ELSEVIER

Coordination Chemistry Reviews
209 (2000) 99–160

COORDINATION CHEMISTRY REVIEWS

www.elsevier.com/locate/ccr

Lanthanides and actinides: annual survey of their organometallic chemistry covering the year 1996

Frank T. Edelmann *, Volker Lorenz

Chemisches Institut der Otto-von-Guericke-Universität Magdeburg, Universitätsplatz 2, D-39106 Magdeburg, Germany

Received 9 July 1999; accepted 9 July 1999

Contents

* Corresponding author. Fax: +49-391-6712933.
E-mail address: frank.edelmann@ust.uni-magdeburg.de (F.T. Edelmann).

0010-8545/00/$ - see front matter © 2000 Elsevier Science S.A. All rights reserved.
PII: S0010-8545(99)00204-0

Keywords: Lanthanides; Actinides; Cyclopentadienyl complexes; Cyclooctatetraenyl complexes; Organometallic chemistry

1. Introduction

The review presents complexes of the lanthanides, actinides and also scandium and yttrium, which contain metal–carbon bonds as defined by section 29 of Chemical Abstracts. Abstracts of papers presented at conferences, dissertations and patents have mostly been excluded.

Deacon [1] published a review on complexes of lanthanoids with neutral π donor ligands. The synthesis, structures and reactions of lanthanoid complexes with alkenes, alkynes and arenes have been described. Whilst the discussion is focused mainly on neutral π donors, including intramolecular π-arene-lanthanoid bonding, some formal $[Sm^{III}(C_5Me_5)_2(\pi\text{-donor})^-]$ complexes, derived from $Sm(C_5Me_5)_2$ and neutral π donors, have been included, especially examples which readily dissociate into the reactants (77 references).

Another short review written by Krishnamurthy [2] with 15 references under the headline 'Lanthanide organometallic chemistry springs a surprise: A serendipitous route to a 'nonclassical carbocation' described the unexpected Sm-carbocation product of CO reaction with $(C_5Me_5)_3Sm$ reported by Evans et al. (1995).

2. Lanthanides

2.1. Lanthanide complexes without supporting cyclopentadienyl and cyclopentadienyl-like ligands

2.1.1. Alkyl, alkynyl and arene complexes

Bochkarev et al. [3] reported the synthesis and characterization of Eu(II) and Sm(II) complexes containing the cyclopentadienyl–vanadiumnaphthalene anion. The trinuclear complexes $[(\eta^5\text{-}C_5H_5)V(\mu_2\text{-}\eta^6\text{:}\eta^6\text{-}C_{10}H_8)]_2Ln(THF)(DME)$ (Ln = Eu, Sm) consist of two $[(C_5H_5)V(C_{10}H_8)]$ sandwiches, bonded η^6 to the lanthanide atom via the naphthalene bridges (Fig. 1). However, there is no interaction between the cyclopentadienyl group and the europium or samarium. The angle V–Eu–V is 126°. The naphthalene ligands remain planar. The distances of the europium atoms to the carbon atoms of both η^6-coordinating rings are in the ranges 284.5 and 301.9 pm with an average of 292.7 pm for C(6) to C(11), and 286.1 and 308.4 pm with an average of 297.0 pm for C(24) to C(29). The C–C bonds in the naphthalene ring

coordinated to europium are elongated and equalized compared with free naphthalene.

The compounds were prepared by the reaction of $LnI_2(DME)_3$ with an equimolar mixture of $K(C_5H_5)$ and $K(C_5H_5)V(C_{10}H_8)$ in DME followed by treatment with THF. The complexes $[(\eta^5\text{-}C_5H_5)V(\mu_2\text{-}\eta^6\text{:}\eta^2\text{-}C_{10}H_8)Ln(\eta^5\text{-}C_5H_5)(THF)]_n$ were observed as side products. The authors also described a route to synthesize these compounds in better yields (Section 2.2.1).

$$LnI_2(DME)_3 + K(C_5H_5) + K[(C_{10}H_8)V(C_5H_5)] \xrightarrow[-2KI]{THF} [(C_5H_5)V(C_{10}H_8)]_2Ln(THF)(DME) + [(C_5H_5)V(C_{10}H_8)Ln(C_5H_5)(THF)]_n$$

Taube et al. [4] synthesized the first neutral tris(allyl)lanthanide complexes $La(\eta^3\text{-}C_3H_5)_3\cdot 1.5$dioxane and $Nd(\eta^3\text{-}C_3H_5)_3\cdot$dioxane and tested them as 'single site' catalysts for the stereospecific polymerization of butadiene. The title complexes were obtained by reaction of tetrakis(allyl)lanthanide(III) complexes $Li[Ln(C_3H_5)_4]\cdot 1.5$dioxane (Ln = La or Nd) with BEt_3 in dioxane. The addition of BEt_3 led to the abstraction of allyllithum. The compounds were characterized by elemental analysis, by IR, ^{1}H- and ^{13}C-NMR spectroscopy and also by X-ray crystal structure analysis:

$$Li[Ln(C_3H_5)_4]\cdot 1.5\text{dioxane} + BEt_3 \xrightarrow{\text{dioxane}} Ln(C_3H_5)_3\cdot x\text{dioxane} + Li[BEt_3(C_3H_5)]\cdot 1.5\text{dioxane}$$

where Ln = La ($x = 1.5$) or Nd ($x = 1$).

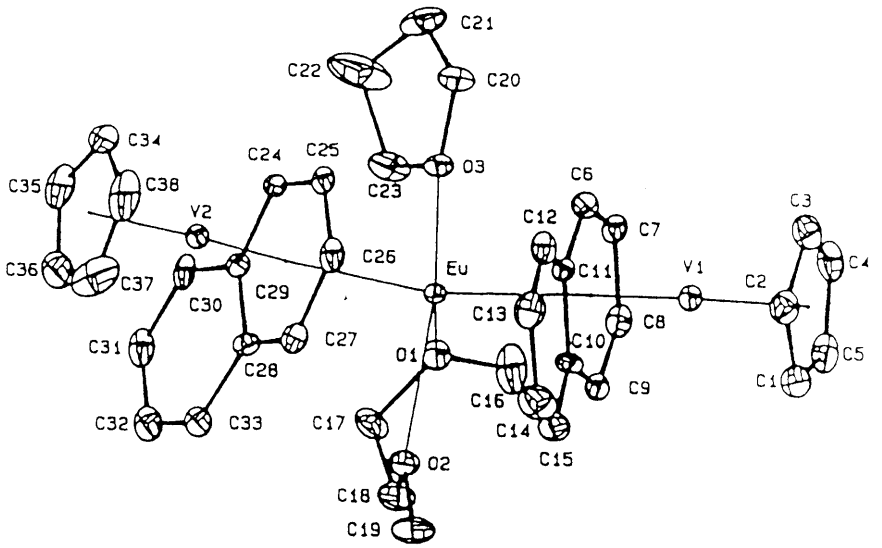

Fig. 1. ORTEP projection of one molecule of $[(\eta^5\text{-}C_5H_5)V(\mu_2\text{-}\eta^6\text{:}\eta^6\text{-}C_{10}H_8)]_2Eu(THF)(DME)$.

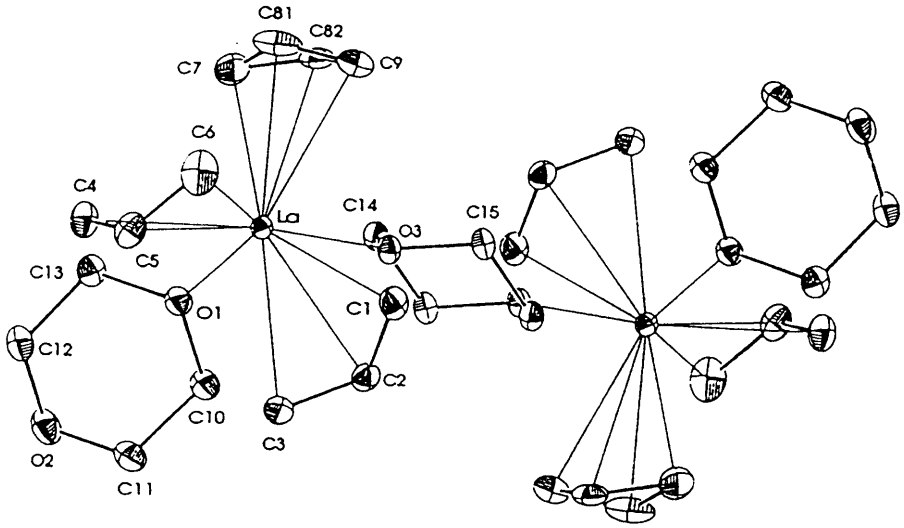

Fig. 2. Structure of $[\{La(\eta^3\text{-}C_3H_5)_3(\eta^1\text{-}C_4H_8O_2)\}_2(\mu\text{-}C_4H_8O_2)]$.

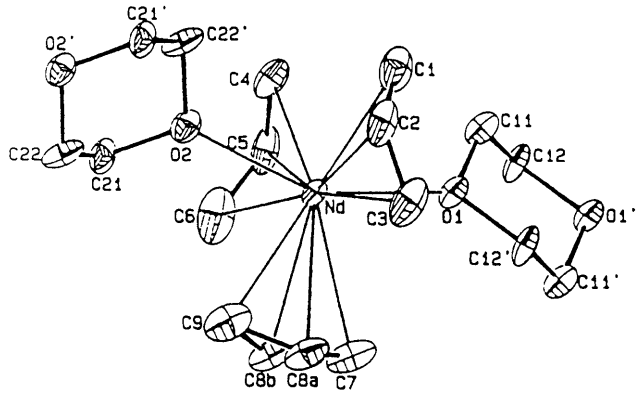

Fig. 3. Structure of a unit of $[Nd(\eta^3\text{-}C_3H_5)_3(\mu\text{-}C_4H_8O_2)]_\infty$.

In both complexes the three allyl anions are η^3 coordinated. By the coordination of dioxane in the case of lanthanum the dimeric structure $[\{La(\eta^3\text{-}C_3H_5)_3(\eta^1\text{-}C_4H_8O_2)\}_2(\mu\text{-}C_4H_8O_2)]$ (Fig. 2) and with neodymium a polymeric structure $[Nd(\eta^3\text{-}C_3H_5)_3(\mu\text{-}C_4H_8O_2)]_\infty$ (Fig. 3) is formed. The dioxane can be split off easily at 50°C without further decomposition. The compounds catalyze the 1,4-*trans* polymerisation of butadiene in toluene with high selectivity.

Windisch and Taube [5] also reported the characterization of allyl lanthanum complexes by ^{139}La NMR spectroscopy. ^{139}La NMR chemical shifts were measured for several anionic complexes of formulae $[Li(C_4H_8O_2)_{1.5}][La(\eta^3\text{-}C_3H_5)_4]$, $[Li(C_4H_8O_2)_2][Cp'_nLa(\eta^3\text{-}C_3H_5)_{4-n}]$ ($Cp' = (\eta^5\text{-}C_5H_5)$, $n = 1$, 2 and $Cp' = (\eta^5\text{-}$

C_5Me_5), $n = 1$) and $Li[R_nLa(\eta^3\text{-}C_3H_5)_{4-n}]$ ($R = N(SiMe_3)_2$, $n = 1$, 2 and $R = C{\equiv}CSiMe_3$, $n = 4$), and as well as for neutral compounds of formulae $La(\eta^3\text{-}C_3H_5)_3L_n$ [$L_n = (C_4H_8O_2)_{1.5}$, $(HMPT)_2$, TMEDA], $Cp'_nLa(\eta^3\text{-}C_3H_5)_{3-n}$ ($Cp' = (\eta^5\text{-}C_5H_5)$, $(\eta^5\text{-}C_5Me_5)$, $n = 1$, 2) and $La(\eta^3\text{-}C_3H_5)_3X(THF)_2$ (X = Cl, Br, I). Typical ranges of the ^{139}La NMR shifts were found for the different types of complexes independent of number and kind of organic groups directly bonded to lanthanum.

Smith et al. [6] described the synthesis and characterization of alkyl europium(II) and ytterbium(II) derivatives. The dialkyls EuR_2 ($R = C(SiMe_3)_3$) and YbR_2 ($R = [C(SiMe_3)_2(SiMe_2X)]$, X = Me, $CH{=}CH_2$, or CH_2CH_2OEt) have been obtained from reactions between KR and LnI_2, and the ytterbium analogues of Grignard reagents, $Yb[C(SiMe_3)_2(SiMe_2X)]I{\cdot}OEt_2$ (X = Me, $CH{=}CH_2$, Ph or OMe), were prepared from reactions between RI and Yb metal. The new complexes were characterized by their ^1H, ^{13}C, ^{29}Si NMR spectra, and the Yb-compounds were also investigated by ^{171}Yb-NMR spectroscopy. Single crystals of $Eu[C(SiMe_3)_3]_2$, $Yb[C(SiMe_3)_2(SiMe_2CH{=}CH_2)]I{\cdot}OEt_2$ and $Yb[C(SiMe_3)_2(Si\,Me_2OMe)]I{\cdot}OEt_2$ were used to determine the structures (Figs. 4 and 5) of the compounds in the solid state. The compounds YbR_2 and EuR_2 crystallize as solvent-free monomers with C–Ln–C = 136–137°. The alkylytterbium iodides crystallize from diethyl ether as solvated iodide-bridged dimers in which the coordination number at Yb is 4 for X = Me but is increased to 5 by chelation from the group X when X = OMe. When

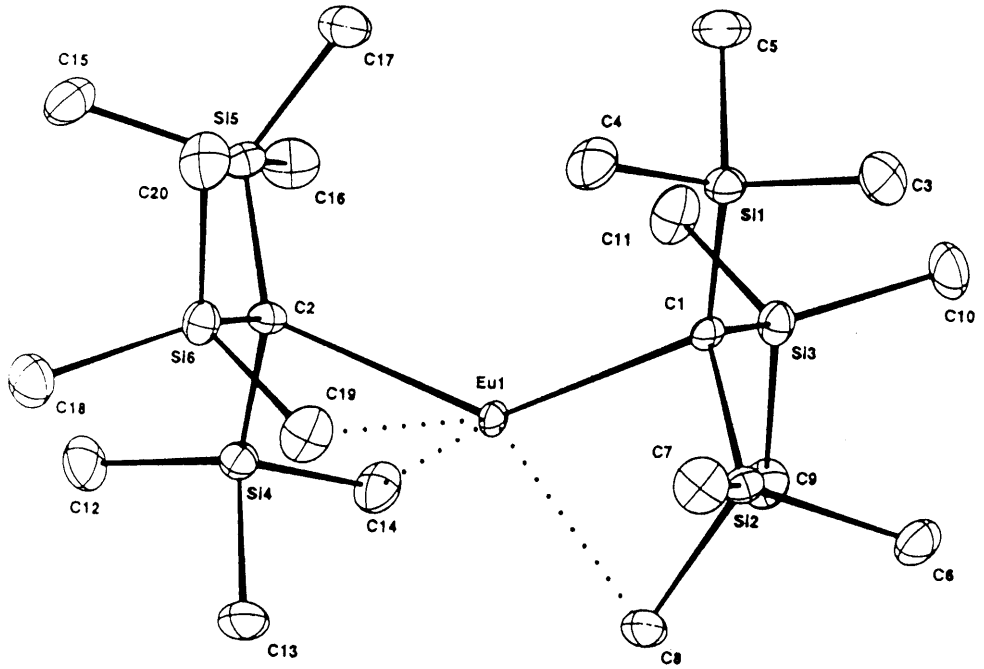

Fig. 4. Molecular structure of $Eu[C(SiMe_3)_3]_2$.

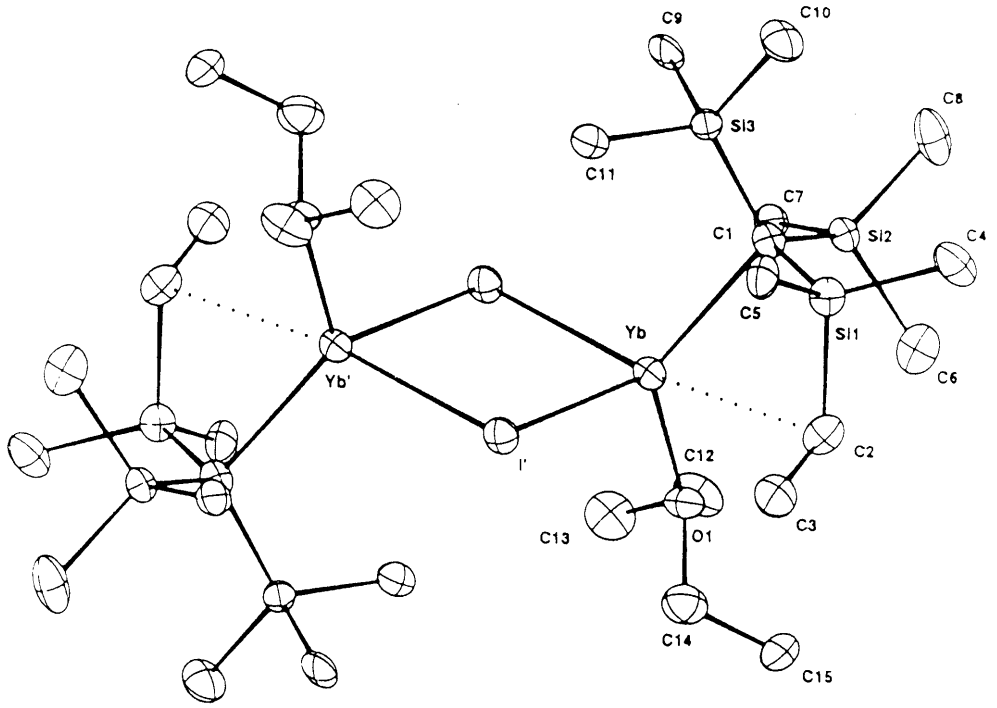

Fig. 5. Molecular structure of $Yb[C(SiMe_3)_2(SiMe_2CH{=}CH_2)]I{\cdot}OEt_2$.

$X = CH{=}CH_2$, the Yb···X interaction is weak. The reaction $2RYbI \rightarrow R_2Yb + YbI_2$ is not observed when X = Me, but takes place readily when X = Ph, $CH{=}CH_2$, or OMe and provides a route to the dialkyls LnR_2 in these cases where the alkylpotassium reagent KR cannot be obtained, e.g. for X = OMe. The dialkyl $Yb[C(SiMe_3)_2(SiMe_2X)]_2$ with X = Me reacts with ethers R′OEt (R′ = Et, Bu, Bu^t) to give ethene and the corresponding alkoxides RYbOR′. This reaction does not take place when X = OMe and is very slow in the case of $X = CH{=}CH_2$.

Jank and Amberger [7] investigated the electronic structure of organometallic complexes of f-elements. The crystal field parameters of base-free $(Me_3SiC_5H_4)_3Pr$, the adducts $(C_5H_5)_3Pr{\cdot}NCCH_3$, $(C_5H_5)_3La(NCCH_3)_2$:Pr, cationic $[Pr(C_8H_8)]^+$ and $Nd[N(SiMe_3)_2]_3$ as model compounds for $Nd[CH(SiMe_3)_2]_3$ were inserted into the corresponding energy matrices of a model spin-free f^1 system. Diagonalizing these matrices the crystal field splitting patterns of the f orbitals were calculated. These experimentally based molecular orbital schemes are compared with the results of previous model calculations.

Makioka et al. [8] studied the reactivity of lanthanide(II) acetylides generated from lanthanide–benzophenone complexes and 1-alkynes. Ytterbium and samarium-benzophenone complexes react with 1-alkynes to generate lanthanide(II) acetylides having an additional diphenylmethoxo ligand. It has been found that

these acetylides act as reductants as well as nucleophiles, depending on the electrophiles used. Their reaction with aldehydes and aliphatic ketones gives propargylic alcohols in very good yields, while with aromatic ketones and alkyl halides the reductive coupling products are obtained selectively. The reaction of Yb with benzophenone in THF/1,3-dimethylimidazolidinone followed by treatment with $C_4H_9C{\equiv}CH$ gave $Ph_2CHOYbC{\equiv}C{-}C_4H_9$. Reaction of $Ph_2CHOYbC{\equiv}C{-}C_4H_9$ with C_3H_7CHO in the same solvent system gave $C_3H_7CH(OH)C{\equiv}C{-}C_4H_9$ with an 88% yield.

2.1.2. Endohedral metallofullerenes, lanthanide-filled carbon nanotubes and lanthanide carbonyls

Pasqualini et al. [9] reported about the carbon nanoencapsulation of uranium dicarbide. Nanoparticles of uranium dicarbide encapsulated in carbon smaller than 100 nm have been obtained by chemical reactions at high temperature. Two types of nanocapsules were identified and characterized. The majority of them had small diffuse kernel surfaces, with dimensions between 5 and 15 nm, surrounded by a thick spherical carbon cover. Others, formed in minor quantity and ranging from 15 to 40 nm, were polyhedral and surrounded with several perfect graphite layers oriented parallel to their external surface. The nanocapsules are as chemically inert as graphite.

Yositaka and Oguro [10] investigated variable range hopping conduction in LaC_2, CeC_2, or GdC_2 crystals encapsulated in carbon nanocages. An experimental study of electrical transport phenomena in magnetic fields (H up to 15 T) in pressed samples of three porous systems composed of carbon nanocages in which LaC_2, CeC_2, or GdC_2 crystals are encapsulated was reported. The $\exp[(T_0/T)^{1/3}]$ temperature dependence in the zero-field dc electrical resistance $R(0)$ was found at low temperatures. Below 50, 50, and 35 K for the LaC_2, CeC_2, and GdC_2 system, respectively, transverse magnetoresistance (MR), [R(H)–R(0)]/R(0), is negative. In the weak field region ($H < 0.15$ T), the negative MR is quadratic in H, and becomes linear in the field range 0.15–0.5 T. The linear and negative MR shows $T^{-1.04\pm0.10}$ temperature dependence. The temperature dependence of $R(0)$ is described in terms of Mott's law for two-dimensional variable range hopping (2D VRH) conduction. The low field magnetotransport features support a predicted quantum interference effect on 2D VRH conduction.

Lin et al. [11] studied the geometry, electronic structure and bond of LaCO with SCM-DV-X_a methods. From the results it is certified that the LaCO is a linear molecule, in which the bond length of La–C and C–O are 0.2273 nm and 0.1179 nm respectively, the σ coordinate bond and the π-back bond are formed between La and CO. It was also shown that the La–C bond has more than 90% covalent character and the 4f orbitals play a certain role in the bonding of LaCO.

2.2. Cyclopentadienyl complexes

2.2.1. Mono(cyclopentadienyl) complexes

As already mentioned in Section 2.1.1 Bochkarev et al. [3] synthesized also complexes of the composition $[(\eta^5\text{-}C_5H_5)V(\mu_2\text{-}\eta^6{:}\eta^2\text{-}C_{10}H_8)Ln(\mu_2\text{-}\eta^5{:}\eta^5\text{-}C_5H_5)\text{-}(THF)]_n$ (Ln = Sm, Eu). First the authors observed these compounds as side products in the reactions to prepare $[(\eta^5\text{-}C_5H_5)V(\mu_2\text{-}\eta^6{:}\eta^6\text{-}C_{10}H_8)]_2Ln\text{-}(THF)(DME)$. The reaction of $(C_{10}H_8)Ln(DME)_2$ with equimolar amounts of dicyclopentadienylvanadium in THF-DME results in the formation of $[(\eta^5\text{-}C_5H_5)V(\mu_2\text{-}\eta^6{:}\eta^2\text{-}C_{10}H_8)Ln(\mu_2\text{-}\eta^5{:}\eta^5\text{-}C_5H_5)(THF)]_n$ (Ln = Sm, Eu) in better yields.

$$(C_{10}H_8)Ln(DME)_2 + V(C_5H_5)_2 \xrightarrow[-\,DME]{THF} [(C_5H_5)V(C_{10}H_8)Ln(C_5H_5)(THF)]_n$$

Ln = Sm, Eu

The X-ray crystal structure analysis for $[(\eta^5\text{-}C_5H_5)V(\mu_2\text{-}\eta^6{:}\eta^2\text{-}C_{10}H_8)Ln(\mu_2\text{-}\eta^5{:}\eta^5\text{-}C_5H_5)(THF)]_n$ shows a polymeric structure, built from infinite zig-zag chains formed by $[Eu(\mu_2\text{-}\eta^5{:}\eta^5\text{-}C_5H_5)]$ units. Each europium atom of this chain is further coordinated η^2 by the naphthalene of the $[(C_5H_5)V(C_{10}H_8)]$ unit and by the oxygen of the THF ligand (Fig. 6).

Piers et al. [12] reported the use of alkane elimination in the one-step synthesis of organoscandium complexes containing a new multidentate cyclopentadienyl ligand. The new multidentate ligand, $Me_2NCH_2\text{-}CH_2\text{–}C_5H_4\text{–}SiMe_2\text{–}NH\text{–}^t$Bu was prepared in 71% yield as a mixture of 1,3 and 1,2 isomers ($\sim$7:3) in one step from $LiC_5H_4\text{–}CH_2\text{–}CH_2\text{–}NMe_2$, Me_2SiCl_2 and *tert*-butylamine. The ligand was attached to scandium in an efficient alkane elimination reaction by treatment of in situ generated $Sc(CH_2SiMe_3)_3\cdot 2THF$ with $Me_2NCH_2\text{–}CH_2\text{–}C_5H_4\text{–}SiMe_2\text{–}NH\text{–}^t$Bu, yielding the alkylscandium species $(Me_2NCH_2\text{–}CH_2\text{–}C_5H_3\text{–}SiMe_2\text{–}N\text{–}^t\text{Bu})\text{-}ScCH_2SiMe_3$ directly in 52% yield. Treatment of $(Me_2NCH_2\text{–}CH_2\text{–}C_5H_3\text{–}SiMe_2\text{–}$

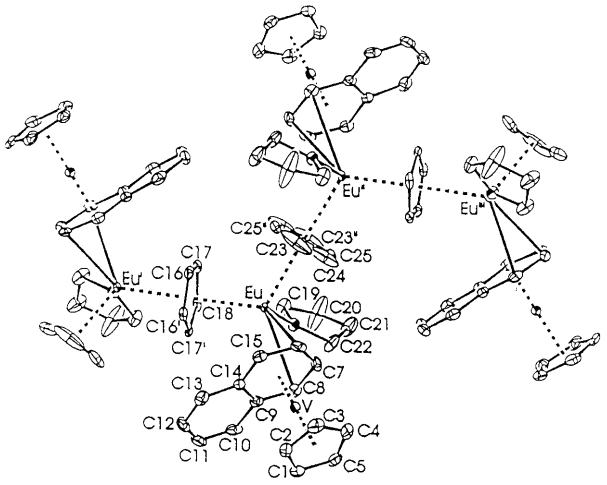

Fig. 6. ORTEP projection of one molecule of $[(\eta^5\text{-}C_5H_5)V(\mu_2\text{-}\eta^6{:}\eta^2\text{-}C_{10}H_8)Eu(\mu_2\text{-}\eta^5{:}\eta^5\text{-}C_5H_5)(THF)]_n$.

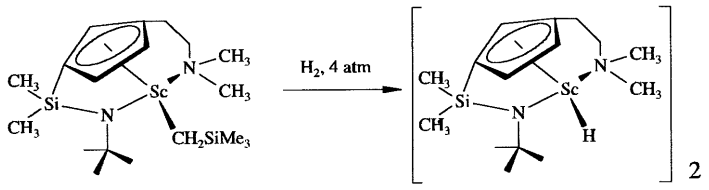

Scheme 1. Treatment of $(Me_2NCH_2–CH_2–C_5H_3–SiMe_2–N–^tBu)ScCH_2SiMe_3$ with H_2.

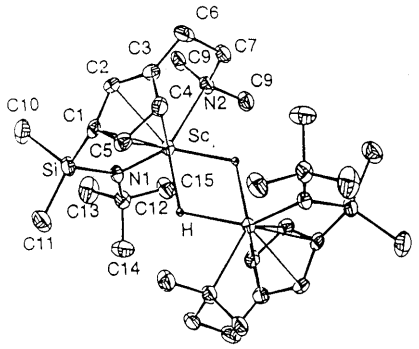

Fig. 7. Structure of the 1R-*trans*-1′S diastereomer $[(Me_2NCH_2–CH_2–C_5H_3–SiMe_2–N–^tBu)Sc]_2(\mu^2\text{-}H)_2$.

$N–^tBu)ScCH_2SiMe_3$ with H_2 gave two of four possible diastereomeric μ-dihydrides (Scheme 1). The C_i symmetric 1R-*trans*-1′S diastereomer $[(Me_2NCH_2–CH_2–C_5H_3–SiMe_2–N–^tBu)Sc]_2(\mu^2\text{-}H)_2$ was characterized crystallographically. Thermolysis of $(Me_2NCH_2–CH_2–C_5H_3–SiMe_2–N–^tBu)ScCH_2SiMe_3$ at 70°C for 3 days resulted in the metalation of an *N*-methyl group and loss of Me_4Si. A mixture of two dimeric compounds with bridging methylene units was formed, one of which was identified as the C_i symmetric 1R-*trans*-1′S diastereomer by X-ray crystallography (Fig. 7).

Taube et al. [13] published the synthesis and characterization of anionic allyl neodymium(III) complexes and their use as catalysts for the stereospecific polymerization of butadiene. For the already known tetrakis(allyl) complex $Li[Nd(\eta^3\text{-}C_3H_5)_4]\cdot 1.5$dioxane an essentially improved method of preparation from anhydrous $NdCl_3$ and LiC_3H_5·dioxane in dimethoxyethane was found.

$$Sn(C_3H_5)_4 + 4Li(n\text{-}C_4H_9) \xrightarrow[2.\ \text{dioxane}]{1.\ Et_2O} 4LiC_3H_5\cdot C_4H_8O_2 + Sn(n\text{-}C_4H_9)_4$$

$$NdCl_3 + 4LiC_3H_5\cdot C_4H_8O_2 \xrightarrow[2.\ Et_2O/\text{dioxane}]{1.\ DME/50°C} Li[Nd(\eta^3\text{-}C_3H_5)_4]\cdot 1.5C_4H_8O_2$$

By partial protolysis with cyclopentadiene and pentamethylcyclopentadiene from $Li[Nd(\eta^3\text{-}C_3H_5)_4]\cdot 1.5C_4H_8O_2$ the complexes $Li[Nd(C_5H_5)(\eta^3\text{-}C_3H_5)_3]\cdot 2C_4H_8O_2$ and $Li[Nd(C_5Me_5)(\eta^3\text{-}C_3H_5)_3]\cdot$3DME were obtained. Both compounds were also synthesized from the appropriate $(C_5H_5)NdCl_2\cdot$3THF. The new compounds $Li[Nd(C_5H_5)(\eta^3\text{-}C_3H_5)_3]\cdot 2C_4H_8O_2$ and $Li[Nd(C_5Me_5)(\eta^3\text{-}C_3H_5)_3]\cdot$3DME were characterized by elemental analyses, IR and ^{1}H-NMR spectroscopy and $Li[Nd(C_5Me_5)\text{-}(\eta^3\text{-}C_3H_5)_3]\cdot$3DME also by X-ray crystal structure analysis (Fig. 8).

Shen et al. [14] described the synthesis and structural investigation of $\{(C_5H_5)Pr[CH(COOC_2H_5)_2][\mu\text{-}CH(COOC_2H_5)_2]\}_2$. The reaction of a 1:2 molar ratio of $(C_5H_5)_3Pr$ with diethyl malonate in *n*-hexane results in the formation of

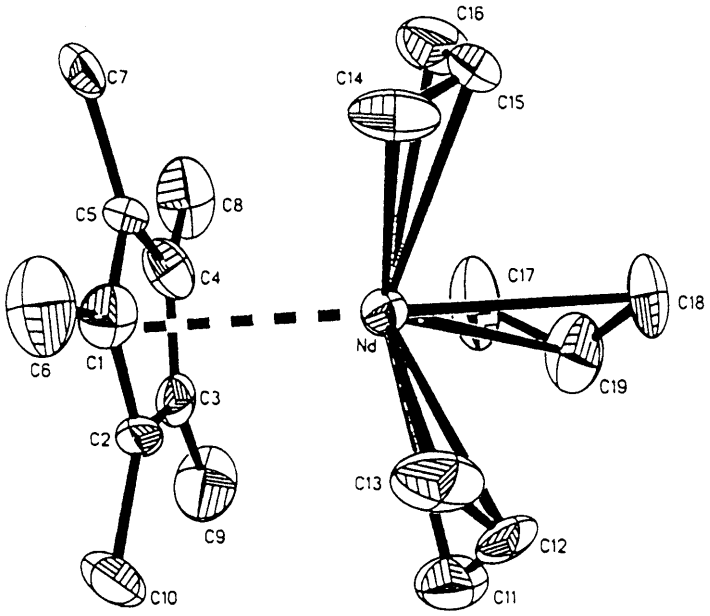

Fig. 8. Structure of $[Nd(C_5Me_5)(\eta^3\text{-}C_3H_5)_3]^-$.

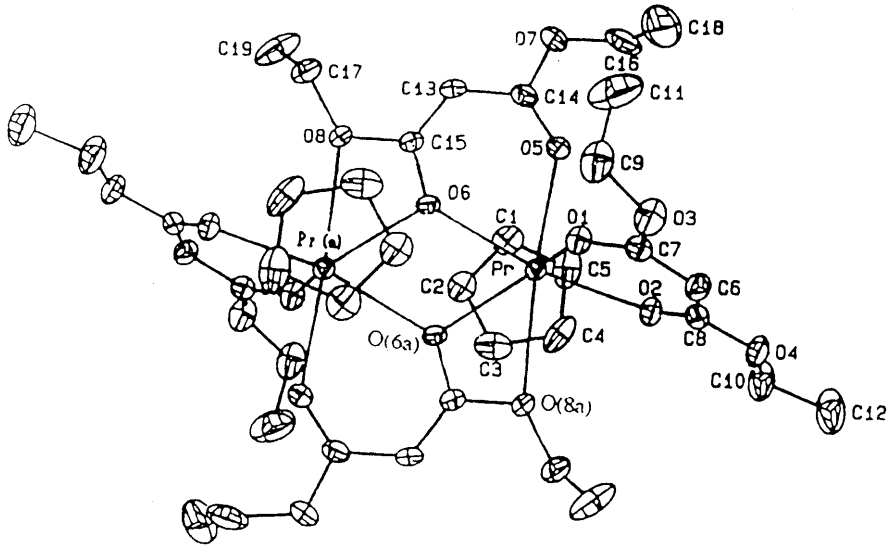

Fig. 9. The structure of $\{(C_5H_5)Pr[CH(COOC_2H_5)_2][\mu\text{-}CH(COOC_2H_5)_2]\}_2$.

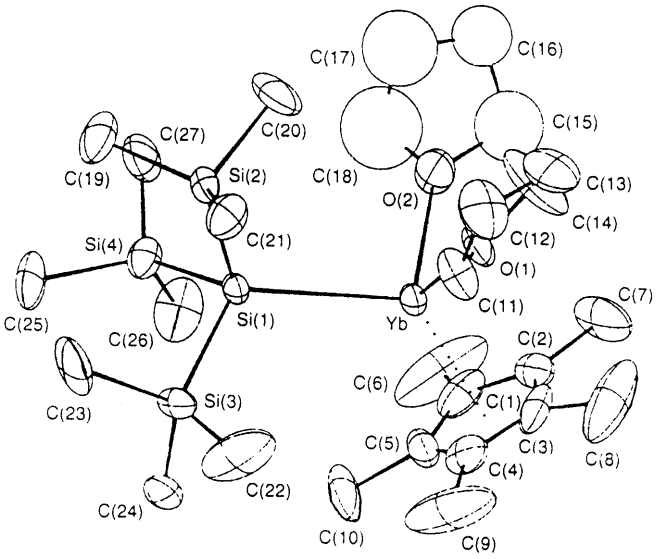

Fig. 10. Molecular structure of $[(C_5Me_5)Yb\{Si(SiMe_3)_3\}(THF)_2]$.

$\{(C_5H_5)Pr[CH(COOC_2H_5)_2][\mu\text{-}CH(COOC_2H_5)_2]\}_2$ (Fig. 9). X-ray analysis demonstrates that the complex is a dimer and the two praseodymium atoms are bridged by two oxygen atoms of the independent diethyl malonate ligands. The bridging ligands coordinate to the praseodymium in a bidentate mode. The complex crystallizes in the monoclinic system, space group $P2_1/a$ with unit cell constants $a = 9.675(4)$, $b = 18.134(3)$, $c = 12.795(3)$ Å, $\beta = 92.53(3)°$, $D_c = 1.55$ g cm^{-3}, $M_r = 1048.65$, $V = 2243(2)$ Å^3, for $Z = 2$, $\mu = 22.01$ cm^{-1} and $F(000) = 1056$. The structure was solved by heavy atom methods (DIRDIF) and full-matrix least-squares refinement to the final $R = 0.040$, $wR = 0.048$.

Lawless et al. [15] published the synthesis, structure and reactivity of $[(C_5Me_5)Yb\{Si(SiMe_3)_3\}(THF)_2]$. The reaction of $[(C_5Me_5)_2Yb(OEt)_2]$ with one equivalent of $[Li\{Si(SiMe_3)_3\}(THF)_3]$ in toluene afforded $[(C_5Me_5)Yb\{Si(SiMe_3)_3\}(THF)_2]$ in high yields (75%). The title compound was initially characterized by its ^{171}Yb NMR spectrum in toluene solution, which displayed a single resonance at δ 421ppm with satellites corresponding to $^1J(^{171}Yb–^{29}Si)$ 829 Hz. The ^{29}Si NMR spectrum comprised two resonances at δ −2.9 and −158 ppm, with the latter assigned to $Si(SiMe_3)_3$ possessing satellites confirming the previously measured $^1J(^{171}Yb–^{29}Si)$ and also displaying a $^1J(^{29}Si–^{29}Si)$ coupling of 26 Hz; the former, assigned to $Si(SiMe_3)_3$, showed a $^2J(^{171}Yb–^{29}Si)$ coupling of 11.5 Hz and a $^1J(^{29}Si–^{13}C)$ coupling of 40 Hz. The ^{13}C NMR spectrum of $[(C_5Me_5)Yb\{Si(SiMe_3)_3\}(THF)_2]$ revealed $^2J(^{13}C–^{29}Si)$ 8 Hz for $Si(SiMe_3)_3$ and a $^1J(^{13}C–^{171}Yb)$ coupling of 10 Hz for C_5Me_5. The molecular structure (Fig. 10) of $[(C_5Me_5)Yb\{Si(SiMe_3)_3\}(THF)_2]$ was determined from a single-crystal X-ray diffraction study. The ligand geometry around the Yb atom is

distorted tetrahedral, with the angle between the bulky silyl substituent and the Cp* centroid, Cp*–Yb–Si, being expanded to 128° and a corresponding compression of the angle O(THF1)–Yb–O(THF2) to 89°. The Yb–Si distance, 3.032(3) Å, is somewhat shorter than that reported for the other previously recorded Yb^{II}–Si compounds.

Mandel and Magull [16] published new benzyl rare earth metal complexes and studied the synthesis and crystal structures of $[(C_5Me_5)_2Y(CH_2C_6H_5)(THF)]$, $[(C_5Me_5)_2Sm(CH_2C_6H_5)_2K(THF)_2]_\infty$, and $[(C_5Me_5)Gd(CH_2C_6H_5)_2(THF)]$.

The gadolinium complex $[(C_5Me_5)Gd(CH_2C_6H_5)_2(THF)]$ as a mono(cyclopentadienyl) compound was synthesized according to the following equation:

$$GdBr_3 + K(C_5Me_5) + 2KCH_2C_6H_5 \xrightarrow{THF} 2KBr + (C_5Me_5)Gd(CH_2C_6H_5)_2(THF)$$

(yield: 64%)

$[(C_5Me_5)_2Y(CH_2C_6H_5)(THF)]$ and $[(C_5Me_5)_2Sm(CH_2C_6H_5)_2K(THF)_2]_\infty$ are discussed in Section 2.2.2.

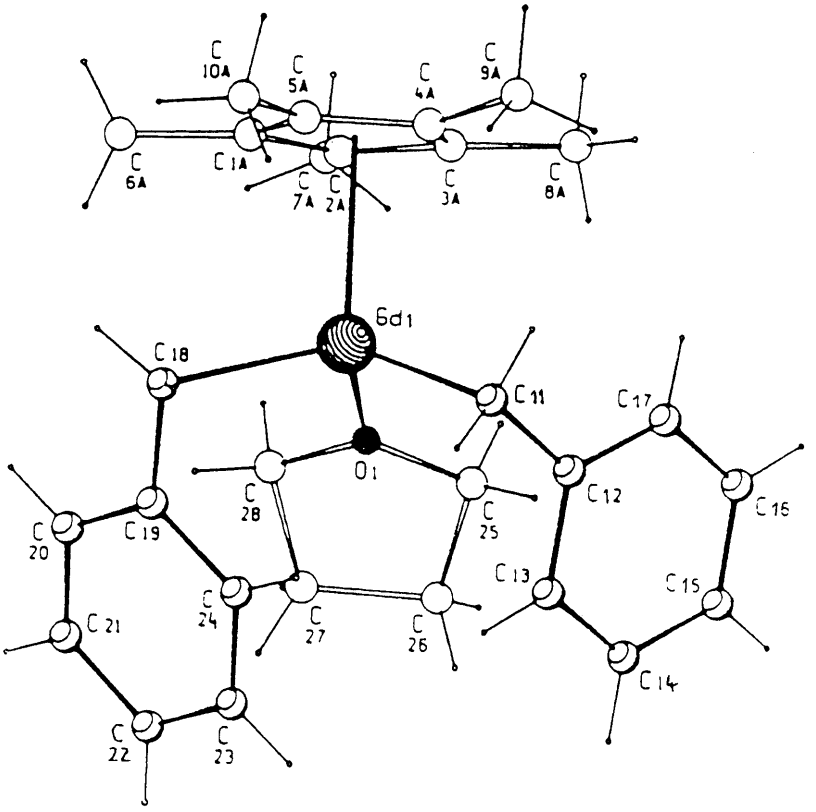

Fig. 11. Molecular structure of $(C_5Me_5)Gd(CH_2C_6H_5)_2(THF)$.

As shown in Fig. 11, the ligand geometry around the Gd atom in $(C_5Me_5)Gd(CH_2C_6H_5)_2(THF)$ is distorted tetrahedral. The angles Gd–C–C_{ipso}(benzyl) are strikingly smaller than the angles Ln–C–C_{ipso}(benzyl) in $[(C_5Me_5)_2Sm(CH_2C_6H_5)_2K(THF)_2]_\infty$ and $(C_5Me_5)Gd(CH_2C_6H_5)_2(THF)$. Additionally the Gd–$C_{ipso}$(benzyl) distance is shorter than those observed in the other benzyl complexes. This result of the X-ray crystal structure analysis indicates a week interaction of the Gd atom with the C_{ipso}(benzyl) in the solid state.

Lawless et al. [17] investigated the spontaneous self-assembly of a hexanuclear ytterbium(II) octaiododianion in the complex $\{Yb_6[\eta\text{-}C_5Me_4(SiMe_2^tBu)]_6I_8\}\{Li(THF)_4\}_2$. The reaction of 1 equivalent of $[LiC_5Me_4(SiMe_2^tBu)]$ with YbI_2 affords the novel half-sandwich polyatomic species. The molecular structures and solid- and solution-state ^{171}Yb NMR data for $\{Yb_6[\eta\text{-}C_5Me_4(SiMe_2^tBu)]_6I_8\}\{Li(THF)_4\}_2$ and, for comparison, the dimeric half sandwich derivatives $[\{Yb(\eta\text{-}C_5Me_5)(\mu\text{-}I)L_n\}_2]$ (L = THF, $n = 2$; L = DME, $n = 1$) are presented. The molecular structure of $\{Yb_6[\eta\text{-}C_5Me_4(SiMe_2^tBu)]_6I_8\}\{Li(THF)_4\}_2$ comprises two Li^+ cations, each tetrahedrally coordinated by four THF molecules, and a $\{Yb_6[\eta\text{-}C_5Me_4(SiMe_2^tBu)]_6I_8\}^{2-}$ dianion (Fig. 12). Each face of the I_8 cube is bridged in a μ_4-fashion by a $Yb[\eta\text{-}C_5Me_4(SiMe_2^tBu)]$ moiety.

Richter and Edelmann [18] published a new synthetic route to organolanthanide tetrahydroborates. The well-known chlorolanthanide bis(tetrahydroborates) have been employed as starting materials for the preparation of organolanthanide complexes. Treatment of $LnCl(BH_4)_2$ with one equivalent of $K(C_5Me_5)$ produced the new organolanthanide tetrahydroborates $(C_5Me_5)Ln(BH_4)_2$ (Ln = Sm, Dy, Yb).

$$LnCl_3 + 2LiBH_4 \xrightarrow[-2LiCl]{(THF)} LnCl(BH_4)_2 \xrightarrow[-KCl]{+K(C_5Me_5)} (C_5Me_5)Ln(BH_4)_2$$

A similar reaction of $SmCl(BH_4)_2$ with $K[HB(3,5\text{-}Me_2pz)_3]$ (pz = pyrazolyl) afforded the disubstituted pyrazolylborate derivative $[HB(3,5\text{-}Me_2pz)_3]_2SmCl$. All new compounds were characterized by their ^1H NMR, ^{11}B NMR, IR and mass spectra and elemental analyses.

Hou et al. [19,20] synthesized beside several samarium(II) aryloxide compounds also $[(C_5Me_5)SmOAr(HMPA)_2]$ (Ar = C_6H_2-2,6-$^tBu_2$-4-Me). In the presence of 2 equivalents HMPA, the reaction of $[(ArO)Sm(\mu\text{-}I)(THF)_3]_2$ with 2 equivalents of C_5Me_5K in THF yielded $[(C_5Me_5)SmOAr(HMPA)_2]$ as dark brown crystals. When $[(ArO)Sm(\mu\text{-}I)(THF)_3]_2$ was mixed with 2 equivalents of C_5Me_5K in THF, polymeric $[ArOSm(\mu\text{-}C_5Me_5)K(\mu\text{-}C_5Me_5)(THF)_2]_\infty$ (Fig. 14) was obtained. The $[C_5Me_5K]$-unit acted as a neutral ligand and could be easily removed by addition of HMPA to give$[(C_5Me_5)SmOAr(HMPA)_2]$. An X-ray analysis of $[(C_5Me_5)SmOAr(HMPA)_2]$ reveals that the central Sm(II) ion is bonded to one C_5Me_5, one ArO, and two HMPA ligands in a distorted tetrahedral fashion (Fig. 13). The bonding angles and atomic distances are unexceptional for $(C_5Me_5)Sm$ and ArO–Sm complexes, respectively.

Bochkarev et al. [21] published the synthesis of mixed cyclopentadienyl-naphthalene complexes of rare earth elements. The reaction of $(C_5H_5)LnCl_2(THF)_3$ (Ln = Y, Gd, Er and Tm) with sodium naphthalide in 1,2-dimethoxyethane (DME) led to the formation of mononuclear complexes $(C_5H_5)LnC_{10}H_8(DME)$.

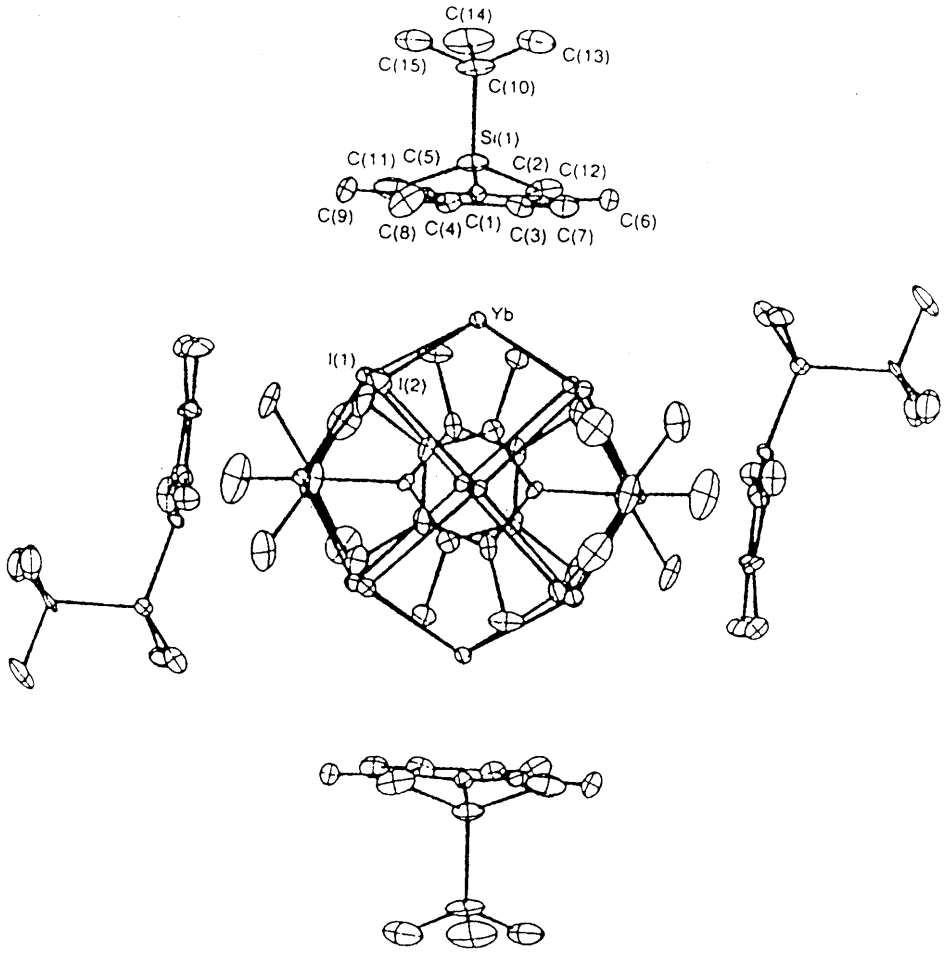

Fig. 12. Structure of the dianion $\{Yb_6[\eta\text{-}C_5Me_4(SiMe_2^tBu)]_6I_8\}^{2-}$.

$$(C_5H_5)LnCl_2 + 2C_{10}H_8\cdot^-Na^+ \xrightarrow{DME} (C_5H_5)LnC_{10}H_8(DME) + C_{10}H_8 + 2NaCl$$

Ln = Y, Gd, Er, Tm

Binuclear complexes $[(C_5H_5)Ln]_2C_{10}H_8(THF)_4$ (Ln = Sm and Yb) containing the Ln atoms in the oxidation state +2 were formed in similar reactions of Sm and Yb complexes.

$$2(C_5H_5)LnCl_2 + 4C_{10}H_8\cdot^-Li^+ \xrightarrow{THF} [(C_5H_5)Ln]_2C_{10}H_8(THF)_4 + 3C_{10}H_8 + 4NaCl$$

Ln = Sm, Yb

The structure of $(C_5H_5)YC_{10}H_8(DME)$ (Fig. 15) was determined by X-ray diffraction. The coordinated naphthalene ring linked to the Y atom is nonplanar

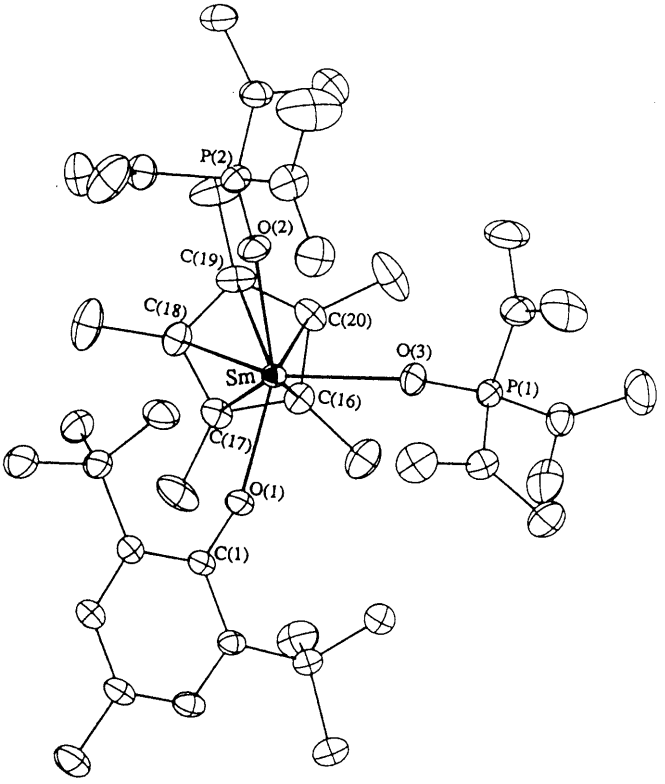

Fig. 13. Molecular structure of $[(C_5Me_5)SmOAr(HMPA)_2]$.

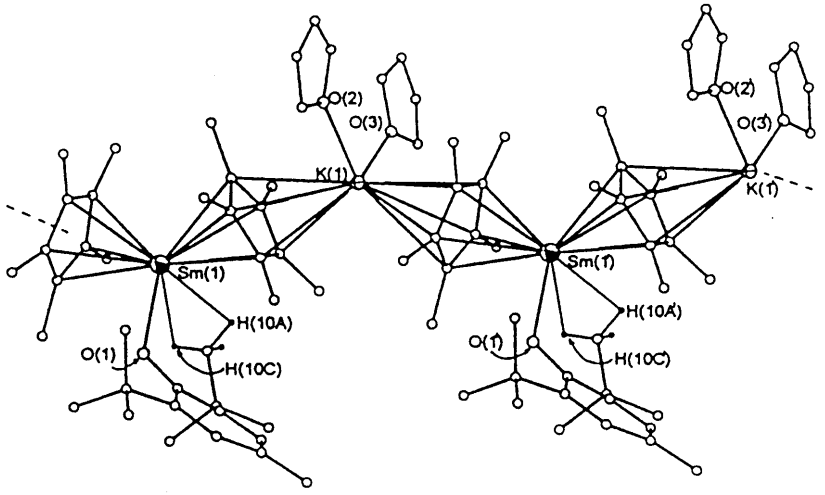

Fig. 14. Structure of $[ArOSm(\mu\text{-}C_5Me_5)K(\mu\text{-}C_5Me_5)(THF)_2]_\infty$.

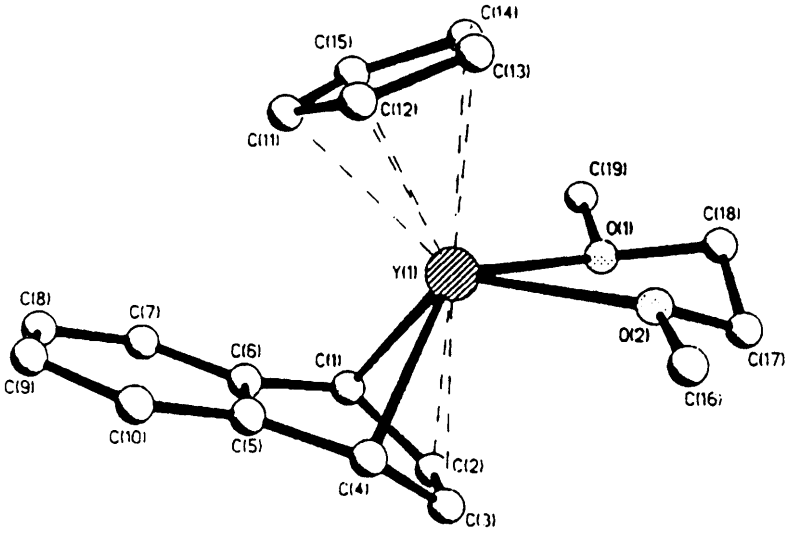

Fig. 15. Molecular structure of $(C_5H_5)YC_{10}H_8(DME)$.

and is bent by an angle of 26.1° over the C(1)–C(4) line. The existence of two short, Y(1)–C(1) and Y(1)–C(4) [2.438(6) and 2.452(6) Å], Y–C($C_{10}H_8$) bonds reflects the $2\eta^1{:}\eta^2$-interaction of the Y atom with the naphthalene dianion. The same yttrium complex was formed as a mixture with $(C_5H_5)_3Y$ in the reaction of $(C_5H_5)_2YCl$ with sodium naphthalenide.

2.2.2. Bis(cyclopentadienyl) complexes

Gautheron et al. [22] reported the synthesis of three bis(diphenylphosphinocyclopentadienyl)yttrium chloride complexes and the heterobimetallic derivative $[(CO)_4Mo(Ph_2PC_5H_4)_2Y(\mu\text{-}Cl)]_2$. The products were characterized by elemental analyses, IR, ^1H-, ^{13}C- and ^{31}P NMR. The crystal structure of $[(Ph_2PC_5H_4)_2Y(\mu\text{-}Cl)]_2$ is remarkable in that the crystal exhibits two independent chloride-bridged dimers that differ in the arrangement (*syn*, *anti*) of the diphenylphosphino groups.

$$2Ph_2PC_5H_4Li + YCl_3(THF)_3 \xrightarrow[25°C]{THF} (Ph_2PC_5H_4)_2Y(\mu\text{-}Cl)_2Li(THF)_2$$

$$4Ph_2PC_5H_4Li + 2YCl_3 \xrightarrow[25°C]{toluene} [(Ph_2PC_5H_4)_2Y(\mu\text{-}Cl)]_2 + 4LiCl$$

$$[(Ph_2PC_5H_4)_2Y(\mu\text{-}Cl)]_2 \xrightarrow[25°C]{THF} (Ph_2PC_5H_4)_2YCl(THF)$$

$$[(Ph_2PC_5H_4)_2Y(\mu\text{-}Cl)]_2 + Mo(CO)_6 \xrightarrow[110°C]{toluene} 2CO + (CO)_4Mo[(Ph_2PC_5H_4)_2Y(\mu\text{-}Cl)]_2$$

Evans [23] published the synthesis of organosamarium diarylpnictide complexes by cleavage reactions of group 15 E–E and E–C bonds by samarium(II). $(C_5Me_5)_2Sm$ and $(C_5Me_5)_2Sm(THF)_2$ react with EPh_3 or $Ph_3E–EPh_3$ (E = P, As, Sb, Bi) by three modes: coordination, E–C cleavage, and E–E cleavage. E–C cleavage

is most common for the heavier congeners, which have weaker E–C bonds. Hence, $(C_5Me_5)_2SmPh$ products were found in reactions with Sb and Bi but not with P and As (Fig. 16).

$$8(C_5Me_5)_2Sm + 2Ph_3Bi \xrightarrow{C_6D_6} [(C_5Me_5)_2Sm]_2(\mu\text{-}\eta^2\text{:}\eta^2\text{-}Bi_2) + 6(C_5Me_5)_2SmPh$$

E–E cleavage occurs with all of the systems studied: P, As, Sb, Bi. For the lighter congeners with stronger E–C bonds, the E–E cleavage products were isolated as the EPh_2 complexes $(C_5Me_5)_2Sm(PPh_2)$ and $(C_5Me_5)_2Sm(AsPh_2)$.

$$2(C_5Me_5)_2Sm + Ph_2EEPh_2 \xrightarrow{\text{toluene}} 2(C_5Me_5)_2Sm(EPh_2)$$

where E = P, As.

$$4(C_5Me_5)_2Sm + Ph_2EEPh_2 \xrightarrow{\text{toluene}} 2(C_5Me_5)_2Sm(\mu^2\text{-}EPh_2)Sm(C_5Me_5)_2$$

where E = P, As.

$$2\ (C_5Me_5)_2Sm(THF)_2 + Ph_2EEPh_2 \xrightarrow{\text{toluene}} (C_5Me_5)_2Sm(EPh_2)(THF)$$

where E = P, As.

The THF adducts display further chemistry and provide a system in which THF coordination and ring opening can be separately defined. This ring opening occurs over a period of several days at room temperature in benzene, toluene, hexane, or THF. $(C_5Me_5)_2Sm[O(CH_2)_4AsPh_2](THF)$ (Fig. 17) can be produced on a preparative scale by heating $(C_5Me_5)_2Sm(EPh_2)(THF)$ in refluxing THF for 16 h.

$$(C_5Me_5)_2Sm(EPh_2)(THF) \xrightarrow[16\ h]{\text{THF/reflux}} (C_5Me_5)_2Sm[O(CH_2)_4EPh_2](THF)$$

where E = P, As.

Schumann et al. [24] reported the synthesis and crystal structures of bis(cyclopentadienyl) rare earth acetates of the type $[Cp_2LnO_2CCH_3]_2$. Organolanthanide chlorides $Cp_2Ln(\mu\text{-}Cl)_2M(L)_2$ ($Cp = C_5H_5$, C_5HMe_4, C_5Me_5; M = Na, Li; L = THF,

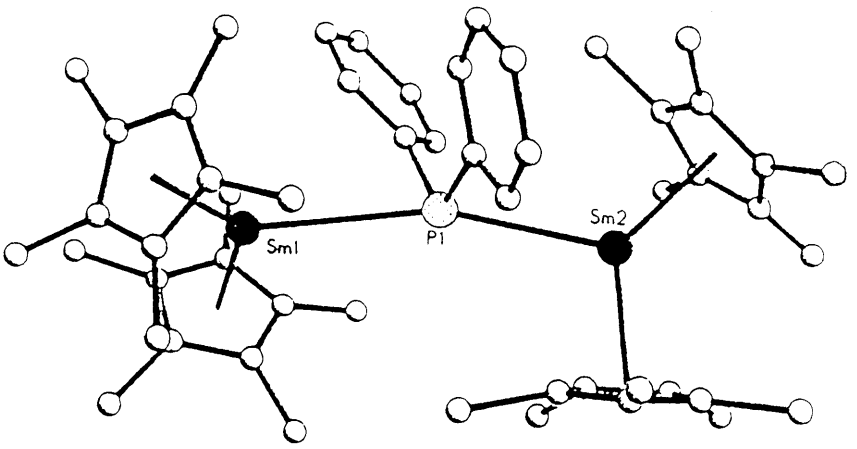

Fig. 16. Structure of $(C_5Me_5)_2Sm(\mu^2\text{-}PPh_2)Sm(C_5Me_5)_2$.

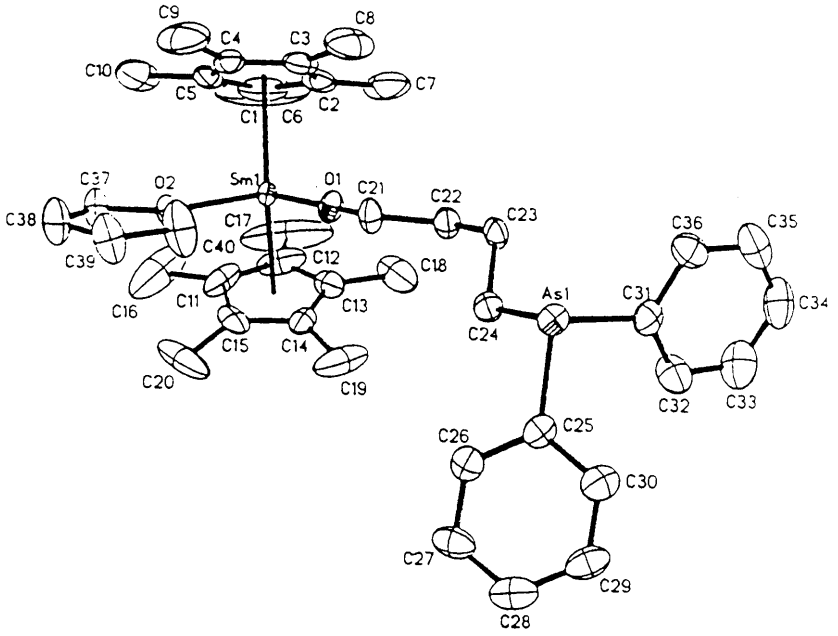

Fig. 17. Structure of $(C_5Me_5)_2Sm[O(CH_2)_4AsPh_2](THF)$.

Et_2O) react with sodium acetate yielding the corresponding dimeric organo rare earth acetates $[(C_5H_5)_2Ln(\mu\text{-}O_2CMe)]_2$ (Ln = Sc, Y, Sm, Lu), $[(C_5HMe_4)_2Ln(\mu\text{-}O_2CMe)]_2$ (Ln = Y, La, Sm, Lu) and $[(C_5Me_5)_2Ln(\mu\text{-}O_2CMe)]_2$ (Ln = Y, La, Sm, Lu).

$$n(C_5R_5)_2LnCl_2M(L)_2 + n NaO_2CCH_3 \xrightarrow{THF/Et_2O} [(C_5R_5)_2Ln(\mu\text{-}O_2CCH_3)]_n + NaCl + n MCl$$

The compounds were characterized by elemental analysis, NMR, IR, Raman and mass spectra. The dimeric structure of the complexes $[(C_5HMe_4)_2Y(\mu\text{-}O_2CMe)]_2$, $[(C_5HMe_4)_2La(\mu\text{-}O_2CMe)]_2$ and $[(C_5HMe_4)_2Sm(\mu\text{-}O_2CMe)]_2$ could be verified by X-ray crystallographic determination. Single crystal X-ray structure analyses show bidentate briging acetate groups in the yttrium (Fig. 18) and samarium compound with eight coordinate Y^{3+} and Sm^{3+} and tridentate bridging acetate groups with nine coordinate La^{3+} in the lanthanum complex (Fig. 19).

The same authors [25] also published the synthesis and single crystal structure analysis of the monomeric organolanthanide acetates $[(C_5Me_4^tBu)_2LnO_2CCH_3]$ (Ln = La, Lu). The monomeric structures are a result of the sterical demanding ^{t}Bu groups at the cyclopentadienyl ligands. The single crystal X-ray structure analysis of $[(C_5Me_4^tBu)_2LuO_2CCH_3]$ (Fig. 20) as well as a cryoscopic molecular weight determination of $[(C_5Me_4^tBu)_2LaO_2CCH_3]$ verify the monomeric structure of these complexes.

Shen et al. [26] reported about the reactivity of lanthanide alkyl compounds with phenylacetylene and the synthesis and structure of $[(^tBu\text{–}C_5H_4)_2LnC{\equiv}CPh]_2$ (Ln =

Nd, Gd) (Fig. 21). $[(^tBu–C_5H_4)_2LnCH_3]_2$ (Ln = Nd, Gd) react with PhC≡CH to form the dimeric alkynide–bridged complexes $[(^tBu–C_5H_4)_2LnC{\equiv}CPh]_2$. Both compounds crystallized from toluene in the monoclinic space group C2/*c*. The two complexes are homologous, composed of asymmetric metal–alkynide bridges with Nd–C, Gd–C(alkynide) bond lengths of 2.602(4), 2.641(5) (Nd) and 2.532(6), 2.601(7) Å (Gd), respectively. The average Nd–C(ring) and Gd–C(ring) distances are 2.746(13) and 2.703(19) Å.

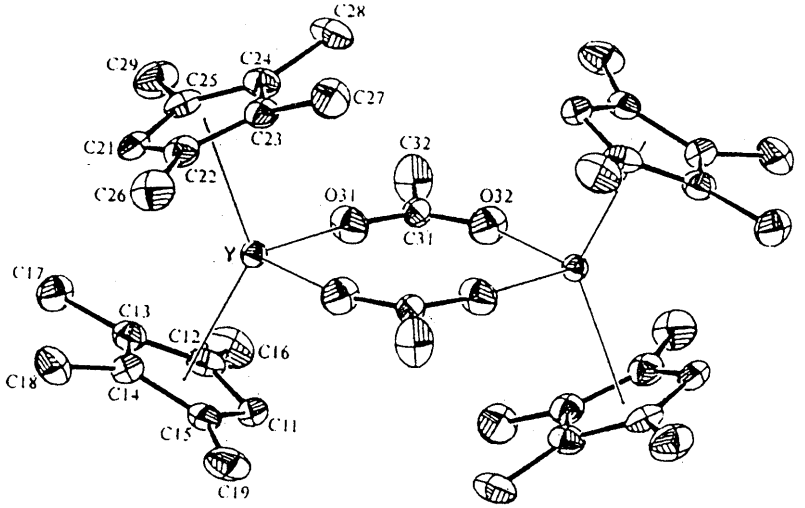

Fig. 18. Structure of $[(C_5HMe_4)_2Y(\mu\text{-}O_2CMe)]_2$.

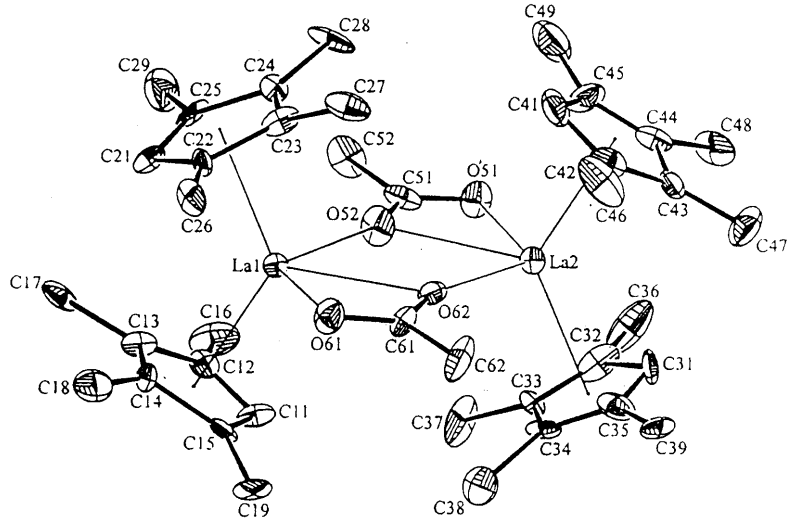

Fig. 19. Structure of $[(C_5HMe_4)_2La(\mu\text{-}O_2CMe)]_2$.

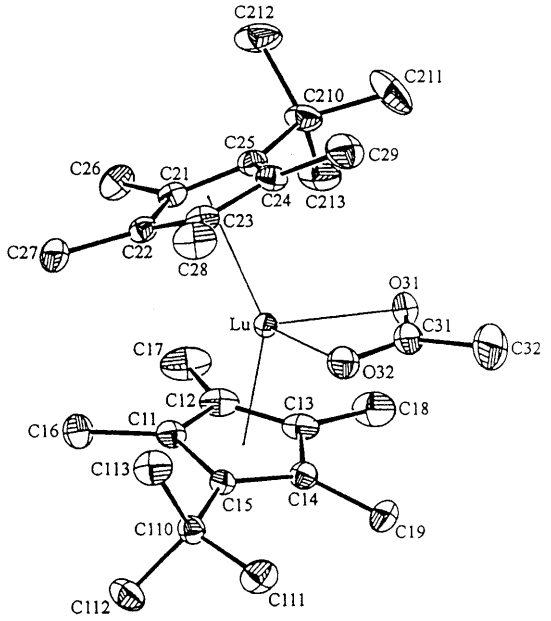

Fig. 20. ORTEP drawing of $[(C_5Me_4^tBu)_2LuO_2CCH_3]$.

Rogers [27] reported the crystal and molecular structure of $[\eta^5\text{-}C_5H_3(SiMe_3)_2]_2$-Yb(THF) (Fig. 22). The compound crystallizes in the orthorhombic space group Pbcn with $a = 11.345(4)$, $b = 13.552(4)$, $c = 21.185(6)$ Å, and $D_{calc.} = 1.354$ mg m^{-3} for $Z = 4$. The Yb and O atoms reside on a crystallographic two-fold axis. The formally seven-coordinate Yb(II) ion is symmetrically coordinated to the $[C_5H_3(SiMe_3)_2]$ ligands with an average Yb–C bond length of 2.67(2) Å. The Yb–O bond length and the centroid–Yb–centroid angle are 2.34(1) Å and 136°, respectively.

Tilley et al. [28] published the syntheses of neutral lanthanide silyl complexes via σ-bond metathesis reactions. The alkyl complexes $(C_5Me_5)_2LnCH(SiMe_3)_2$ (Ln = Sm, Nd, Y) and $(C_5Me_4Et)_2LnCH(SiMe_3)_2$ (Ln = Sm, Nd) react with neat $H_2Si(SiMe_3)_2$ (ca. 5 equivalents) at 85°C to give the new silyl complexes $(C_5Me_5)_2LnSiH(SiMe_3)_2$ (Ln = Sm, Nd, Y) and $(C_5Me_4Et)_2LnSiH(SiMe_3)_2$ (Ln = Sm, Nd). These neutral silyl complexes have been characterized, and are monomeric in pentane solution at room temperature. The structure of $(C_5Me_5)_2SmSiH(SiMe_3)_2$ (Fig. 23) reveals that this compound forms dimers in the solid state via intramolecular Sm···CH_3–Si interactions. The Sm–Si bond length in $(C_5Me_5)_2LnSiH(SiMe_3)_2$ is 3.052(8) Å. Initial reactivity studies characterize the Ln–Si bonds as being highly reactive.

Thiele et al. [29] reported the synthesis, properties and X-ray crystal structure of bis(decamethyllanthanocene)-anthracene. $[(C_5Me_5)_2La]_2[\mu\text{-}\eta^3\text{:}\eta^3\text{-}C_{14}H_{10})]\cdot 2C_6H_5$-$CH_3$ was obtained by reaction of $[(C_5Me_5)_2La(\mu\text{-}Cl)_2K(dme)_2]$ with disodiumanthracenide $[Na_2(C_{14}H_{10})]$ in toluene in the molar ratio 2:1.

$$2[(C_5Me_5)_2La(\mu\text{-}Cl)_2K(DME)_2] + [Na_2(C_{14}H_{10})] \xrightarrow{\text{toluene}} [(C_5Me_5)_2La]_2[\mu\text{-}\eta^3\text{:}\eta^3\text{-}C_{14}H_{10})]\cdot 2C_6H_5CH_3 + 2\ NaCl + 2\ KCl + 2\ DME \qquad \text{black–green crystals}$$

The title compound was characterized by elemental analyses, ^{1}H- and ^{13}C NMR spectroscopy as well as X-ray crystal structure determination. $[(C_5Me_5)_2La]_2[\mu\text{-}\eta^3\text{:}\eta^3\text{-}C_{14}H_{10})]\cdot 2C_6H_5CH_3$ (Fig. 24) crystallizes in the triclinic space group $P\bar{1}$ with $Z = 1$, $a = 10.471(2)$, $b = 11.234(2)$, $c = 11.382(3)$ Å, and $\alpha = 81.22(2)$, $\beta = 86.36(2)$, $\gamma = 77.36(2)°$, $V = 1291.8(5)$ Å^3. The molecule contains two $(C_5Me_5)_2$ La moieties which are η^3-coordinated to two of the aromatic rings from opposite sides of the anthracene ligand.

Huang et al. [30] described the synthesis and crystal structure of binuclear biscyclopentadienyl ytterbium *n*-propyl thiolate $[(C_5H_5)_2Yb(\mu\text{-}SCH_2CH_2CH_3)]_2$. The reaction of Cp_3Yb ($Cp = C_5H_5$) with equimolar *n*-propanethiol in THF at room temperature resulted in the formation of the new complex $[Cp_2Yb(\mu\text{-}SCH_2CH_2CH_3)]_2$ in good yield (Fig. 25), which was characterized by elemental analysis and mass spectra, and studies by X-ray crystallography. The title complex crystallized from the saturated THF solution in dimeric form with thiolate ligands as bridging groups. The bridging unit Yb_2S_2 is planar. The ytterbium atom was coordinated by two Cp groups and two bridging sulfur atoms to form a distorted

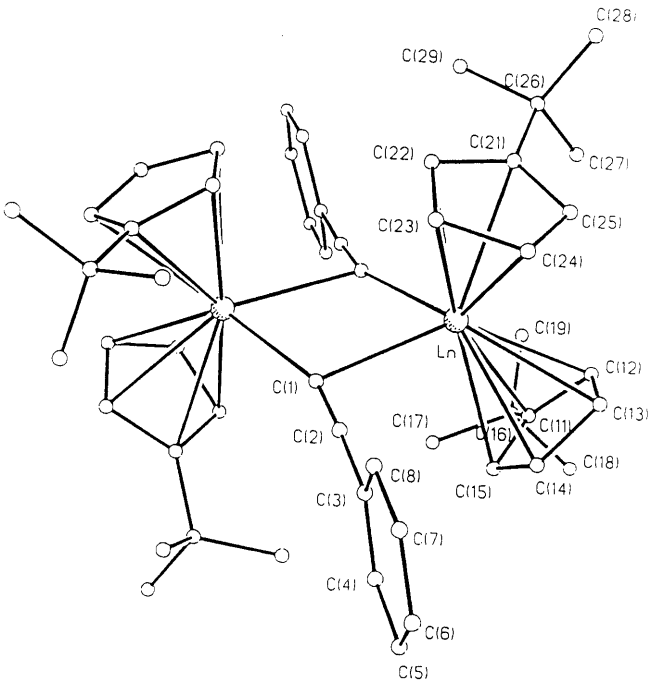

Fig. 21. Structure of $[(^t\text{Bu–}C_5H_4)_2LnC{\equiv}CPh]_2$.

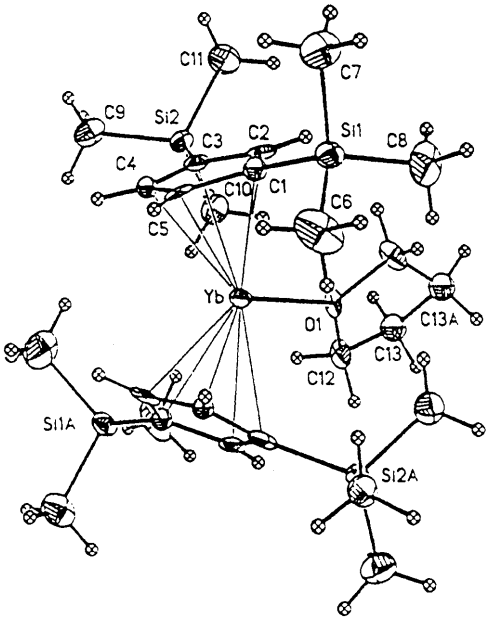

Fig. 22. Structure of $[\eta^5\text{-}C_5H_3(SiMe_3)_2]_2Yb(THF)$.

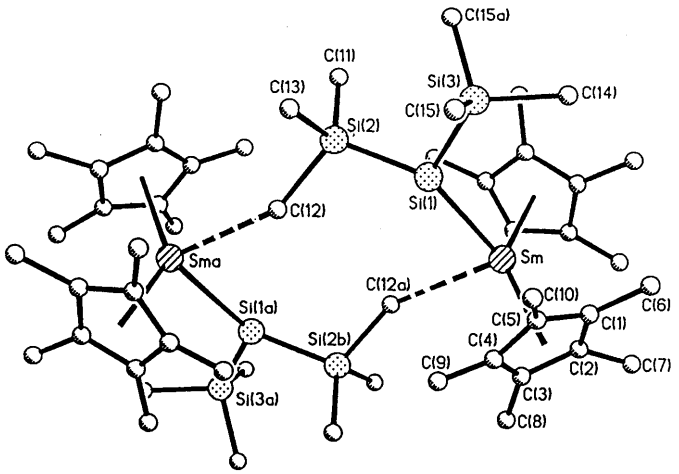

Fig. 23. Structure of $(C_5Me_5)_2SmSiH(SiMe_3)_2$.

tetrahedral geometry. The Yb–C(Cp) distances range from 2.48(2) to 2.71(2) Å, averaging 2.60(2) Å. The Yb–S bond lengths range from 2.69(7) to 2.71(8) Å, averaging 2.705(8) Å.

Molander et al. [31] published the synthesis and molecular structures of donor-functionalized chiral cyclopentadienyl complexes of calcium, samarium(II), and

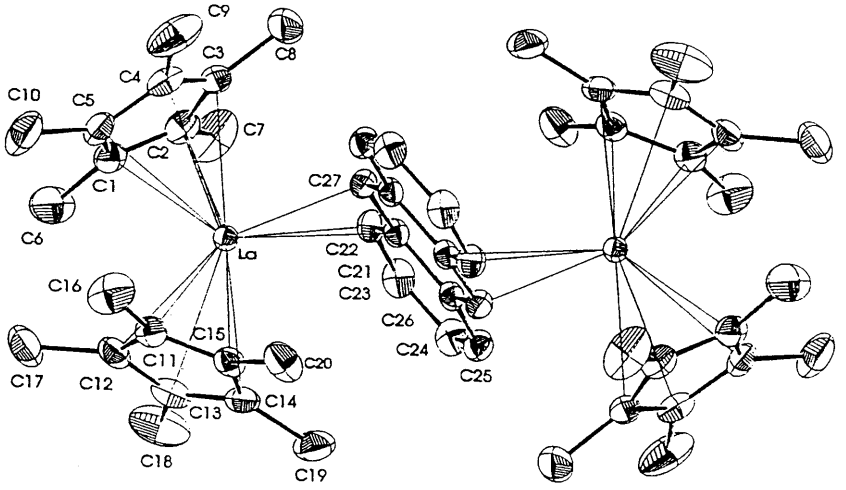

Fig. 24. Structure of $[(C_5Me_5)_2La]_2[\mu\text{-}\eta^3\text{:}\eta^3\text{-}C_{14}H_{10})]\cdot 2C_6H_5CH_3$.

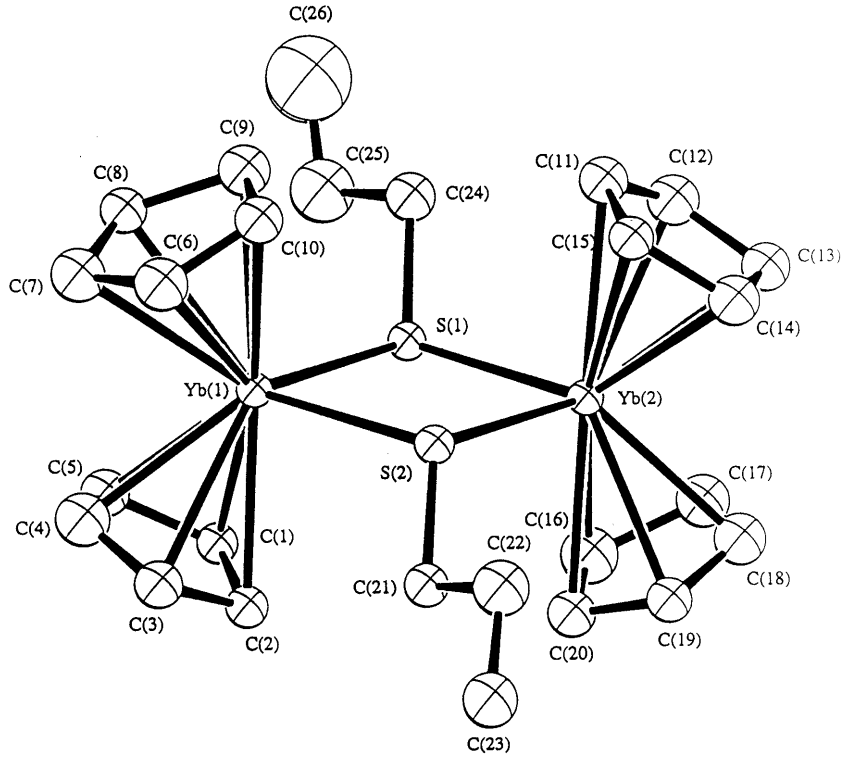

Fig. 25. Molecular structure of $[Cp_2Yb(\mu\text{-}SCH_2CH_2CH_3)]_2$ (the hydrogen atoms are omitted for clarity).

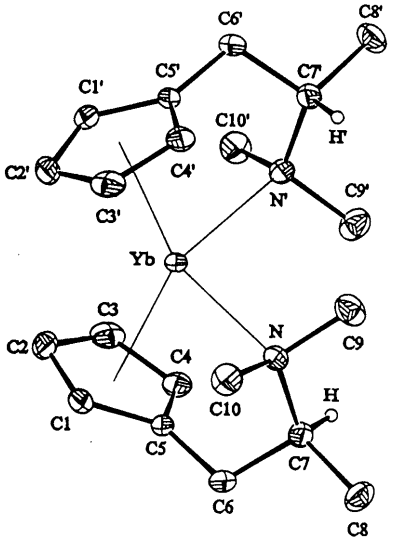

Fig. 26. Molecular structure of $[Yb\{(S)\text{-}\eta^5\text{:}\eta^1\text{-}C_5H_4CH_2CH(Me)NMe_2\}_2]$. For clarity, all hydrogens except those on the chiral center are omitted.

ytterbium(II) as new class of chiral metallocenes. Twelve optically active metallocene complexes of Ca, Sm(II), and Yb(II) containing cyclopentadienyl systems with a chiral N- or O-substituted side chain as ligands have been described. Specifically, the ligand systems (S)–(2-methoxy–2-propyl)cyclopentadienyl $\{(S)\text{–}C_5H_4\text{–}CH_2CH(Me)OMe\}$, (S)–(2-methoxy-2-phenylethyl)cyclopentadienyl $\{(S)\text{–}C_5H_4CH_2CH(Ph)OMe\}$, and the novel (S)-[2-(dimethylamino)propyl]cyclopentadienyl $\{(S)\text{–}C_5H_4CH_2CH(Me)NMe_2\}$ and (S)–[2-(dimethylamino)-1-phenylethyl]cyclopentadienyl $\{(S)\text{–}C_5H_4CH(Ph)CH_2NMe_2\}$ systems were employed. The starting materials for their synthesis are ethyl (S)-(−)-lactate, (R)-(−)-2-methoxy-2-phenylethanol, (S)-(+)-2-amino-1-propanol, and (R)-(−)-2-phenylglycinol, respectively. Each of the cyclopentadienyl systems was converted by a 2:1 reaction of the potassium salt with the metal diiodide into the corresponding metallocene. The novel compounds have been characterized by C, H, N analysis, mass spectrometry, NMR spectroscopy, and optical rotation. Additionally, X-ray structural analyses of $[Yb\{(S)\text{-}\eta^5\text{:}\eta^1\text{-}C_5H_4CH_2CH(Me)NMe_2\}_2]$, $[Ca\{(S)\text{-}\eta^5\text{:}\eta^1\text{-}C_5H_4CH_2CH(Ph)OMe\}_2]$ and $[Ca\{(S)\text{-}\eta^5\text{:}\eta^1\text{-}C_5H_4CH(Ph)CH_2NMe_2\}_2]$ were performed (Fig. 26).

Buchwald et al. [32] reported the carbon–hydrogen bond activation of aromatic imines by $[(C_5Me_5)_2SmH]_2$. Aromatic imines react with $[(C_5Me_5)_2SmH]_2$ via *ortho*-metalation, rather than the anticipated 1,2-insertion of the imine into the Sm–H bond to form an amide complex. The facile conversion to the *ortho*-metalated complex (Scheme 2) was observed when the reaction between $[(C_5Me_5)_2SmH]_2$ was followed by ^{1}H-NMR spectroscopy.

The $(C_5Me_5)_2Sm$(2-phenyl-1-pyrroline) complex was characterized spectroscopically and by single crystal X-ray diffraction. The *ortho*-metalation pathway is not

limited to cyclic imines. This reaction also occurs with acyclic imines, halogen-containing ketimine substrates, and aldimines.

Lawless et al. [33] studied a series of ytterbium(II) cyclopentadienyl derivatives by high-resolution solid-state ^{171}Yb CP MAS (cross-polarisation magic angle spinning) NMR spectroscopy; the principal components of the chemical shift tensors have been determined from spinning sideband analysis. Examining the ^{171}Yb NMR data reveals that: (i) with the exception of $[Yb(C_5Me_5)_2(py)_2]$, the isotropic chemical shifts are in general in good agreement with the solution data thereby providing strong support for the retention of very similar structures in solution; (ii) the addition of the O-centred Lewis base to $[Yb(C_5Me_5)_2]$ (which exhibits two magnetically inequivalent Yb atoms within the unit cell) results in a high frequency shift of some 40–60 ppm; (iii) the difference between solid- and solution-state ^{171}Yb NMR chemical shifts for $[Yb(C_5Me_5)_2(py)_2]$, some 160 ppm, is too large to be explained by magnetic susceptibility changes alone. This high frequency shift is supposedly due to a solution equilibrium between the bis- and tris-pyridine adducts. Support for this conclusion also derives from the large temperature dependence of the ^{171}Yb resonance displayed by pyridine solutions of $[Yb(C_5Me_5)_2]$.

Jin et al. [34] described the synthesis and crystal structure of bis[bis(cyclopentylcyclopentadienyl)methylerbium] $[(C_5H_9C_5H_4)_2ErCH_3]_2$. The reaction of $(C_5H_9C_5H_4)_2ErCl$ with $LiCH_3$ in Et_2O/THF at room temperature gave $[(C_5H_9C_5H_4)_2ErCH_3]_2$, which was extracted with toluene several times to remove LiCl. To the extract was added a certain amount of hexane and then the solution was placed in a refrigerator for crystallisation. A pink single crystal was selected for X-ray analysis. The structure analysis shows that the title complex is a dimer. Two cyclopentylcyclopentadienyl- and two methyl groups are bonded to Er^{3+} forming a tetrahedral coordination geometry. Each cyclopentyl group in $[(C_5H_9C_5H_4)_2ErCH_3]_2$ has two conformations and the two cyclopentyl substituents in the cyclopentylcyclopentadienyls on the same erbium atom are located on the opposite sides.

Deacon et al. [35] described the synthesis, characterization and properties of new lanthanoid(III) complexes with pyrazolate ligands. The tris(pyrazolate) complexes $Ln(Ph_2pz)_3(THF)_n$ (Ph_2pz = 3,5-diphenylpyrazolate; Ln = Sc, Y, Gd, Er) contain just N–Ln bonds whereas the complexes $(C_5Me_5)_2Ln(Me_2pz)(THF)_n$ (Ln = Y, Lu;

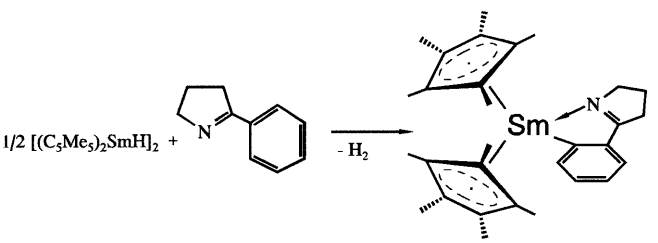

Scheme 2. Carbon–hydrogen bond activation of aromatic imines by $[(C_5Me_5)_2SmH]_2$.

pz = pyrazolate, Mepz = 3-methylpyrazolate, Me_2pz = 3,5-dimethylpyrazolate), $(C_5Me_5)_2Y(pz)(THF)$, $(C_5Me_5)_2Y(Mepz)(THF)$, $(C_5Me_5)_2Y(Me_2pz)(THF)_2$ have also η^5-bonded cyclopentadienyl ligands. These compounds were synthesized through reactions of the corresponding $(C_5H_5)_2LnCl$ derivatives and sodium pyrazolates.

$$(C_5H_5)_2LnCl + Na(Me_2pz) \xrightarrow{THF} (C_5H_5)_2Ln(Me_2pz) + NaCl$$

Lappert et al. [36] published the synthesis and structures of $[K(18\text{-crown-6})][Ln\{\eta^5\text{-}C_5H_3(SiMe_3)_2\text{-}1,3\}_2(C_6H_6)]$ (Ln = La, Ce), the first metal complexes containing the 1,4-cyclohexa-2,5-dienyl ligand (benzene 1,4-dianion). Treatment of $[Ln\{\eta^5\text{-}C_5H_3(SiMe_3)_2\text{-}1,3\}_3]$ or $[(Ln\{\eta^5\text{-}C_5H_3(SiMe_3)_2\text{-}1,3\}_2(\mu\text{-}Cl))_2]$ with a potassium mirror or C_8K and 18-crown-6 in benzene under mild conditions afforded the tight ion pairs $[K(18\text{-crown-6})][Ln\{\eta^5\text{-}C_5H_3(SiMe_3)_2\text{-}1,3\}_2(C_6H_6)]$ (Ln = La, Ce) containing the remarkable anions $[Ln\{\eta^5\text{-}C_5H_3(SiMe_3)_2\text{-}1,3\}_2(C_6H_6)]^-$, which in principle can be regarded as either (benzene)lanthanocenate(II) or (1,4-cyclohexa-2,5-dienyl)-lanthanocenate(III) anions. The latter representation is the more appropriate in the light of X-ray crystallographic and UV-vis and NMR spectral data, as well as with respect to their hydrolysis products which included (GCMS) cyclohexa-1,4-diene and a smaller proportion of benzene. The X-ray structure of $[K(18\text{-crown-6})][La\{\eta^5\text{-}C_5H_3(SiMe_3)_2\text{-}1,3\}_2(C_6H_6)]$ is illustrated in Fig. 27. The cerium complex displays an isomorphous structure.

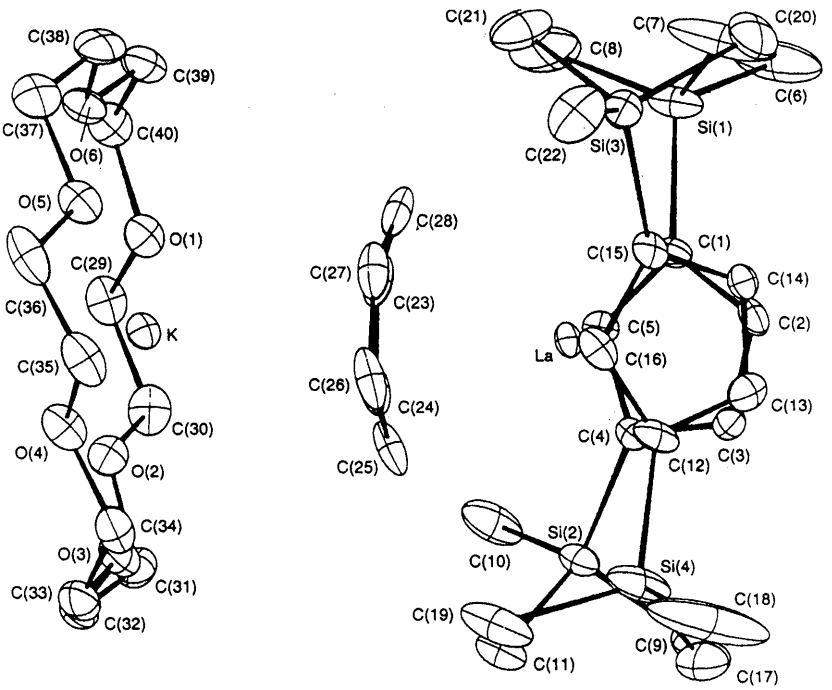

Fig. 27. Structure of $[K(18\text{-crown-6})][La\{\eta^5\text{-}C_5H_3(SiMe_3)_2\text{-}1,3\}_2(C_6H_6)]$.

Schumann et al. [37] described the synthesis and characterisation of cationic metallocene complexes of the lanthanides. These cationic organolanthanide compounds $[(C_5H_4R)_2Sm(THF)_2][BPh_4]$ ($R = {}^tBu$, $SiMe_3$), $[Pyr^*_2Sm(THF)][BPh_4]$ ($Pyr^* = NC_4H^t_2Bu_2$-2,5), $[(C_5Me_5)_2Ln(THF)_2][BPh_4]$ (Ln = Y, Yb), and $[(C_5Me_4Et)_2Ln(THF)_2][BPh_4]$ (Ln = Sm, Y) have been synthesized by oxidation of the divalent metallocenes $[(C_5H_4R)_2Sm(THF)_2]$, $[Pyr^*_2Sm(THF)]$, $[(C_5Me_5)_2Yb(THF)]$, and $[(C_5Me_4Et)_2Sm(THF)]$ with $Ag[BPh_4]$ and by protolysis of the lanthanide alkyls $[(C_5Me_5)_2LnMe(THF)]$, $[(C_5Me_5)_2YbCH(SiMe_3)_2]$, and $[(C_5Me_4Et)_2LnCH(SiMe_3)_2]$ (Ln Y, Sm) by $[NEt_3H][BPh_4]$. The ^1H- and ^{13}C-NMR spectra of the new compounds were discussed, $[(C_5Me_5)_2Yb(THF)_2][BPh_4]$ was characterized by X-ray crystal structure analyses (Fig. 28).

$$[(C_5H_4R)_2Sm(THF)_2] + Ag[BPh_4] \xrightarrow[-Ag]{THF,\ 20°C} [(C_5H_4R)_2Sm(THF)_2][BPh_4]$$

where $R = {}^tBu$, $SiMe_3$.

$$[(C_5Me_4R)_2LnR'(THF)_2] + [HNEt_3][BPh_4] \xrightarrow{THF,\ 20°C} R'H + NEt_3 + [(C_5Me_4R)_2Ln(THF)_2][BPh_4]$$

where R = Me, Et; Ln = Y, Yb, Sm and R′ = Me, $CH(SiMe_3)_2$

Wu et al. [38] described the preparation and X-ray crystallographic characterization of $[(\eta^5\text{-}CH_3C_5H_4)_2Tb(\mu\text{-}Cl)(THF)]_2$. The compound crystallized in the orthorhombic space group Pbcn with $a = 20.414(2)$, $b = 9.548(1)$, $c = 16.390(6)$ Å; $Z = 4$, $d_c = 1.77$; $R = 0.032$, $Rw = 0.044$ for 1915 reflections. The Tb^{3+} ion is coordinated by two $CH_3C_5H_4$ groups, two chloride ions and one O atom from THF to form a distorted trigonal bipyramidal geometry. Two bridging Tb–Cl bond lengths are 2.716(2) and 2.709(2) Å, respectively. The Tb–O (THF) and Tb–C ($CH_3C_5H_4$) bond length are 2.559(6) and 2.670(4) Å, respectively.

Wong and Lin [39] published the synthesis and structural characterization of Cp-functionalized organolanthanide complexes $[(\eta^5\text{-}C_5H_4PPh_2)_2Ln(diglyme)]$ (Ln =

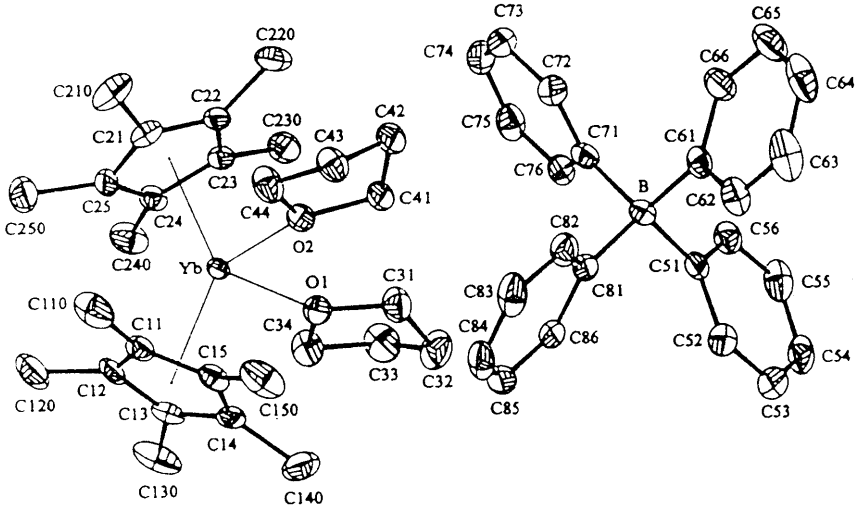

Fig. 28. Structure of $[(C_5Me_5)_2Yb(THF)_2][BPh_4]$.

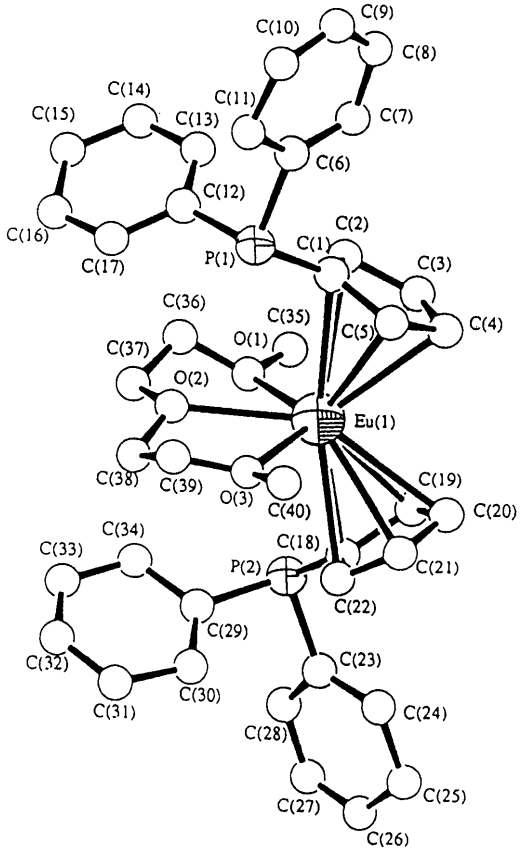

Fig. 29. Molecular structure of $[(\eta^5\text{-}C_5H_4PPh_2)_2Eu(diglyme)]$.

Eu, Yb, diglyme) = diethyleneglycoldimethylether). The reaction of [(diphenylphosphino)cyclopentadienyl]thallium $[Tl(C_5H_4PPh_2)]$ with metallic europium or ytterbium powder in THF at 60°C in the presence of metallic mercury, followed by crystallization from a mixture of dimethoxyethane and diethyleneglycoldimethylether (diglyme) (10: 1), afforded $[(\eta^5\text{-}C_5H_4PPh_2)_2Eu(diglyme)]$ and $[(\eta^5\text{-}C_5H_4\text{-}PPh_2)_2Yb(diglyme)]$ respectively.

$$2[Tl(C_5H_4PPh_2)] + Ln \xrightarrow[2.\ DME/diglyme\ (10:1)]{1.\ THF,\ 60°C\ [Hg]} [(\eta^5\text{-}C_5H_4PPh_2)_2Ln(diglyme)] + 2Tl$$

Crystal and molecular structures of both complexes have been determined by X-ray crystallography. The molecular structure of $[(\eta^5\text{-}C_5H_4PPh_2)_2Eu(diglyme)]$ is shown in Fig. 29.

Wong et al. [40] synthesized and characterized $[(\eta^5\text{-}C_5H_4'Bu)_2Yb(Cl)CH_2P\text{-}(Me)Ph_2]$. The interaction of $[(\eta^5\text{-}C_5H_4'Bu)_2YbCl{\cdot}LiCl]$ with one equivalent of $Li[(CH_2)(CH_2)PPh_2]$ in tetrahydrofuran at room temperature for 16 h, work up gave white crystals of stoichiometry $[Ph_2PMe_2][(C_5H_4'Bu)_2Li]$ and yellow crystals of

the stoichiometry $[(C_5H_4^tBu)_2Yb(Cl)CH_2P(Me)Ph_2]$ in 10% and 30% yields, respectively, after successive recrystallization from a THF/toluene mixture. Both compounds have been fully characterized by analytical, spectroscopic and X-ray diffraction methods. The molecular structure of $[(C_5H_4^tBu)_2Yb(Cl)CH_2P(Me)Ph_2]$ is shown in Fig. 30 and can be described as a distorted tetrahedron if one considers that the metal is coordinated to the centroid of the *tert*-butylcyclopentadienyl rings.

The *tert*-butylcyclopentadienyl rings are bonded to the Yb atom in a η^5-fashion with Yb–C(ring) distances ranging from 2.57(3) to 2.86(3) Å. The Yb–C(ylide) distance is 2.51(3) Å. The P–C(19) distance of 1.71(2) Å is within the range of a P = C double bond distance (1.665 Å) and a P–C single bond distance (1.872 Å).

Ren et al. [41] described the synthesis and structure of $[(C_5H_4{}^tBu)_2Er(\mu\text{-}Cl)]_2$. The title compound was prepared from $[C_5H_4{}^tBuNa]$ and $ErCl_3$ in THF and characterized by X-ray crystallography. The molecular structure shows that the compound is a dimer in which the two $(C_5H_4{}^tBu)_2Er$ units are connected by two bridging chlorine atoms. The erbium atom is coordinated by two $C_5H_4{}^tBu$ groups and two chlorine atoms to form a distorted tetrahedron.

Mandel and Magull [16] published new benzyl complexes and studied the synthesis and crystal structures of $[(C_5Me_5)_2Y(CH_2C_6H_5)(THF)]$, $[(C_5Me_5)_2Sm(CH_2C_6H_5)_2K(THF)_2]_\infty$, and $[(C_5Me_5)Gd(CH_2C_6H_5)_2(THF)]$. These compounds were synthesized according to the equations.

$$YBr_3 + 2K(C_5Me_5) + KCH_2C_6H_5 \xrightarrow{THF} [(C_5Me_5)_2Y(CH_2C_6H_5)(THF)] + 3KBr \quad \text{(yield: 29\%)}$$

$$SmBr_3 + K(C_5Me_5) + 2KCH_2C_6H_5 \xrightarrow{THF} [(C_5Me_5)_2Sm(CH_2C_6H_5)_2K(THF)_2]_\infty + 2KBr \quad \text{(yield: 54\%)}$$

$$GdBr_3 + K(C_5Me_5) + 2KCH_2C_6H_5 \xrightarrow{THF} [(C_5Me_5)Gd(CH_2C_6H_5)_2(THF)] + 2KBr \quad \text{(yield: 64\%)}$$

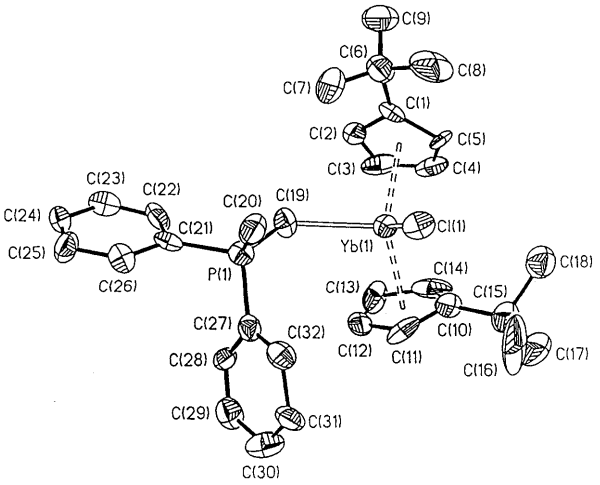

Fig. 30. Molecular structure of $[(C_5H_4^tBu)_2Yb(Cl)CH_2P(Me)Ph_2]$.

$[K(C_5Me_5)]$ and $[KCH_2C_6H_5]$ were allowed to react in different ratios with $LnBr_3$. The gadolinium complex $[(C_5Me_5)Gd(CH_2C_6H_5)_2(THF)]$ as a mono(cyclopentadienyl) compound has been discussed in Section 2.2.1. The structures of the new benzyl complexes were determined by X-ray single crystal structure analysis. The structure of $[(C_5Me_5)_2Y(CH_2C_6H_5)(THF)]$ is unexceptional for bis(cyclopentadienyl) compounds of the rare earth metals. Fig. 31 shows the polymeric structure of $[(C_5Me_5)_2Sm(CH_2C_6H_5)_2K(THF)_2]_\infty$. The polymer chain is formed by η^6-coordination of the $K(THF)_2$-fragment with two benzyl ligands of different $(C_5Me_5)_2Sm(CH_2C_6H_5)_2$ units. The C_5Me_5(centroid)–Sm bond length is 250 pm whereas the C_6H_5(centroid)–K distance is determined with 288–290 pm.

Tilley et al. [42] reported the samarium-mediated redistribution of silanes and formation of trinuclear samarium–silicon clusters. Reaction of $(C_5Me_5)_2SmCH(SiMe_3)_2$ with $PhSiH_3$ (1 equiv.) in D_6-benzene occurs rapidly after a variable induction time (5–20 min) to produce a deep red solution. By ^{1}H-NMR spectroscopy, this reaction gives a quantitative yield of $CH_2(SiMe_3)_2$, along with H_2 (26%), $PhSiH_2$–SiH_2Ph (11%), Ph_2SiH_2 (46%), and Ph_3SiH (trace). Quantitative transfer of the deuterium label from $PhSiD_3$ to the alkyl group [to produce $CHD(SiMe_3)_2$] implies that the first step in the reaction is the formation of $(C_5Me_5)_2SmSiH_2Ph$, but this species has not been identified as an intermediate. In contrast, $(C_5Me_5)_2SmCH(SiMe_3)_2$ reacts slowly with Ph_2SiH_2 via redistribution at silicon, to give $PhSiH_3$ (10% after 2 days) and unidentified silicon-containing compounds, but no $PhSiH_3$ or Ph_2HSi–$SiHPh_2$. Crystals from such reactions over 2 days contain the cluster $[\{(C_5Me_5)_2Sm\}_3(\mu\text{-}SiH_3)(\mu^3\text{-}\eta^1,\eta^1,\eta^2\text{-}SiH_2SiH_2)]$ shown in Fig. 32. This cluster possesses a planar Sm_3Si_3 core and lies on a crystallographic twofold axis that passes through Sm(1)–Si(1) and Si(2). The Sm–Si distances in this molecule [Sm(1)–Si(1) 3.174(4), Sm(2)–Si(1) 3.093(4), Sm(2)–Si(2) 2.954(2) Å] are similar to the corresponding distance of 3.052(8) Å in $[(C_5Me_5)_2SmSiH(SiMe_3)_2]_2$. As described above the reaction of $(C_5Me_5)_2SmCH(SiMe_3)_2$ with $PhSiH_3$ is rather complex, and produces a number of soluble silane products. Two other cluster compounds were also identified by X-ray structure analysis.

Huang et al. [43] described the syntheses and thermal stability of binuclear bis(cyclopentadienyl) lanthanide thiolates. The trivalent lanthanide metallocenes $[(C_5H_5)_3Ln]$ (Ln = Dy, Yb) react with thiols, HSR ($R = CH_2CH_2CH_3$ or $CH_2CH_2CH_2CH_3$) to give the dimeric complexes $[(C_5H_5)_2Ln(\mu\text{-}SR)]_2$ in THF at room temperature. They have been characterized by elemental analysis and mass spectroscopy or ^{1}H NMR spectra, indicating that they are dimers bridged through the sulfur atoms of the thiolate ligands. Crystals of $[(C_5H_5)_2Yb(\mu\text{-}SCH_2CH_2CH_2CH_3)]_2$ are monoclinic, space group $P2_1/a$ with $a = 8.928(3)$, $b = 17.620(7)$ and $c = 9.208(4)$ Å, $\beta = 103.94(3)°$, $V = 1405.8(9)$ Å^3, $Z = 2$ and $D_c = 1.85$ g cm^{-3}. The molecular structure of $[(C_5H_5)_2Yb(\mu\text{-}SCH_2CH_2CH_2CH_3)]_2$ (Fig. 33) shows a planar Yb_2S_2 unit. The geometry around the ytterbium atom is pseudotetrahedral although the geometry is pyramidal at sulfur so that the *n*-butyl groups are *anti* relative to the Yb_2S_2 ring. The average Yb–C(Cp) and Yb–S bond distances are 2.59(1) and 2.708(3) Å, respectively. It was found that these complexes are thermally unstable and tend to decompose to form $(C_5H_5)_3Ln$ species upon heating.

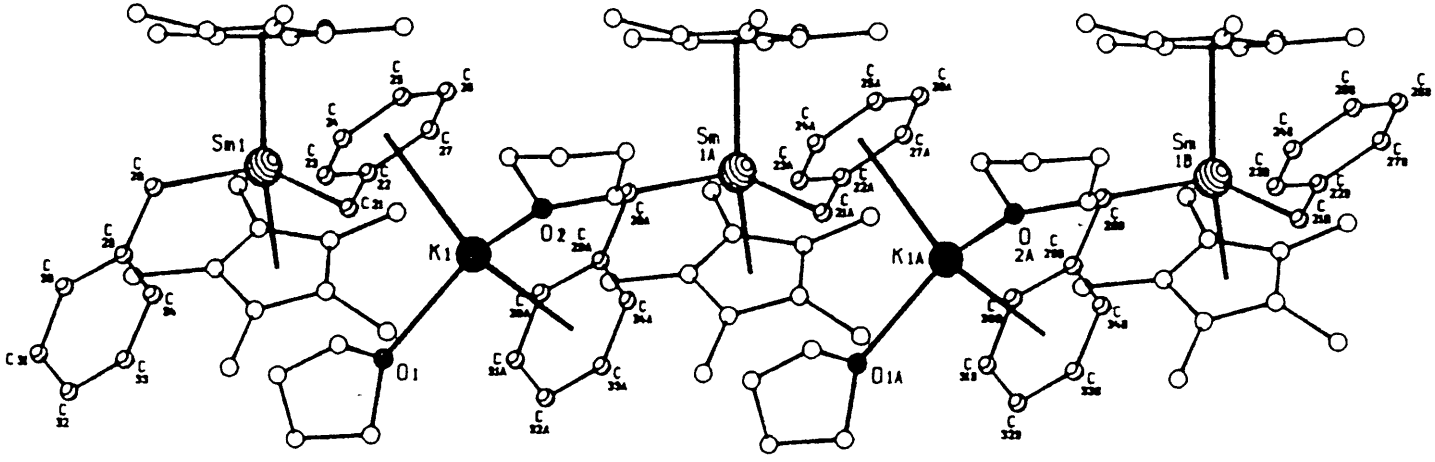

Fig. 31. Section of the polymeric structure of $[(C_5Me_5)_2Sm(CH_2C_6H_5)_2K(THF)_2]_\infty$.

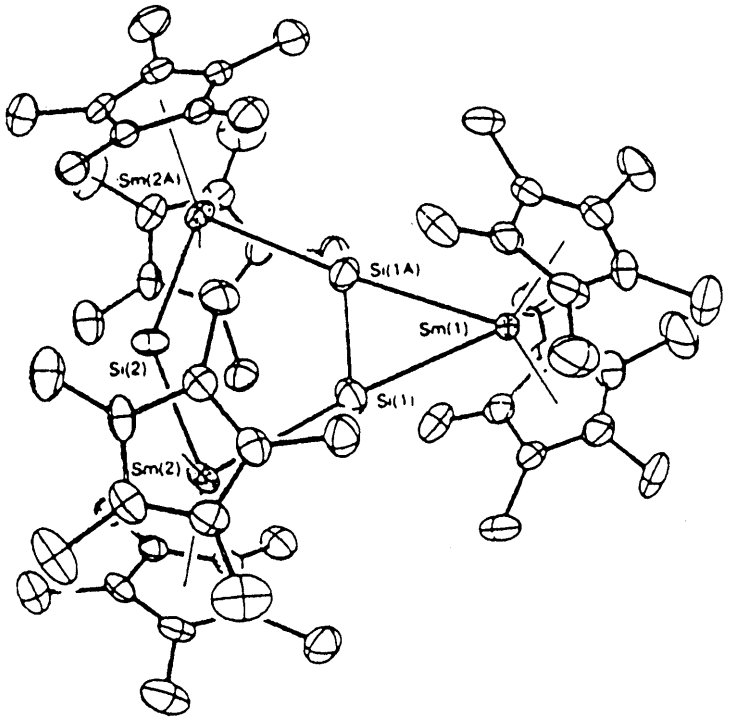

Fig. 32. Molecular structure of $[\{(C_5Me_5)_2Sm\}_3(\mu\text{-}SiH_3)(\mu^3\text{-}\eta^1,\eta^1,\eta^2\text{-}SiH_2SiH_2)]$.

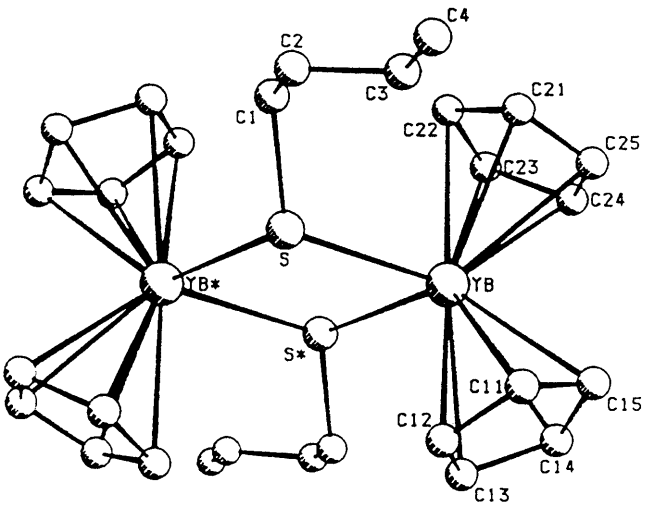

Fig. 33. Molecular structure of $[(C_5H_5)_2Yb(\mu\text{-}SCH_2CH_2CH_2CH_3)]_2$.

Rabe and Sebald [44] published the introduction of ^{171}Yb solid state NMR cross polarisation/magic-angle spinning (CP/MAS) spectroscopy as a new analytical tool for the investigation and structural characterisation of divalent ytterbium complexes. The authors described a convenient procedure to optimize the experimental set-up for ^{171} Yb NMR CP/MAS. The measured isotropic chemical shifts δ ^{171}Yb are +28.5, +29.5 and +440.6 ppm for $(C_5Me_5)_2Yb(THF)\cdot 0.5$toluene, $(C_5Me_5)_2Yb(THF)_2$ and $Yb(PPh_2)_2(THF)_4$, respectively.

Bulychev et al. [45] described the synthesis and catalytic properties of bis(di-*t*-butylcyclopentadienyl)ytterbium(II). Polymeric $[(C_5H_5)_2Yb\cdot THF]_n$, the ionic *ate*-complex $(C_5H_5)_3YbNa$, and the mono-adduct $(^tBu_2C_5H_3)_2Yb\cdot THF$ were prepared through reactions of $(C_5H_5)Na$ or $^tBu_2C_5H_3Na$ with YbI_2 in THF. The $(^tBu_2C_5H_3)_2Yb\cdot THF$ shows catalytic activity in the homogeneous hydrogenation of hex-1-ene and in the polymerization of styrene.

Schwartz [46] investigated the weak interactions of $(C_5Me_5)_2Yb$ and *cis* dihydrido platinum complexes in solution using multinuclear NMR spectroscopy. $(C_5Me_5)_2Yb$ formed 1:1 adducts with the *cis* dihydrido complexes P_2PtH_2 [$P_2 = (c\text{-}C_6H_{11})_2P(CH_2)_2P(c\text{-}C_6H_{11})_2$, $(c\text{-}C_6H_{11})_2P(CH_2)_3P(c\text{-}C_6H_{11})_2$] that undergo slow intermolecular exchange at 25°C on the NMR timescale. There are significant perturbations in the spectral values from those of the free P_2PtH_2 complexes, and JYBX coupling (X = ^{1}H, ^{31}P, ^{195}Pt) is present. The interactions of $(C_5Me_5)_2Yb$ with $[(C_6H_5)_2P(CH_2)_2P(C_6H_5)_2]PtMe_2$ and $[(C_6H_5)_2P(CH_2)_2P(C_6H_5)_2]Pt(H)Me$ have also been investigated. The NMR spectral values of the adducts were discussed in detail, and correlated with the solid state structures.

Visseaux et al. [47] studied paramagnetic Nd–H species by NMR measurements. The new bis(cyclopentadienyl)neodymium triethylborohydrides $(C_5H_4CH_2CH_2OCH_3)_2NdHBEt_3$ and $(C_5H_4'Bu)_2NdHBEt_3\cdot n$THF were obtained by reaction of $NaHBEt_3$ with the corresponding chlorides.

$$[(C_5H_4CH_2CH_2OCH_3)_2NdCl]_2 \xrightarrow[-2NaCl]{2NaHBEt_3} 2(C_5H_4CH_2CH_2OCH_3)_2NdHBEt_3$$

$$(C_5H_4CH_2CH_2OCH_3)_2NdHBEt_3 \xrightarrow{O{=}CMe_2} (C_5H_4CH_2CH_2OCH_3)_2NdOCHMe_2$$

$$(C_5H_4CH_2CH_2OCH_3)_2NdHBEt_3 \xrightarrow{BH_3} (C_5H_4CH_2CH_2OCH_3)_2NdBH_4$$

$$(C_5H_4CH_2CH_2OCH_3)_2NdHBEt_3 \xrightarrow{RT,\ 2\ weeks} (C_5H_4CH_2CH_2OCH_3)_3Nd$$

The Nd–H NMR signals are found at 200 ppm ($w_{1/2} = 1000$ Hz). The reactivity of these moderately stable complexes is similar to that of the known dimeric cyclopentadienyllanthanide hydrides.

2.2.3. Ansa-cyclopentadienyl complexes

Bercaw et al. [48] reported the synthesis and structural characterization of $\{(\eta^5\text{-}C_5Me_4)_2SiMe_2\}YCH(SiMe_3)_2$, its hydrogenation to $[\{(\eta^5\text{-}C_5Me_4)_2SiMe_2\}Y]_2\text{-}(\mu_2\text{-}H)_2$ and facile ligand redistribution to $Y_2[\mu_2\text{-}\{(\eta^5\text{-}C_5Me_4)SiMe_2(\eta^5\text{-}C_5Me_4)\}]_2\text{-}(\mu_2\text{-}H)_2$. Alkylation of $[\{(\eta^5\text{-}C_5Me_4)_2SiMe_2\}Y]_2(\mu_2\text{-}Cl)_2Li(OEt_2)_2$ with $LiCH(SiMe_3)_2$ proceeds readily in toluene. Removal of the toluene in vacuo, followed by extrac-

tion of the product from LiCl with petroleum ether affords $\{(\eta^5\text{-}C_5Me_4)_2SiMe_2\}$-$YCH(SiMe_3)_2$ in moderate yields (Scheme 3).

The structure of $\{(\eta^5\text{-}C_5Me_4)_2SiMe_2\}YCH(SiMe_3)_2$ has been examined by single crystal X-ray diffraction methods (Fig. 34). The bis(trimethylsilyl)methyl ligand is distorted in the equatorial plane such that one of the methyl groups of the $[CH(SiMe_3)_2]$ bridges yttrium and a silicon in a 3-center, 2-electron bridging fashion. Hydrogenolysis of $\{(\eta^5\text{-}C_5Me_4)_2SiMe_2\}YCH(SiMe_3)_2$ results, initially, in the formation of the *ansa* yttrocene hydride dimer $[\{(\eta^5\text{-}C_5Me_4)_2SiMe_2\}Y]_2(\mu_2\text{-}H)_2$. This compound is unstable with respect to ligand redistribution affording the hydride- and $\{(\eta^5\text{-}C_5Me_4)_2SiMe_2\}$-bridged ('flyover') hydride dimer $Y_2[\mu_2\text{-}\{(\eta^5\text{-}C_5Me_4)SiMe_2(\eta^5\text{-}C_5Me_4)\}]_2(\mu_2\text{-}H)_2$.

Yasuda et al. [49] explored ethylene polymerization by using *racemic* $[(2\text{-}SiMe_3\text{-}4\text{-}{}^t BuC_5Me_2)_2SiMe_2]Sm(THF)_2$, *meso* type $[(3\text{-}{}^t BuC_5H_2)_2SiMe_2(SiMe_2OSiMe_2)]Sm(THF)_2$, and *C1*-symmetric $[(2,4\text{-}(SiMe_3)_2C_5H_2)(3,4\text{-}(SiMe_3)_2C_5H_2)SiMe_2]Sm(THF)_2$ in the absence of methylalumoxane. The complexes were prepared as purple crystals by reaction of the corresponding potassium salts of the cyclopentadienes with SmI_2

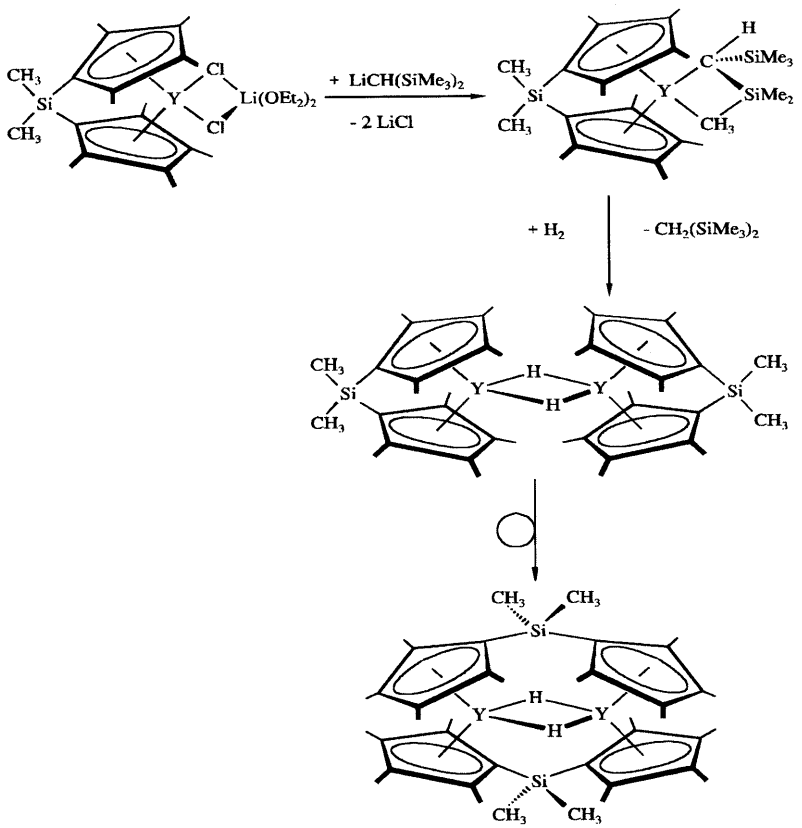

Scheme 3. Synthesis and hydrogenation of $\{(C_5Me_4)_2SiMe_2\}YCH(SiMe_3)_2$ and facile ligand redistribution of $[\{(C_5Me_4)_2SiMe_2\}Y]_2(\mu_2\text{-}H)_2$.

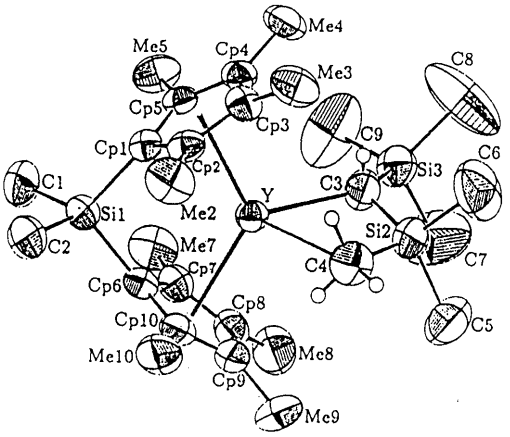

Fig. 34. Structure of $\{(\eta^5\text{-}C_5Me_4)_2SiMe_2\}YCH(SiMe_3)_2$.

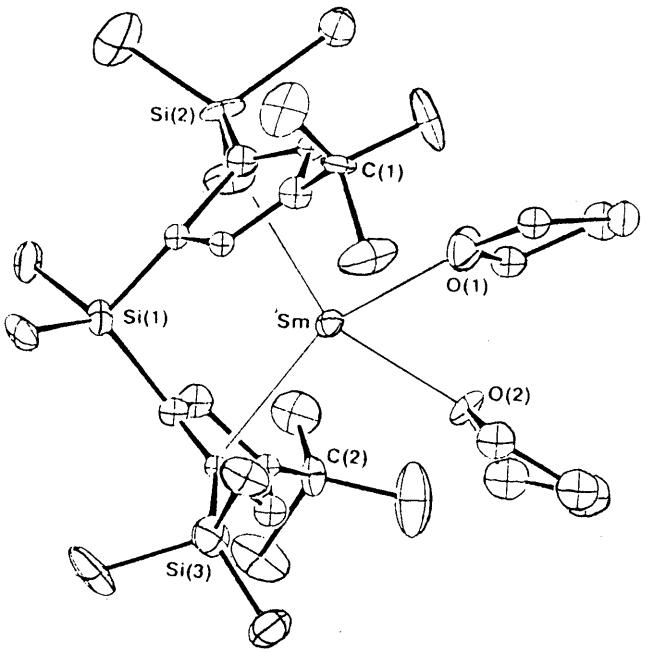

Fig. 35. Structure of *rac*-$[(2\text{-}SiMe_3\text{-}4\text{-}^tBuC_5Me_2)_2SiMe_2]Sm(THF)_2$.

in THF. Single crystal X-ray analysis of $[(2\text{-}SiMe_3\text{-}4\text{-}^tBuC_5Me_2)_2SiMe_2]Sm(THF)_2$ clearly reveals the *racemic* structure (Fig. 35). The Cp′(centroid)-Sm-Cp′(centroid) bite angle is 117.08 (4)°, 18.6° smaller than that of $(C_5Me_5)_2Sm(THF)_2$.

Qian et al. [50] described the syntheses of 1,1′-(3-oxa-pentamethylene)-dicyclopentadienyl divalent organolanthanides (Ln = Sm, Yb) and the X-ray molec-

ular structure of $[O(CH_2CH_2C_5H_4)_2Yb(DME)]$. The interaction of $LnCl_3$ (Ln = Sm, Yb) and 1,1′-(3-oxa-pentamethylene)dicyclopentadienyl disodium salt in THF provided the trivalent complexes $[O(CH_2CH_2C_5H_4)_2LnCl]$ (Ln = Sm, Yb). The chlorides were then reduced with sodium metal in THF at room temperature for 3 days, purple-black (Ln = Sm) and red-black (Ln = Yb) solutions were being formed, respectively. Following precipitation by the addition of *n*-hexane and drying in vacuum, new divalent organolanthanide complexes, i.e. the purple compound $[O(CH_2CH_2C_5H_4)_2Sm(THF)_2]$ and the red-orange compound $[O(CH_2CH_2C_5H_4)_2Yb(THF)_2]$, were obtained in good yield:

$$LnCl_3 + O(CH_2CH_2C_5H_4)_2Na_2 \xrightarrow[-2NaCl]{(THF)} O(CH_2CH_2C_5H_4)_2LnCl$$

$$O(CH_2CH_2C_5H_4)_2LnCl + Na \xrightarrow[-NaCl]{(THF)} O(CH_2CH_2C_5H_4)_2Ln(THF)_2$$

where Ln = Sm, Yb.

Another method was also used to synthesize the Sm compound. Thus, SmI_2 reacted with $O(CH_2CH_2C_5H_4)_2K_2$ in THF to give $[O(CH_2CH_2C_5H_4)_2Sm(THF)_2]$ in good yields. Both compounds are soluble in THF and DME, but insoluble in aromatic and aliphatic solvents. The Yb complex dissolves in DME to give a red-green solution. Recrystallization from DME gave red single crystals of $[O(CH_2CH_2C_5H_4)_2Yb(DME)]$. Fig. 36 shows the molecular structure of this compound.

2.2.4. Tris(cyclopentadienyl) complexes

Amberger et al. [51] published the electronic structure of Pr^{3+} in ψ-trigonal bipyramidal organic coordination. By doping a $(C_5H_5)_3La(NCCH_3)_2$ matrix with different amounts of Pr^{3+}, relatively stable $(C_5H_5)_3La_{1-x}Pr_x(NCCH_3)_2$ ($x = 0.6$,

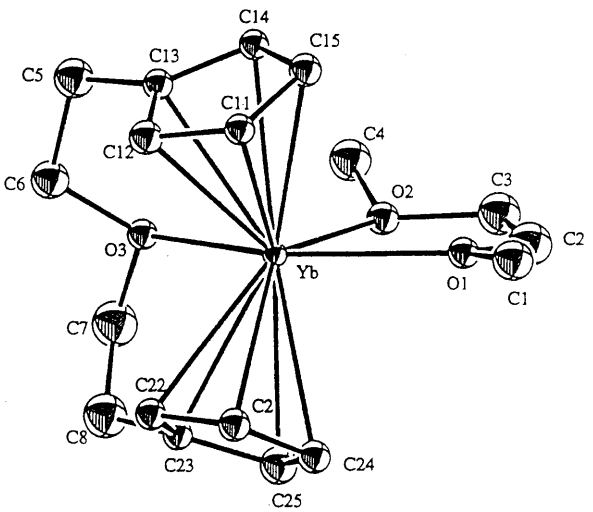

Fig. 36. Molecular structure of $[O(CH_2CH_2C_5H_4)_2Yb(DME)]$.

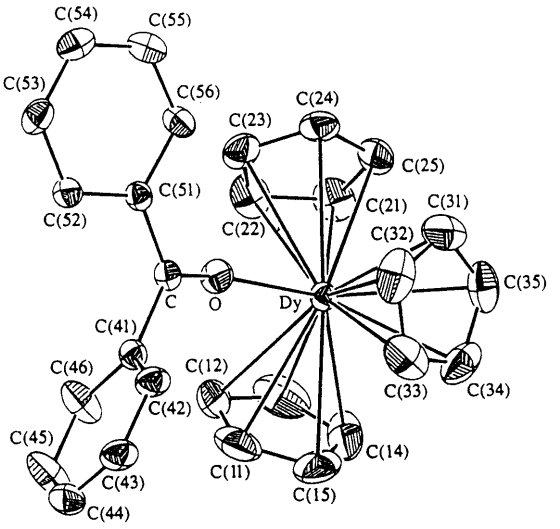

Fig. 37. Molecular structure of $[(C_5H_5)_3Dy{\cdot}O{=}CPh_2]$.

0.3, 0.1) single crystals have been grown. On the basis of absorption, luminescence and, in part, magnetic CD spectroscopic measurements, the crystal field splitting pattern of $(C_5H_5)_3La_{1-x}Pr_x(NCCH_3)_2$ and also of $(CH_3OCH_2CH_2C_5H_4)_3Pr$ could be derived. The parameters of an empirical Hamiltonian were fitted to the energies of 25 and 24 levels, respective, to give r.m.s. derivations of 27 and 24 cm^{-1} for $(C_5H_5)_3La_{1-x}Pr_x(NCCH_3)_2$ and $(CH_3OCH_2CH_2C_5H_4)_3Pr$. The experimentally detected temperature dependencies of the paramagnetic susceptibility of powdered $(C_5H_5)_3Pr(NCCH_3)_2$ and $(CH_3OCH_2CH_2C_5H_4)_3Pr$ were simulated from the eigenvalues and wavefunctions obtained using the empirically detected 'best fit' parameters.

Zhou et al. [52] reported the X-ray single crystal structure of the benzophenone adduct of tris(cyclopentadienyl)dysprosium. The compound $[(C_5H_5)_3Dy{\cdot}O{=}CPh_2]$ is a distorted tetrahedral complex (Fig. 37). The central Dy atom is η^5-bonded to three cyclopentadienyl groups and η^1-bonded to one benzophenone molecule. The average Dy–O and Dy–C(Cp) distances are 2.384(3) and 2.733(6) Å, respectively. The Dy–O–C angle is 170.6(3)°. The C–O bond distance of the coordinated benzophenone ligand is comparable to the corresponding value reported for free benzophenone.

The same authors [53] published the X-ray crystal structure of a new form of tris(cyclopentadienyl) neodymium. From a solution containing a mixture of $(C_5H_5)_3Nd$ and $(C_5H_4Me)_3Nd$ in THF, crystals of the so far unreported modification $(C_5H_5)_3Nd{\cdot}THF$ were obtained. The new structure differs markedly from the previously reported data for the same compound in cell dimension parameters, space group and Z-value (Table 1).

2.2.5. Complexes with cyclopentadienyl and cyclooctatetraenyl ligands

Chen et al. [54] described the synthesis and crystal structure of $[(C_8H_8)_3(C_6H_5CH_2C_5H_4)Nd_2K(THF)_3]$. $NdCl_3$ reacted with $C_6H_5CH_2C_5H_4Na$ in the ratio 1:1 at $-78°C$ giving $[C_6H_5CH_2C_5H_4)NdCl_2{\cdot}nTHF]$, which was then treated with $C_8H_8K_2$/THF to yield the title compound ($C_6H_5CH_2C_5H_4$ = benzyl cyclopentadienyl). The crystal structure of the Nd complex (Fig. 38) was determined by X-ray diffraction and revealed that the benzyl group is η^3-coordinated to the potassium ion to form a new type of trinuclear triangular shape.

Table 1
Comparison of selected crystal structure data of the two forms of $(C_5H_5)_3Nd{\cdot}THF$

$(C_5H_5)_3Nd{\cdot}THF$	from $(C_5H_5)_3Nd/(C_5H_4Me)_3Nd$ mixture THF solution	from $(C_5H_5)_3Nd$
Crystal system	Monoclinic	Monoclinic
Space group	$C2/c$	$P2_1/n$
a (Å)	12.839(7)	8.364(3)
b (Å)	10.520(3)	24.467(9)
c (Å)	26.599(9)	8.254(3)
β (°)	98.50	101.42
V (Å^3)	3553(3)	1655.6(4)
Z	8	4
D_c (g cm^{-3})	1.54	1.65
(Nd–C)ave. (Å)	2.76(2)	2.78(2)
Nd–O (Å)	2.54(1)	2.54(1)

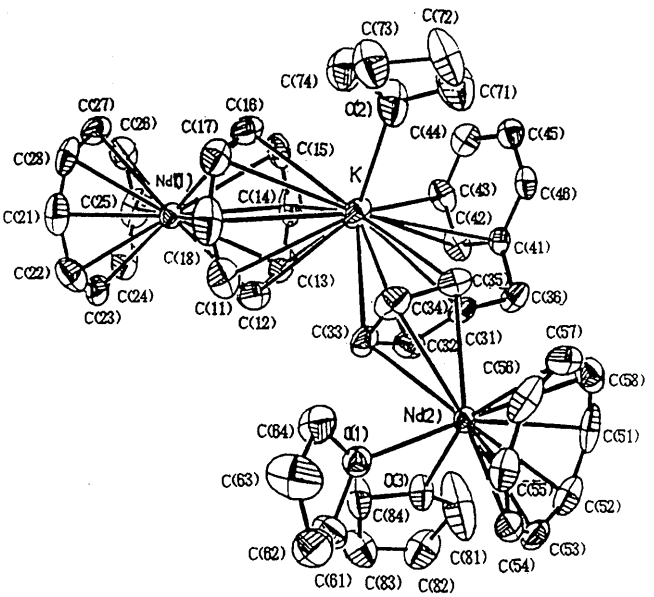

Fig. 38. Structure of $[(C_8H_8)_3(C_6H_5CH_2C_5H_4)Nd_2K(THF)_3]$.

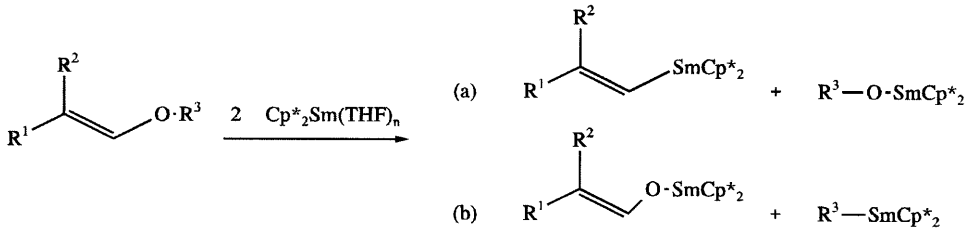

Scheme 4. Reductive cleavage of alkyl vinyl ethers with $(C_5Me_5)_2Sm(THF)_n$.

The complex consists of the two parts of $[(\eta^8\text{-}C_8H_8)Nd(\eta^8\text{-}C_8H_8)]^-$ and $[C_6H_5CH_2C_5H_4)Nd(THF)_2(\eta^8\text{-}C_8H_8)]$ connected by the K^+ ion, to which the $\eta^3\text{-}C_6H_5$ ring of a benzyl cyclopentadienyl and a THF molecule are coordinated. The coordination number around K^+ is 11.

2.3. Complexes with cyclooctatetraenyl ligands

Edelstein et al. [55] investigated the oxidation state of Ce in the sandwich molecule cerocene $[Ce(C_8H_8)_2]$. X-ray absorption near-edge structure (XANES) measurements were used for determining the oxidation state of Ce atoms in several inorganic and organometallic Ce(III) and Ce(IV) compounds. The XANES spectra in this paper give the assignment of the oxidation state of the Ce ion in substituted cerocene molecules as trivalent. The Ce ion in the substituted cerocenes appears to be less electron-rich than in their alkali metal salts, as shown by a 4.5 eV shift toward higher oxidation state of their X-ray K-edges. This argument is supported by structural data which show the Ce ring centroid distance for the substituted cerocenes is ~ 1.97 Å as compared to ~ 2.07 Å for the $K[Ce(C_8H_8)_2]$ diglyme salt. The experimental results therefore support the conclusion of the sophisticated ab initio calculations that the cerocene ground configuration should be formulated primarily as a $4f^1_{e2u}\pi^3_{e2u}$ singlet.

2.4. Organolanthanide complexes in organic synthesis

Petrov et al. [56] studied the reaction of ytterbium and its derivatives with carboxylic acid bromides. The reaction of RYbI (R = Me, Ph) with R′COBr (R′ = Ph, Me) gave acetophenone and the corresponding tertiary alcohols, with the latter predominating when R = Ph. This addition reaction is analogous to the Grignard reaction. For example, reaction of 4 equivalents of PhYbI with MeCOBr at 20°C in THF gave 87% Ph_2MeCOH. Acid bromides upon reaction with Yb(0) are converted into α-diketones, which in presence of the $YbBr_2$ formed in the reactions gave some products resulting from their partial reduction.

Takaki et al. [57] studied the regioselectivity on the reductive cleavage of alkyl vinyl ethers with $(C_5Me_5)_2Sm(THF)_n$, i.e. competition (Scheme 4) between sp^2 C–O fission (a) leading to vinyl species and alkoxides and sp^3 C–O (b) to enolates and alkyl complexes.

Interestingly, it was found that the selectivity depends on the substituent R^3. Path (a) was observed for $R^3 = Me$ ($R^1 = Ph$, $R^2 = H$), while (b) was found for $R^3 =$ Benzyl. The reactions were detected by ^1H NMR spectroscopy. Hydrolysis, deuterolysis and electrophilic trapping of the intermediates were used to prove the kind of bond cleavage.

The same authors [58] also investigated the generation of lanthanide complexes via reductive C–O bond cleavage and their reaction. The reductive C–O bond cleavage of allylic and propargylic benzyl ethers with two equivalents of $(C_5Me_5)_2Sm(THF)_n$ ($n = 0$–2) gives allylic and allenic samarium complexes, respectively, in high yields along with equimolar amounts of $(C_5Me_5)_2SmOBn$ (Bn = benzyl). Stereoselectivity at the electrophilic trapping of these complexes has been studied. Reactions of the allylic complexes with acetophenone and pivalaldehyde affords selectively more substituted *anti* homoallylic alcohols. With aldimines, *syn* homoallylic alcohols were obtained predominantly. The allenic samarium complexes react with acetophenone to yield *anti* homopropargylic alcohols with high regio- and stereoselectivities.

Heathcock et al. [59] used an in situ obtained organo-Ce(III) compound as selective reagent in one step (Scheme 5) of the total synthesis of zaragozic acid (squalestatin S1).

Addition of the Grignard reagent prepared from 4-bromo-1-butene and magnesium led to elimination of the benzyloxy group β to the carbonyl unit in **I**. This problem was circumvented by transmetalation to the cerium reagent $CH_2{=}CHCH_2CH_2CeCl_2$.

Krief et al. [60] summarized the use of $(C_5H_5)_2Sm$ as a valuable reagent for the addition of alkyl-, allyl-, benzyl- and acyl moieties to carbonyl compounds. $(C_5H_5)_2Sm$ and SmI_2 have been successfully used in Barbier type reactions involving organic halides and carbonyl compounds. $(C_5H_5)_2Sm$ proved to be in some instances the superior reagent.

$$R{-}X + 2(C_5H_5)_2Sm \rightarrow (C_5H_5)_2Sm{-}R + Cp_2Sm{-}X$$

$$(C_5H_5)_2Sm{-}R + R'{-}C(=O){-}R'' \rightarrow RR'{-}C[{-}O{-}Sm(C_5H_5)_2]{-}R''$$

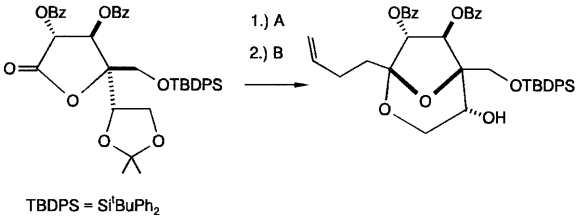

TBDPS = Si^tBuPh_2

I **II**

A $CH_2{=}CHCH_2CH_2MgBr$ / $CeCl_3$ (THF), -78 °C

B HCl, H_2O, (THF)

Scheme 5. In situ obtained organo–Ce(III) compound as selective reagent.

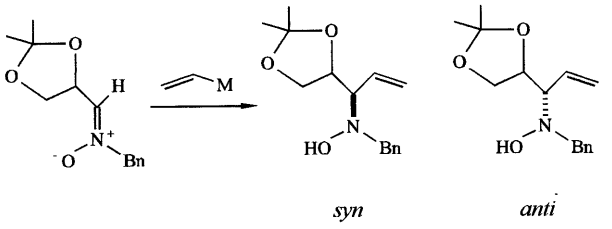

Scheme 6. Vinylcerium derivative as stereoselective reagent.

It also offers the unique advantage in being able to produce, via radical intermediates, soluble and stable organosamarium derivatives, which can be further reacted with electrophiles. These stepwise conditions proved to be crucial for the success of several reactions involving allyl-, benzyl- and acid halides.

Kawasaki et al. [61] used $(C_5Me_5)_2Sm(THF)_2$ as an efficient catalyst for the acylation of alcohols with vinyl esters to give the corresponding esters in moderate to good yields. In addition, SmI_2 was found to catalyze an aldol type reaction of imines in the presence of a formate to the corresponding α,β-unsaturated imines in satisfactory yields.

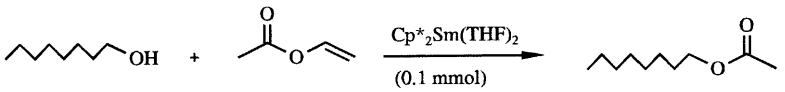

Merino et al. [62] investigated the direct vinylation and ethynylation of nitrones for the stereodivergent synthesis of allyl and propargyl amines (Scheme 6).

The best result for preparing the *syn*-hydroxylamine was obtained using 1.2 equivalents of vinyl magnesium bromide at 0°C in THF as a solvent. The stereoselective course of the reaction changes dramatically when several Lewis acids were used for precomplexing the nitrones. Similar results were obtained with vinylcerium and vinylcuprate derivatives.

2.5. Organolanthanide catalysis

Taube et al. [13] reported the stereospecific polymerisation of butadiene with $Li[Nd(\eta^3\text{-}C_3H_5)_4]\cdot 1.5$dioxane, $Li[Nd(\eta^5\text{-}C_5H_5)(\eta^3\text{-}C_3H_5)_3]\cdot 2$dioxane and $Li[Nd(\eta^5\text{-}C_5Me_5)(\eta^3\text{-}C_3H_5)_3]\cdot 3$DME as catalysts (synthesis Section 2.2.1). The catalytic reactivity of these compounds depends obviously on how far a dissociation of the complexes with formation of LiC_3H_5 takes place under the reaction conditions. By addition of proper acceptor or donor molecules, like BEt_3, Ph_2SnCl_2, Et_2AlCl and THF or dipiperidylethane, the reactivity can be controlled accordingly.

The same authors [4] published also the synthesis of neutral tris(allyl)-lanthanide complexes $La(\eta^3\text{-}C_3H_5)_3\cdot 1.5$dioxane and $Nd(\eta^3\text{-}C_3H_5)_3\cdot$dioxane and their test as 'single site' catalysts for the stereospecific polymerization of butadiene. The title

Table 2
Butadiene polymerization catalyzed by La(η^3-C_3H_5)$_3$·1.5 dioxane (A) and Nd(η^3-C_3H_5)$_3$·dioxane (B)

Catalyst	Lewis acid	$[BD]_0$	BD:Ln	T (°C)	t (h:min)	Yield (%)	Activity [mol BD (mol La)$^{-1}$ h^{-1}]	*cis*	*trans*
A	–	2.0	2000	50	1:35	53	590	15	82
A	–	2.0	2000	50	2:30	59	470	9	83
B	–	2.0	2000	50	1:00	42	600	3	94
A	Et_2AlCl	2.0	2000	50	3:15	51	320	11	84
B	$2Et_2AlCl$	2.0	2000	50	0:20	28	1800	94	5
A	$0.5EtAlCl_2$	2.0	2000	50	2:10	57	520	12	82
B	$EtAlCl_2$	2.0	2000	50	0:05	38	8300	94	5
A	30MAO	2.0	5000	50	0:19	53	8400	62	36
B	30MAO	2.2	2000	50	0:06	50	10 000	59	37
B	30MAO	2.0	30 000	25	1:20	14	2100	91	8

Table 3
Ethylene polymerization initiated by organosamarium complexes with a bridged bis(substituted cyclopentadienyl) ligand

Initiator	Polym. Time (min)	Activity (kg PE $mol^{-1} \cdot h^{-1}$)	Efficiency (%)	M_n 10^{-4}	M_w/M_n
rac-[(2-$SiMe_3$-4-$^tBuC_5Me_2)_2SiMe_2$]$Sm(THF)_2$	1	62	2	11.6	1.43
	3	139	32	35.6	1.60
meso-[(3-$^tBuC_5H_2)_2SiMe_2(SiMe_2OsiMe_2)$]$Sm(THF)_2$	5	149	87	1.9	3.29
	10	470	256	1.7	3.49
C1-[(2,4-$(SiMe_3)_2C_5H_2)$(3,4-$(SiMe_3)_2C_5H_2)SiMe_2$]$Sm(THF)_2$	15	16	1	100.8	1.60
	30	15	2	150.3	1.80
Non-bridged ($^nBuC_5H_4)_2Sm(THF)_2$	5	6	4	1.6	2.14

complexes were obtained by reaction of tetrakis(allyl)lanthanide(III) complexes $Li[Ln(C_3H_5)_4]\cdot 1.5$ dioxane (Ln = La or Nd) with BEt_3 in dioxane (Section 2.1.1). The compounds catalyzed the 1,4-*trans* polymerisation of butadiene in toluene with high selectivity. By addition of appropriate Lewis acids such as Et_2AlCl, $EtAlCl_2$ or $(MeAlO)_x$, catalysts for the 1,4-*cis* polymerisation are obtainable. The results allow to draw first conclusions on the mechanism of the lanthanide-complex-catalyzed butadiene polymerization (Table 2).

Yasuda et al. [49] explored the ethylene polymerization by using the *racemic* $[(2\text{-}SiMe_3\text{-}4\text{-}^tBuC_5Me_2)_2SiMe_2]Sm(THF)_2$, *meso* type $[(3\text{-}^tBuC_5H_2)_2SiMe_2\text{-}(SiMe_2OSiMe_2)]Sm(THF)_2$, and *C1*-symmetric $[(2,4\text{-}(SiMe_3)_2C_5H_2)(3,4\text{-}(SiMe_3)_2\text{-}C_5H_2)SiMe_2]Sm(THF)_2$ in the absence of methylalumoxane. As a result, the *meso* isomer exhibits the highest initiating activity(Table 3), but the number-average molecular weight is relatively low ($M_n = 50\ 000$). In contrast to these complexes the *C1*-symmetric complex provides the highest molecular weight of polyethylene, $M_n > 1\ 000\ 000$, with relatively narrow moleculare weight distribution ($M_w/M_n = 1.60$). Only the racemic complex exhibits good activity for the polymerization of propylene, 1-pentane and 1-hexane.

The same authors [63] reported the synthesis and the polymerization activities (Table 4) of *ansa*-samarocene complexes (Scheme 7), monocyclopentadienyl samarium complexes with an allyl or benzyl group one the cyclopentadienyl ring, and the use of 2,6-dialkoxyphenyl groups as new ligands for samarium-based polymerization initiators.

Table 4
Ethylene polymerization by $Ph_2Si[(Me_3Si)_2C_5H_3]_2Sm(THF)$

Time (min)	Activity (10^{-4} g mol^{-1} h^{-1})	$10^{-5}M_n$	M_w/M_n
5	10.4	1.60	1.84
10	5.22	4.96	2.42
14	9.58	$\gg 10$	–

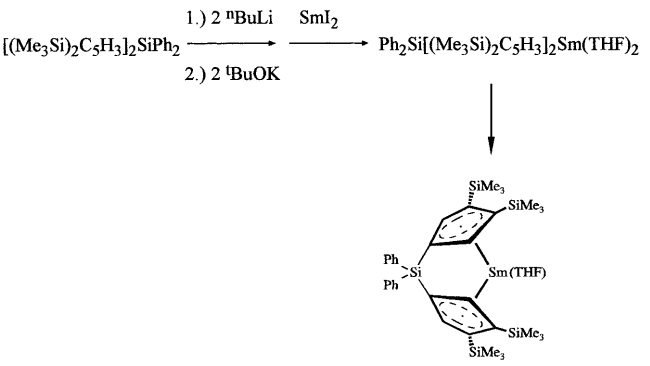

Scheme 7. Synthesis of $Ph_2Si[(Me_3Si)_2C_5H_3]_2Sm(THF)$.

Yasuda et al. (Showa Denko KK) [64] also described in a patent new lanthanide complexes and their use for the production highly syndiotactic unsaturated carboxylic ester polymers and polyolefins with broad molecular weight distribution. These complexes are expressed by the following formula:

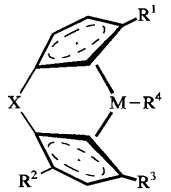

where M = lanthanide-series atom; X = substituted alkylene or a substituted silylene in the crosslinked structure of two cyclopentadienyl rings; R^1–$R^3 = C_{1-10}$ hydrocarbon or C_{1-10} alkylsilyl, being different from one another; R^4 = H, C_{1-10} hydrocarbon, e.g. dimethylsilylene(3-*tert*-butyl-cyclopentadienyl)[2-triethylsilyl-3-dimethyl(*tert*-butyl)silylcyclopentadienyl]samarium hydride.

Evans et al. [65] used field desorption mass spectrometry (FD-MS) in conjunction with NMR spectroscopy to study how olefins larger than ethylene are incorporated into polyethylene using $(C_5Me_5)_2Sm$-based catalysts under hydrogen. Polymerization reactions of propene, 1-pentene, *cis*- and *trans*-2-pentene, 1-heptene, *trans*-2-heptene, *trans*-3-heptene, 1-octene, and 1-nonadecene with ethylene under H_2 and with CD_2=CD_2 under D_2 were studied as well as reactions of ethylene with propene-d_6 and 3,3,3-propene-d_3 using $(C_5Me_5)_2Sm$ and $(C_5Me_5)_2Sm(\eta^3$-$CH_2CHCHR)$ precursors where R = H, Et, and Bu. For the olefins listed above, the combined analytical techniques with the appropriate deuterium labeling indicate that one olefine is selectively incorporated per polyethylene chain and that incorporation occurs by insertion into a Sm–H bond in the system rather than via an allyl group. Metalation of the olefin by growing polymer chains was found to be competitive with hydrogenolysis as a termination step and can be used to control molecular weight. 2-Pentene and 2-heptene do not incorporate as readily as their α-olefin analogs and 3-heptene incorporation was not detectable, but these internal olefins are effective termination agents via metalation.

Marks et al. [66] reported the ring-opening Ziegler polymerization of methylenecycloalkanes catalyzed by highly electrophilic d^0/f^n metallocenes. The authors described the reactivity, the scope, the reaction mechanism, and routes to functionalized polyolefins. A series of zirconium and lanthanide metallocene catalysts are active in the regioselective ring-opening polymerization of strained *exo*-methylenecycloalkanes to yield *exo*-methylene-functionalized polyethylenes. Methylenecyclobutane affords the polymer $[CH_2CH_2CH_2C(CH_2)]_n$ under the catalytic action of $[\{1,2\text{-}Me_2C_5H_3\}_2ZrCH_3]^+[CH_3B(C_6F_5)_3]^-$, and methylenecyclopropane affords the polymer $[CH_2CH_2C(CH_2)]_n$ under the catalytic action of $[(C_5Me_5)_2LuH]_2$. Reversible deactivation of the $[(C_5Me_5)_2LuH]_2$ catalyst is observed in the methylenecyclopropane polymerization reaction and is ascribed to formation of a Lu-allyl species based on D_2O quenching experiments. In contrast, the catalysts $[(C_5Me_5)_2SmH]_2$ and $[(C_5Me_5)_2LaH]_2$ yield the dimer 1,2-dimethylene-3-methylcy-

clopentane from methylenecyclopropane with high chemoselectivity. The mechanism of dimerization is proposed to involve the intermediacy of 3-methylene-1,6-heptadiene and is supported by the observation that independently synthesized 3-methylene-1,6-heptadiene is smoothly converted to 1,2-dimethylene-3-methylcyclopentane under catalytic conditions. Methylenecyclopropane-ethylene copolymerization to yield high molecular weight $\{[CH_2CH_2]_x[CH_2CH_2C(CH_2)]_y\}$ having an exclusively ring-opened microstructure is catalyzed by $[(C_5Me_5)_2LuH]_2$ and $[(C_5Me_5)_2SmH]_2$. When $[(C_5Me_5)_2LaH]_2$ is used as the catalyst, more than 50% of the methylenecyclopropane is located at the chain ends in a dienyl structure. The only zirconium polymerization catalyst which incorporates methylenecyclopropane in the ring-opened form in a moderate percentage is $[C_5Me_4Si(CH_3)_2(N^tC_4H_9)ZrCH_3]^+[B(C_6F_5)_4]^-$.

Marks and Li [67] also described diverse mechanistic pathways and selectivities in organo-f-element-catalyzed hydroamination. Lanthanide metallocenes catalyze the regiospecific intermolecular addition of primary amines to acetylenic, olefinic, and diene substrates at rates which are $\sim 1/1000$ of those of the most rapid intramolecular analogues. Kinetic and mechanistic data argue for turnover-limiting C≡C/C=C insertion into a Ln–N bond, followed by protonolysis of the resulting Ln–C bond. The rigorously anhydrous/anaerobic reaction of primary alkyl amines (0.30 M) with various alkynes, alkenes, and dienes (1.2 M) was carried out in hydrocarbon solvents using $(C_5Me_5)_2LnCH(SiMe_3)_2$ and $[SiMe_2(C_5Me_4)_2]LnCH(SiMe_3)_2$ (Ln = Sm, Nd) as precatalysts (6.0 mM). Reaction rates and selectivities were monitored by ^1H and ^{13}C NMR, and known products were identified by comparison with literature data and/or with those of authentic samples. New compounds were characterized by one- and two-dimensional ^1H and ^{13}C NMR as well as by high-resolution MS. The reactions proceed with $>95\%$ regiospecificity.

Another contribution [68] by the same authors reported the efficent and regiospecific $(C_5Me_5)_2LnCH(SiMe_3)_2$ (Ln = La, Nd, Sm, Lu)- and $[Me_2Si(C_5Me_4)_2]$-$LnCH(SiMe_3)_2$ (Ln = Nd, Sm)-catalyzed hydroamination/cyclization of aliphatic and aromatic aminoalkynes of the formula $RC{\equiv}C(CH_2)_nNH_2$ to yield the corresponding cyclic imines $RCH_2C{=}N(CH_2)_{n-1}CH_2$, where R, n, $N_t\ h^{-1}$ (°C) = Ph, 3, 77 (21°C); Ph, 3, 2830 (60°C); Me, 3, 96 (21°C); and $SiMe_3$, 3, >7600 (21°C), and of aliphatic secondary amino-alkynes of the formula $RC{\equiv}C(CH_2)_3NHR^1$ to generate the corresponding cyclic enamines $RCH{=}CNR^1(CH_2)_2CH_2$ where R, R^1, $N_t\ h^{-1}$(°C) = $SiMe_3$, $CH_2{=}CHCH_2$, 56 (21°C); H, $CH_2{=}CHCH_2$, 27 (21°C); $SiMe_3$, $CH_2{=}CH(CH_2)_3$, 129 (21°C); and H, $CH_2{=}CH(CH_2)_3$, 47 (21°C). Kinetic and mechanistic (Scheme 8) evidence is presented arguing that the turnover-limiting step is an intramolecular alkyne insertion into the Ln–N bond followed by rapid protonolysis of the resulting Ln–C bond. The use of larger metal ionic radius $(C_5Me_5)_2LnCH(SiMe_3)_2$ and more open $[Me_2Si(C_5Me_4)_2]LnCH(SiMe_3)_2$ complexes as the precatalysts results in a decrease in the rate of hydroamination/cyclization, arguing that the steric demands in the –C≡C– insertive transition state are relaxed compared to those of the analogous aminoolefin hydroamination/cyclization. The presented process provides an efficient method for the catalytic synthesis of pyrrole, pyridine, and azepine derivatives.

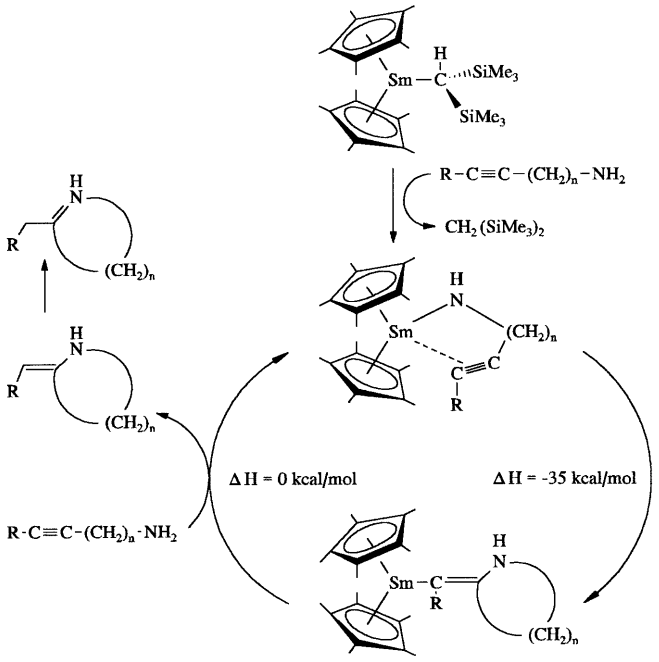

Scheme 8. Simplifed catalytic cycle for the hydroamination/cyclization of aminoalkynes.

Marks and Fu [69] also patented a method for synthesizing polyolefins having a silyl group at one terminus. These polymerizations were carried out in the presence of a metallocene catalyst using silanes (e.g. $PhSiH_3$) as a chain transfer agent. $(C_5H_5)_2LnH$, $(C_5Me_5)_2LnCH(SiMe_3)_2$, $(C_5Me_5)_2LnH$, $Me_2Si(C_5Me_4)_2LnCH(SiMe_3)_2$ (Ln = Sc, Y, La, Ac, Ce–Lu) and several Ti, Zr and Hf complexes were claimed as catalytic active compounds. The activities of the organolanthanide complexes and molecular weight of the polyolefins are inversely proportional to the silane concentration, showing that the silane is a true chain-transfer agent.

Mortreux et al. [70] showed that the ethylene insertion into a Mg–C bond is possible under very mild conditions by a alkyl chain-transfer via chain growing-polymerization catalyzed by a lanthanocene. This new reaction is an efficient method for the synthesis of P–Mg–P′ compounds (P = alkyl chain C_4–C_{200}).

$$\mathrm{BuMgEt} + (n+m)\mathrm{CH_2{=}CH_2} \xrightarrow[80°C,\ 1\ \mathrm{atm}]{[(C_5Me_5)_2SmCl_2Li(OEt_2)_2]} \mathrm{P–Mg–P'}$$

where P = Bu(–CH_2–CH_2)$_n$ and P′ = Et(–CH_2–CH_2)$_m$.

The experiments were usually performed in hydrocarbons at 80 °C. The ethylene reacted immediately and was consumed constantly until the alkyl chain of the dialkyl magnesium compounds grew too long and the products began to precipitate. The treatment of the P–Mg–P′ compounds with CO_2 resulted after hydrolysis in the formation of acids with odd carbon chain lengths between 5 and 13 C-atoms (FAB^+-MS, m/z 101–213). Investigations of the molecular mass distributions the

polymers and the kinetics of several experiments led to the conclusion of a so-called 'pseudo-living or living' polymerisation mechanism.

Mortreux et al. [71] also patented this procedure for long-chain dialkylmagnesium compounds, their preparation by polymerization of ethylene, and their use. Additionally to $[(C_5Me_5)_2SmCl_2Li(OEt_2)_2]$ the authors claim all complexes of the type $[(C_5Me_5)_2LnCl_2Li(OEt_2)_2]$ with Ln = Sc, Y, and lanthanides, as initiators for this process. Further they claim the use of these compounds as macroinitiators for the preparation of ethylene-methylmethacrylate or ε-caprolactone-ethylene block copolymers, etc., and as starting materials for the preparation of alcohols by oxidation and hydrolysis, of acids by reaction with CO_2, etc.

Endo et al. [72] reported the block copolymerization of tetrahydrofuran with δ-valerolactone by samarium iodide-induced transformation. The polymerization behavior of δ-valerolactone with alkylsamarium reagents ($RSmI_2$) was studied, and its application to the block copolymerization of tetrahydrofuran with δ-valerolactone was examined. Polymerization of δ-valerolactone by butylsamarium reagents gave the corresponding polyvalerolactone in good yield. The yield increased with increasing the concentration of valerolactone and decreasing the polymerization temperature, resulting from the equilibrium between δ-valerolactone and polyvalerolactone. The decrease in the molecular weight of polyvalerolactone by extending the polymerization time indicated the existence of a 'back-biting' reaction to form cyclic oligomers (Scheme 9).

The polymerization of δ-valerolactone with polytetrahydrofuran-macroanion obtained by the two-electron reduction of the propagation center of living polytetrahydrofuran with SmI_2 led to the block copolymer of THF with δ-valerolactone. The initiation efficiency of valerolactone polymerization was almost quantitative, and the unit ratio of THF and δ-valerolactone segments could be controlled by both the polymerization time of THF and the amounts of δ-valerolactone.

Tokimitsu et al. (Mitsubishi Rayon) [73,74] patented two kinds of rare earth compounds (A, B) for the preparation of methacrylic ester/olefin block copolymers.

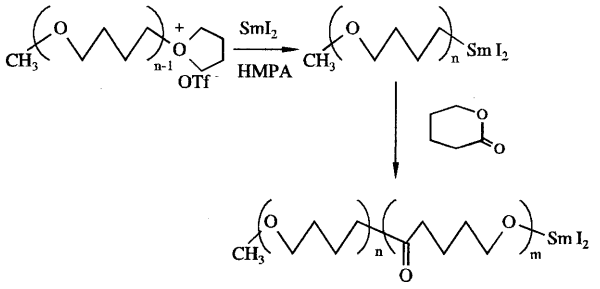

Scheme 9. Polymerization of δ-valerolactone.

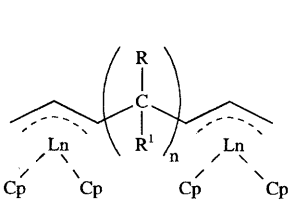

A

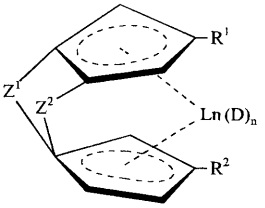

B

where in (A) Ln = Sc, Y, lanthanide metal are R, R^1 = H, C_{1-5} hydrocarbon; and in (B) R^1, $R^2 = C_{1-5}$ hydrocarbon, Ln = Sm, Er, Yb, Z^1, $Z^2 = C_{1-3}$ alkene, alkylsilyl, or alkylsiloxane and D = solvent, $n = 0–3$.

Both polymerization initiators can be used to obtain an A–B–A type block copolymer comprising a polymer block (A) of a (meth)acrylic ester and a polymer block (B) of an olefin and having a narrow molecular weight distribution M_w/M_n of 1.0 to 2.5. The polymerization initiator A is additionally able to produce a B–A–B type block copolymer having a few reaction stages, excellent in weather resistance and having elastomeric properties, etc.

Ota and Ishimaru (Hitachi) [75] patented a monodispersed vinyl polymer with molecular weight dispersion M_w/M_n of 1.01–1.5, a photo-crosslinkable monomer having at least one radical-polymerizable double bond at a terminal and a photopolymerization initiator. The polymer could be obtained by polymerization in the presence of a lanthanide organometallic compound $(AR_5)_aLn(Z)_b(X)_c$ (A = Cp, R = alkyl, $SiMe_3$; R may be same or different from each other; Ln = Sc, Y, La, Ce, Pr, Nd, Yb, Lu; Z = H, alkyl, $SiMe_3$; X = halogene other than F, furane, pyridine, phosphine, amine, ether; $a + b = 3$; $c = 0–5$). The described polymer is used as photosensitive resin composition and photosensitive element.

3. Actinides

3.1. Actinide complexes without supporting cyclopentadienyl ligands

Leonov [76] et al. investigated the oxidation of tetrabenzyl uranium. $(C_6H_5CH_2)_4U{\cdot}MgCl_2$ reacted with O_2 or ^{t}BuOOH in organic solvents at room temperature. Products of different composition were detected depending on the oxidizing reagent and the stoichiometry. The reaction yielded mainly uranium(IV) benzyloxide derivatives. In the case of oxygen the so-called peroxide mechanism took place and the novel complex $(C_6H_5CH_2)_2U(OCH_2C_6H_5)_2{\cdot}MgCl_2$ was obtained.

3.2. Cyclopentadienyl complexes

3.2.1. Mono(cyclopentadienyl) complexes

Baudry et al. [77] published the synthesis and reactivity of mono(diphenylphosphinocyclopentadienyl)uranium trisborohydrides $C_5R_4PPh_2U(BH_4)_3$ (R = H or CH_3) and of their borane adducts. The reactivity of the monocyclopentadienyl

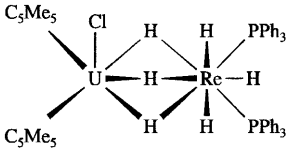

Scheme 10. Preferred conformation of the anion $[(C_5Me_5)_2ClUH_6Re(PPh_3)_2]^-$.

complex $(C_5H_4PPh_2)U(BH_4)_3$ and of its borane adduct $(C_5H_4PPh_2{\cdot}BH_3)U(BH_4)_3$ strongly suggest that in solution these complexes are in equilibrium with the bis(cyclopentadienyls) $(C_5H_4PPh_2)_2U(BH_4)_2$ and $(C_5H_4PPh_2{\cdot}BH_3)_2U(BH_4)_2$ and $U(BH_4)_4$ which is the most reactive species in such systems. Both species rearrange in the presence of neutral ligands and are only characterizable in solution. The analogous tetramethylcyclopentadienyl compound $(C_5Me_4PPh_2{\cdot}BH_3)U(BH_4)_3$, a model of monolinked dimetallics, is stable and has been isolated.

$$(C_5H_4PPh_2)U(BH_4)_3 + BH_3{\cdot}SMe_2 \xrightarrow[-SMe_2]{\text{toluene}} (C_5Me_4PPh_2{\cdot}BH_3)U(BH_4)_3$$

Leonov et al. [78] investigated the reaction of uranium(IV) mono(cyclopentadienyl) complexes with oxygen. The uranium complexes $C_5H_5UCl_3{\cdot}2L$ [L = THF, $(^nBuO)_3P{=}O$] react with molecular oxygen at 298 K in an organic solvent:

$$C_5H_5UCl_3{\cdot}2L + O_2 \xrightarrow{XH} UO_2Cl_2{\cdot}2L + C_5H_6 + 0.5Cl_2$$

where XH = solvent or metal organic compound as proton source

$$C_5H_6 + Cl_2 \rightarrow [C_5H_5Cl]_n + HCl$$

solvents to give uranyl dichloride complexes of the type $UO_2Cl_2{\cdot}2L$ and free cyclopentadiene. The latter is easily halogenated under the reaction conditions to give polymeric products. Possible routes for the transformation of the cyclopentadienyl ligand are proposed.

3.2.2. Bis(cyclopentadienyl) complexes

Cendrowski-Guillaume and Ephritikhine [79] published the synthesis and reactivity of hydrogen-rich uranium-rhenium compounds. The reaction of $(C_5Me_5)_2UCl(THF)$ and $[K(THF)_2][ReH_6(PPh_3)_2]$ did not afford the metathesis product $[(C_5Me_5)_2UH_6Re(PPh_3)_2]$ (Scheme 10) with elimination of KCl but gave the anionic addition compound $[K(THF)_2][(C_5Me_5)_2ClUH_6Re(PPh_3)_2]$; the borohydride analogue $K[(BH_4)(C_5Me_5)_2UH_6Re(PPh_3)_2]$ was prepared similarly. The ^1H- and ^{31}P NMR spectra revealed that $[K(THF)_2][(C_5Me_5)_2ClUH_6Re(PPh_3)_2]$ was reversibly dissociated in THF into $(C_5Me_5)_2UCl(THF)$ and $[K(THF)_2][ReH_6(PPh_3)_2]$; addition of either of these two species caused the equilibrium to be shifted towards the formation of $[K(THF)_2][(C_5Me_5)_2ClUH_6Re(PPh_3)_2]$.

Burns et al. [80] published the preparation of actinide phosphinidene complexes as well as the steric control of their reactivity. The reaction of KPH-2,4,6-$^tBu_3C_6H_2$ with $(C_5Me_5)_2UMeCl$ at room temperature in toluene in the presence of trimethylphosphine oxide yields the complex $(C_5Me_5)_2U{=}P$-2,4,6-$^tBu_3C_6H_2$-$(O{=}PMe_3)$ as black crystals in 62% yield.

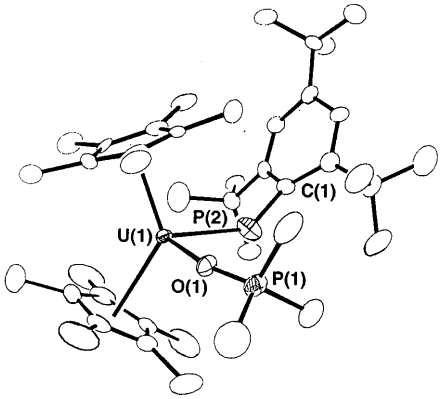

Fig. 39. Structure of $(C_5Me_5)_2U{=}P\text{-}2,4,6\text{-}{}^tBu_3C_6H_2(O{=}PMe_3)$.

$$(C_5Me_5)_2UMeCl + KPH\text{-}2,4,6\text{-}{}^tBu_3C_6H_2 \xrightarrow[12\ h,\ RT]{OPMe_3} (C_5Me_5)_2U{=}P\text{-}2,4,6\text{-}{}^tBu_3C_6H_2\text{-}(O{=}PMe_3) + CH_4 + KCl$$

In the absence of added base, intractable product mixtures result, possibly due to reduction of the metal center or reaction of the formed phosphinidene ligand with the solvent or ancillary ligand. The phosphine oxide adduct has been structurally characterized (Fig. 39).

The reaction of an *ansa*-uranocene dimethyl with $H_2P\text{-}2,4,6\text{-}{}^tBu_3C_6H_2$ led to the formation of $\{[(C_5H_5)_2SiMe_2]U(\mu\text{-}P\text{-}2,4,6\text{-}{}^tBuC_6H_2)\}_2$, a complex containing two U–P 'bridge' bonds. The dimer may be readily disrupted by the addition of an equivalent of phosphine oxide as a Lewis base, yielding a product that may be formulated on the basis of NMR spectroscopy as the analog of the compound $(C_5Me_5)_2U{=}P\text{-}2,4,6\text{-}{}^tBu_3C_6H_2(O{=}PMe_3)$.

$$[(C_5H_5)_2SiMe_2]UMe_2 + H_2P\text{-}2,4,6\text{-}{}^tBu_3C_6H_2 \xrightarrow[6\ days,\ 45°C]{toluene} 0.5\{[(C_5H_5)_2SiMe_2]U(\mu\text{-}P\text{-}2,4,6\text{-}{}^tBuC_6H_2)\}_2$$

Hughes et al. [81] reported the synthesis and molecular structure of a uranocene dichloride containing 1,2-di-*tert*-butylcyclopentadienyl ligands. 1,2-Di-*tert*-butylcyclopentadienyl lithium has been used to prepare 1,1′,2,2′-tetra-*tert*-butyluranocene dichloride and the corresponding compounds of titanium and zirconium for comparison. The bent metallocene structures of these compounds have been confirmed by X-ray crystallography, and illustrate that the 1,2-di-*tert*-butylcyclopentadienyl ligands are arranged with all four *tert*-butyl groups in the open part of the wedge between the two canted cyclopentadienyl rings, but that steric interactions between the substituents afford a conformationally dictated C_2 symmetry for the molecules (Fig. 40).

Eisen et al. [82] reported the synthesis, molecular structure, solution dynamics and interconversion reactions of uranium(IV) bis(amido), imino and bis(acetylide)

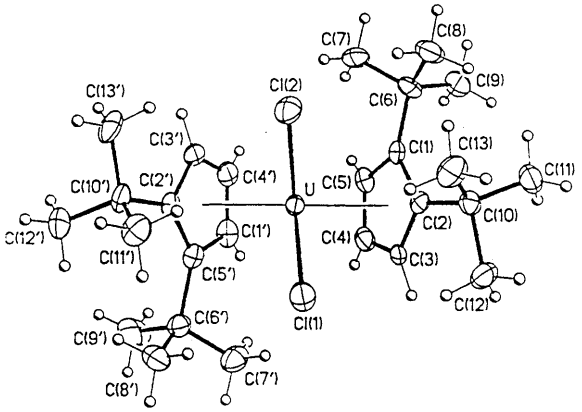

Fig. 40. Molecular structure of $(1,2\text{-}C_5H_3^tBu_2)_2UCl_2$; selected bond distances and angles: U–Cp″1(centroid) = 2.427(4) Å, U–Cp″2(centroid) = 2.435(4) Å, U–Cl1 = 2.591(4) Å, U–Cl2 = 2.576(4) Å, Cp″1–U–Cp″2 = 123.3(8)°, Cl1–U–Cl2 = 97.6(1)°.

complexes (Scheme 11). Reactions of $(C_5Me_5)_2UMe_2$ with primary aromatic or aliphatic amines led to the rapid formation of monomeric uranium(IV) complexes $(C_5Me_5)_2U(NHR)_2$ (R = 2,6-dimethylphenyl, Et, ^{t}Bu). The compounds were characterized by standard techniques, and $(C_5Me_5)_2U(NHC_6H_3Me_2\text{-}2,6)_2$ by X-ray diffraction. In co-ordinating solvents like THF $(C_5Me_5)_2U(NHC_6H_3Me_2\text{-}2,6)_2$ reacted intramolecularly releasing one primary amine and forming the imidouranium(IV) complex $(C_5Me_5)_2U{=}NC_6H_3Me_2\text{-}2,6(THF)$, whereas in non-co-ordinating solvents the base-free compound $(C_5Me_5)_2U{=}NC_6H_3Me_2\text{-}2,6$ was obtained.

The coordinated THF in $(C_5Me_5)_2U{=}NC_6H_3Me_2\text{-}2,6(THF)$ was found not to be in equilibrium with bulk solvents, and different proton chemical shifts for the coordinated base were observed as a function of temperature following a Curie–Weiss behaviour. σ-Bond metathesis reactions of bis(amido) and/or imido complexes with terminal alkynes produced the bis(acetylide) complexes $(C_5Me_5)_2U(C{\equiv}CR)_2$ (R = Ph or ^{t}Bu) as active species for the regioselective oligomerization of terminal alkynes, which can be prepared also from the reaction of $(C_5Me_5)_2UMe_2$ with 2 equiv. of the corresponding terminal alkyne. Reactivity studies show the possible interconversion among these bis(amido), imido, and bis(acetylide) complexes.

Ephritikhine et al. [83] studied a novel ring-opening reaction of THF promoted by the cationic uranium amide compound $[(C_5Me_5)_2U(NMe_2)(THF)][BPh_4]$ and the presence of free amine. The compound $[(C_5Me_5)_2U(NMe_2)(THF)][BPh_4]$ was prepared readily in THF and was isolated in very good yields. However, when the reaction mixture was kept at room temperature for a longer period of time, the red solution of $[(C_5Me_5)_2U(NMe_2)(THF)][BPh_4]$ progressively deposited a yellow microcrystalline powder. This compound, $[(C_5Me_5)_2U\{O(CH_2)_4NMe_2(CH_2)_4O\}][BPh_4]\cdot(0.5\ THF)$, was identified by ^{1}H NMR and by X-ray diffraction analysis of

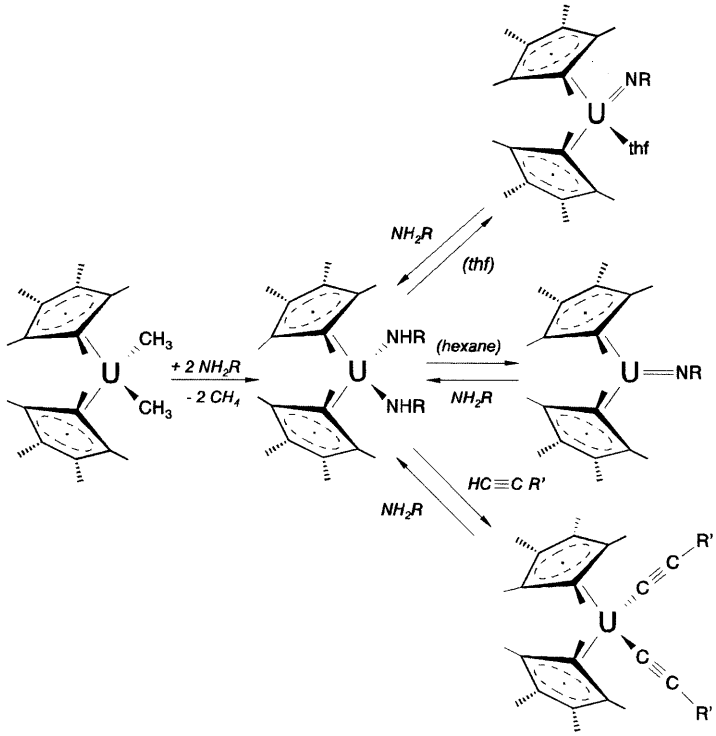

Scheme 11. Reactivity and interconversion reactions of $(C_5Me_5)_2U$-bis(amido), imido and alkynyl complexes. ($R = C_6H_3Me_2$-2,6, $R' = Ph$ or ^tBu).

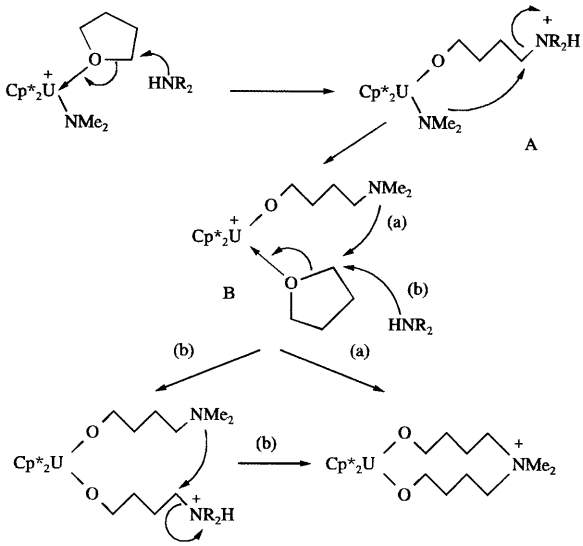

Scheme 12. Proposed mechanism of the THF cleavage and formation of the cation $[(C_5Me_5)_2U\{O(CH_2)_4NMe_2(CH_2)_4O\}]^+$.

the solvate obtained by crystallization from pyridine. $[(C_5Me_5)_2U(NMe_2)(THF)][BPh_4]$ was transformed slowly into $[(C_5Me_5)_2U\{O(CH_2)_4NMe_2(CH_2)_4O\}][BPh_4]\cdot(0.5\ THF)$ (ca. 20% after 4 days) by reaction with two molecules of THF (Scheme 12). In fact, $[Cp^*_2U(NMe_2)(THF)][BPh_4]$ was found to be inert towards THF, except in the presence of free amine; the reactivity sequence was $NHMe_2 > NHEt_2 > NEt_2$.

$$(C_5Me_5)_2U(NMe_2)_2 + [NHEt_3][BPh_4] \xrightarrow{THF} [(C_5Me_5)_2U(NMe_2)(THF)][BPh_4] + NHMe_2 + NEt_3$$

The crystal structure of the cation in the pyridine solvated salt $[(C_5Me_5)_2U\{O(CH_2)_4NMe_2(CH_2)_4O\}][BPh_4]\cdot NC_5H_5$ is shown in Fig. 41. The uranium atom is in a pseudo-tetrahedral environment which is quite familiar for complexes of the type $[(C_5Me_5)_2MX_2]$. The short U–O distances of 2.08(1), 2.09(1) Å and the large U–O–C angles 170.2(5) and 172.8(5)° reflect the strong bonding interaction between the uranium and oxygen atoms.

Marks et al. [84] introduced a new organo-Lewis acid tris(perfluorobiphenylyl)-borane (PBB) as cocatalyst in cationic metallocene polymerization catalysis. Reactions with group 4 and thorium metallocene methyls proceed cleanly to yield cationic complexes, which were characterized by standard ^1H-, ^{13}C- and ^{19}F NMR spectroscopic and analytical techniques. Whereas the $(C_5Me_5)_2ThMe_2$ and

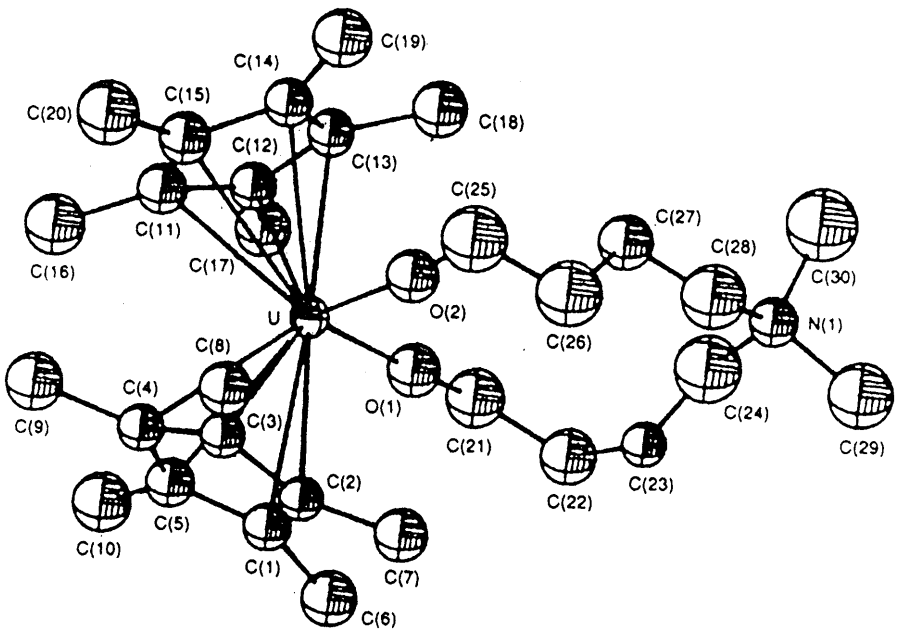

Fig. 41. Molecular structure of the cation $[(C_5Me_5)_2U\{O(CH_2)_4NMe_2(CH_2)_4O\}]^+$

$(C_5H_5)_2Zr(Cl)Me$ reaction with $B(C_6F_5)_3$ yields inseparable mixtures of catalytically inactive products, PBB selectively abstracts a single methyl group to yield cationic, catalytically active ion pairs.

3.2.3. Tris(cyclopentadienyl) complexes

Cendrowski-Guillaume and Ephritikhine [79] reported in addition to the synthesis of $[K(THF)_2][(C_5Me_5)_2ClUH_6Re(PPh_3)_2]$ (Section 3.2.2) also the preparation of some tris(cyclopentadienyl)uranium-rhenium hydrides $(C_5H_4R)_3UH_6Re(PPh_3)_2$ (R = H, ^{t}Bu, $SiMe_3$). These compounds were characterized by elemental analyses and by ^{1}H- and ^{31}P NMR spectra.

$$[U(C_5H_4R)_3][BPh_4] + [K(THF)_2][ReH_6(PPh_3)_2] \overset{THF}{\rightarrow} [(C_5H_4R)_3UH_6Re(PPh_3)_2] + KBPh_4$$

The reaction of ring-substituted $(C_5H_4R)_3UCl$ (R = ^{t}Bu and $SiMe_3$) with one equivalent of $[K(THF)_2][ReH_6(PPh_3)_2]$ remained incomplete, leading to the equilibrium:

$$(C_5H_4R)_3UCl + [K(THF)_2][ReH_6(PPh_3)_2] \overset{THF}{\rightleftharpoons} [(C_5H_4R)_3UH_6Re(PPh_3)_2] + KCl$$

Kanellakopulos et al. [85] synthesized and characterized μ-oxo-bis[tri(cyclopentadienyl)uranium(IV)]. Oxidation of $(C_5H_5)_3U^{III}\cdot THF$ with molecular oxygen in tetrahydrofuran yields the linear bridged complex $[(C_5H_5)_3U]_2(\mu\text{-}O)$ (Fig. 42). Three cyclopentadienyl rings are η^5-bonded to each uranium atom to form a distorted tetrahedron with one bridging oxygen atom. The U–O–U angle is 180° with the oxygen atom situated on a centre of inversion. The U–O distance, 2.0881(4) Å, is among the shortest ever observed. The temperature-dependent paramagnetic susceptibility of the compound was measured in the temperature range between 4.2 and 300 K and was discussed in comparison with the magnetic susceptibilities of $(C_5H_5)_3UOH$, $(C_5H_5)_3USH$ and $[(C_5H_5)_3U]_2(\mu\text{-}S)$. The magnetic moment of the μ-O bridged complex is remarkably lower than the magnetic moment of the OH compound. From the low magnetic moment and the absence of any indication for a temperature-independent paramagnetic behavior at low temperatures, as well as from the slight field dependence of the susceptibility at low temperatures, it can be suggested that a slight long-range U–U magnetic interaction via a bridging oxygen atom within the molecule is present.

Ephritikhine et al. [86] synthesized tris(cyclopentadienyl) uranium thiolates and selenolates. Tris(cyclopentadienyl) uranium(IV) thiolates were prepared by two principal methods namely (1) substitution of the chloride group of $(C_5H_5)_3UCl$ by SR- and (2) oxidation of the trivalent precursors $(C_5H_5)_3U(THF)$, $(C_5H_4SiMe_3)_3U$ and $(C_5H_4'Bu_3)_3U$ with the disulfides RSSR (R = Me, Et, ^{i}Pr, ^{t}Bu or Ph). Similar treatment with MeSeSeMe afforded $(C_5H_5)_3USeMe$ and $(C_5H_4SiMe_3)_3USeMe$. The crystal structure (Fig. 43) of $(C_5H_5)_3USMe$ was determined, the U–S bond length is 2.695(4) Å, the distance U–Cp(centroid) is given with 2.48(1) and 2.39(1) Å and the angle U–S–C(CH_3) is 107.2(5)°. Several reactions of these complexes are described, namely cleavage of the U–S bond by acidic substrates or iodine, insertion of CS_2 and CO_2 into the U–S bond, and reduction to afford the corresponding U(III)

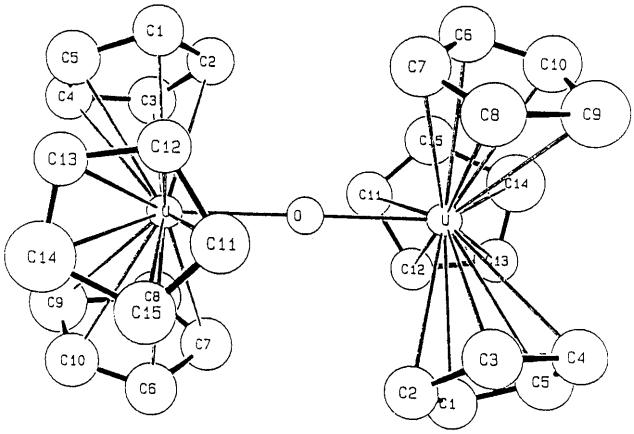

Fig. 42. Molecular structure of $[(C_5H_5)_3U]_2(\mu\text{-O})$.

anions. The synthesis, structure and reactivity of the thiolate compounds are compared with those of the alkoxide analogues.

De Ridder et al. [87] compared the geometry of $(C_5H_5)_3Np(OPh)$ with that of the isostructural uranium analogue. The molecular structure (Fig. 44) consists of one

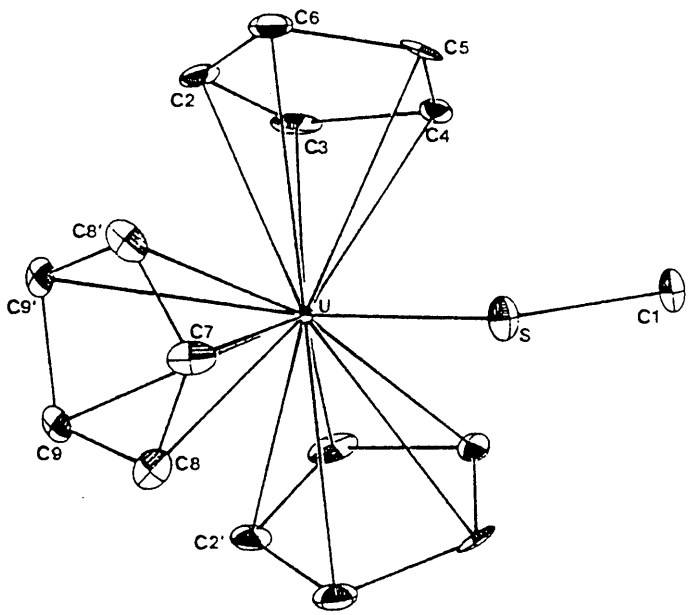

Fig. 43. Molecular structure of $(C_5H_5)_3USMe$.

Np atom coordinated by the O atom of the phenoxide and by three η^5-coordinated cyclopentadienyl rings. If the coordination polyhedron is considered to be formed by the O atom and the centres of the cyclopentadienyl rings, the coordination about the Np atom displays approximate C_{3v} symmetry, with the O atom at the apex and the cyclopentadienyl rings at the base of a flattened tetrahedron. Thus the Cp_3MY ($Cp = C_5H_5$) geometry is maintained in this complex; the Cp–Np–Cp angles are nearly identical and significantly smaller than 109°. The deviation of the structure from a regular tetrahedron is also shown by the distance of the Np atom from the plane defined by the centres of the three cyclopentadienyl rings. If one assumes tetrahedral geometry about the Np atom and an average Np to ring centre distance of 2.47(1) Å, then the Np atom should be located 0.823 Å above the plane. The distance found in the compound is 0.452(4) Å and is a measure for the trigonal distortion from tetrahedral geometry.

3.2.4. Mixed cyclopentadienyl-cyclooctatetraenyl and cyclooctatetraenyl complexes

Ephritikhine et al. [88] studied the reactivity of the cationic uranium amide compound $[U(\eta^8\text{-}C_8H_8)(NEt_2)(THF)_2][BPh_4]$. The reactions of the title compound are summarized in the equations.

$$[U(C_8H_8)(NEt_2)(THF)_2][BPh_4] + MX \rightarrow [U(C_8H_8)(NEt_2)(X)] + M[BPh_4]$$

where $MX = LiCH(SiMe_3)_2$, $NaN(SiMe_3)_2$, KC_5H_5, KC_5Me_5, LiCl or KBH_4.

The chloro- and tetrahydroborato-amide complexes $[U(C_8H_8)(NEt_2)(THF)_x(BH_4)]$, $[U(C_8H_8)(NEt_2)(THF)_x(X)]$, which were readily formed upon addition of

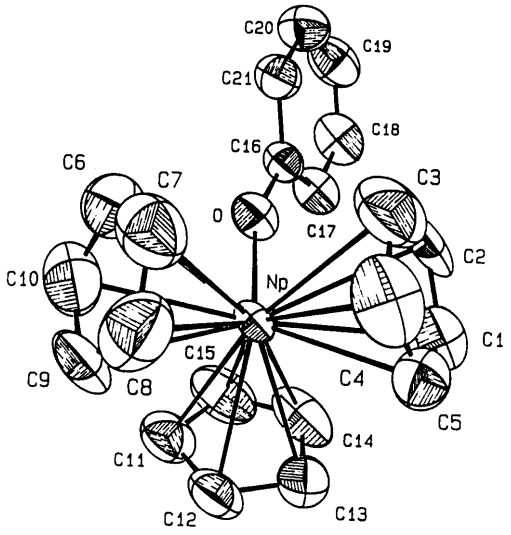

Fig. 44. Moleculare structure of $(C_5H_5)_3Np(OPh)$.

LiCl or KBH_4, were stable in THF solution but could not be isolated in solid form, being decomposed into $[U(C_8H_8)_2]$ and other unidentified species upon desolvation.

$$[U(C_8H_8)(NEt_2)(THF)_2][BPh_4] + CE_2 \rightarrow [U(C_8H_8)(E_2CNEt_2)(THF)_2][BPh_4]$$

where E = O, S.

$$[U(C_8H_8)(NEt_2)(THF)_2][BPh_4] + MeC{\equiv}N$$

$$\rightarrow [U(C_8H_8)(NC\{Me\}\{NEt_2\})(THF)_2][BPh_4]$$

The treatment of $[U(C_8H_8)(NEt_2)(THF)_2][BPh_4]$ with CO_2, CS_2 or acetonitrile led to an insertion of these molecules into the U–N bond to form the carbamate or dithiocarbamate complexes, respectively.

$$[U(C_8H_8)(NEt_2)(THF)_2][BPh_4] + HA \rightarrow [U(C_8H_8)(A)(THF)_2][BPh_4] + HNEt_2$$

where HA = $[HNEt_3]Cl$, C_5H_6, HO^iPr, HS^iPr.

The reaction of $[U(C_8H_8)(NEt_2)(THF)_2][BPh_4]$ with proton acidic substrates HA provides a straightforward route to U–A derivatives. The new compounds were characterized by elemental analyses, their ^{1}H-NMR and IR spectra. The complexes $[U(C_8H_8)(NEt_2)(THF)_3][BPh_4]$ and $[U(C_8H_8)(S_2CNEt_2)(THF)_2][BPh_4]$ have been crystallographically characterized; the structure of the dithiocarbamate complex is shown in Fig. 45.

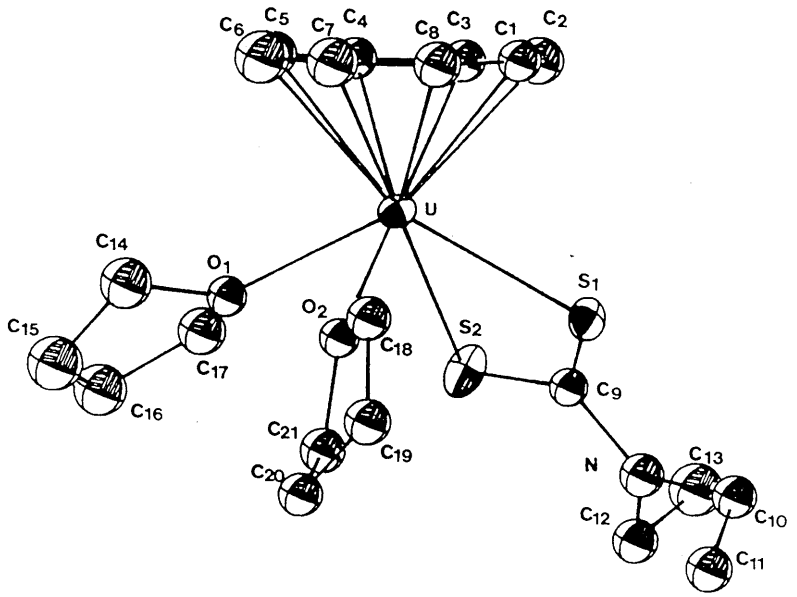

Fig. 45. Structure of the cation $[U(C_8H_8)(S_2CNEt_2)(THF)_2]^+$.

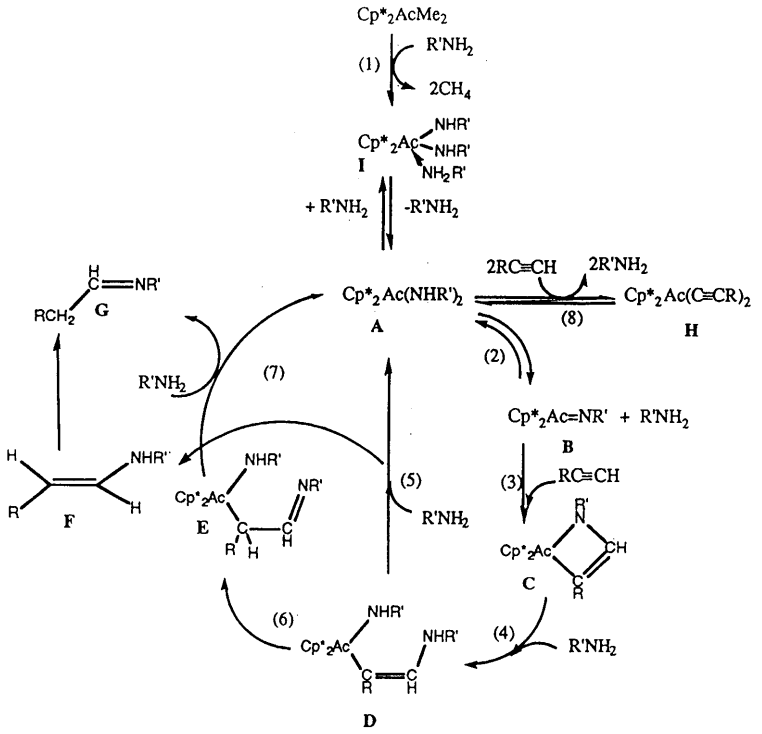

Scheme 13. Reaction mechanism for the intermolecular hydroamination of terminal alkynes with aliphatic amines.

3.3. Organoactinide catalysis

Eisen et al. [89] reported the organoactinide-catalyzed intermolecular hydroamination of terminal alkynes. The regioselectivity of the products can be tuned by varying the alkyne and the metal. Mechanistic studies shows that the rate-limiting step (Scheme 13, step 2) is the formation of an actinide imido complex B.

For thorium, the imido intermediate $[(C_5Me_5)_2Th{=}NC_6H_3Me_2\text{-}2,6(THF)]$ has been characterized by standard techniques, including X-ray diffraction.

Acknowledgements

Financial support by the Deutsche Forschungsgemeinschaft, the Fonds der Chemischen Industrie and the Otto-von-Guericke-Universität Magdeburg is gratefully acknowledged.

References

[1] G.B. Deacon, Q. Shen, J. Organomet. Chem. 511 (1996) 1.
[2] S.S. Krishnamurthy, Curr. Sci. 70 (1996) 769.
[3] I.L. Fedushkin, V.K. Nevodchikov, V.K. Cherkasov, M.N. Bochkarev, H. Schumann, F. Girgsdies, F. Görlitz, G. Kociok-Köhn, J. Pickardt, J. Organomet. Chem. 511 (1996) 157.
[4] R. Taube, H. Windisch, S. Maiwald, H. Hemling, H. Schumann, J. Organomet. Chem. 513 (1996) 49.
[5] H. Windisch, J. Scholz, R. Taube, B. Wrackmeyer, J. Organomet. Chem. 520 (1996) 23.
[6] C. Eaborn, P.B. Hitchcock, K. Izod, Z.-R. Lu, J.D. Smith, Organometallics 15 (1996) 4783.
[7] S. Jank, H.D. Amberger, Acta Phys. Pol. A 90 (1996) 21.
[8] Y. Makioka, K. Takaki, Y. Taniguchi, Y. Fujiwara, Nippon Kagaku Kaishi (1996) 424.
[9] E. Pasqualini, P. Adelfang, M.N. Regueiro, J. Nucl. Mater. 231 (1996) 173.
[10] Y. Yositaka, I. Oguro, Appl. Phys. Lett. 69 (1996) 586.
[11] X. Lin, G. Hong, L. Li, Wuji Huaxue Xebao 12 (1996) 197.
[12] Y. Mu, W.E. Piers, D.C. MacQuarrie, M.J. Zaworotko, V.G. Young, Organometallics 15 (1996) 2720.
[13] R. Taube, S. Maiwald, J. Sieler, J. Organomet. Chem. 513 (1996) 37.
[14] F. Shen, W. Zhang, J. Hu, S. Wang, X. Huanh, J. Organomet. Chem. 523 (1996) 121.
[15] M.M. Corradi, A.D. Frankland, P.B. Hitchcock, M.F. Lappert, G.A. Lawless, Chem. Commun. (1996) 2323.
[16] A. Mandel, J. Magull, Z. Anorg. Allg. Chem. 622 (1996) 1913.
[17] S.P. Constantine, G.M. De Lima, P.B. Hitchcock, J.M. Keates, G.A. Lawless, Chem. Commun. (1996) 2421.
[18] J. Richter, F.T. Edelmann, Eur. J. Solid State Inorg. Chem. 33 (1996) 1063.
[19] Z. Hou, A. Fujita, T. Yoshimura, A. Jesorka, Y. Zhang, H. Yamazaki, Y. Wakatsuki, Inorg. Chem. 35 (1996) 7190.
[20] Z. Hou, T. Yoshimura, Y. Wakatsuki, Kidorui 28 (1996) 290.
[21] A.V. Protchenko, L.N. Zakharov, G.K. Fukin, Yu.T. Struchkov, M.N. Bochkarev, Izv. Akad. Nauk, Ser. Khim. 4 (1996) 993.
[22] R. Broussier, G. Delmas, P. Perron, B. Gautheron, J.L. Petersen, J. Organomet. Chem. 511 (1996) 185.
[23] W.J. Evans, J.T. Leman, J.W. Ziller, S.I. Khan, Inorg. Chem. 35 (1996) 4283.
[24] H. Schumann, K. Zietzke, R. Weimann, Eur. J. Solid State Inorg. Chem. 33 (1996) 121.
[25] H. Schumann, K. Zietzke, F. Erbstein, R. Weimann, J. Organomet. Chem. 520 (1996) 265.
[26] J. Ren, J. Hu, Y. Lin, Y. Xing, Q. Shen, Polyhedron 15 (1996) 2165.
[27] R.D. Rogers, J. Organomet. Chem. 512 (1996) 97.
[28] N.S. Radu, T.D. Tilley, A.L. Rheingold, J. Organomet. Chem. 516 (1996) 41.
[29] K.-H. Thiele, S. Bambirra, H. Schumann, H. Hemling, J. Organomet. Chem. 517 (1996) 161.
[30] Z.-Z. Wu, W.-W. Ma, Z.-E. Huang, R.-F. Cai, Z. Xu, X.-Z. You, J. Sun, Polyhedron 15 (1996) 3427.
[31] G.A. Molander, H. Schumann, E.C.E. Rosenthal, J. Demtschuk, Organometallics 15 (1996) 3817.
[32] N.S. Radu, S.L. Buchwald, B. Scott, C.J. Burns, Organometallics 15 (1996) 3913.
[33] J.M. Keates, G.A. Lawless, M.P. Waugh, Chem. Commun. (1996) 1627.
[34] J. Jin, X. Zhuang, G. Wei, W. Chen, Jiegou Huaxue 15 (1996) 261.
[35] J.E. Cosgriff, G.B. Deacon, B.M. Gatehouse, P.R. Lee, H. Schumann, Z. Anorg. Allg. Chem. 622 (1996) 1399.
[36] M.C. Cassani, Y.K. Gun'ko, P.B. Hitchcock, M.F. Lappert, Chem. Commun. (1996) 1987.
[37] H. Schumann, J. Winterfeld, M.R. Keitsch, K. Herrmann, J. Demtschuk, Z. Anorg. Allg. Chem. 622 (1996) 1457.
[38] Z.-Z. Wu, Z.-E. Huang, R.-F. Cai, X.-G. Zhou, Z. Xu, X.-Z. You, X.-Y. Huang, Jieguo Huaxue 15 (1996) 367.
[39] G. Lin, W.-T. Wong, J. Organomet. Chem. 523 (1996) 93.

[40] W.-K. Wong, L. Zhang, W.-T. Wong, F. Xue, T.C.W. Mak, Polyhedron 15 (1996) 4593.
[41] J.-S. Ren, Q. Shen, J.-Y. Hu, Y.-H. Lin, Y. Xing, Jiegou Huaxue 15 (1996) 379.
[42] N.S. Radu, F.J. Hollander, T.D. Tilley, A.L. Rheingold, Chem. Commun. (1996) 2459.
[43] Z.-Z. Wu, Z.-E. Huang, R.-F. Cai, X.-G. Zhou, Z. Xu, X.-Z. You, X.-Y. Huang, J. Organomet. Chem. 506 (1996) 25.
[44] G.W. Rabe, A. Sebald, Solid State Nucl. Magn. Reson. 6 (1996) 197.
[45] S.Y. Knyazhanskii, A.I. Sizov, A.V. Khvostov, B.M. Bulychev, Izv. Akad. Nauk, Ser. Khim. 7 (1996) 1833.
[46] D.J. Schwartz, Diss. Univ. of California, Berkley, CA (USA) 1995, Bis(pentamethylcyclopentadienyl)ytterbium: an investigation of weak interactions in solution using multinuclear NMR spectroscopy. Diss. Abstr. Int., B 57(3) (1996) 1791; Avail. Univ. Microfilms Int. Order No. DA9621359.
[47] M. Visseaux, D. Baudry, A. Dormond, C. Qian, C. R. Acad. Sci. Ser. IIb 323 (1996) 415.
[48] E.B. Coughlin, L.M. Henling, J.E. Bercaw, Inorg. Chim. Acta 242 (1996) 205.
[49] E. Ihara, M. Nodono, H. Yasuda, N. Kanchisa, Y. Kai, Macromol. Chem. Phys. 197 (1996) 1909.
[50] C. Qian, C. Zhu, Y. Lin, Y. Xing, J. Organomet. Chem. 507 (1996) 41.
[51] H.-D. Amberger, H. Schulz, H. Reddmann, S. Jank, N. Edelstein, C. Qian, B. Wang, Spectrochim. Acta Part A 52 (1996) 429.
[52] X. Zhou, H. Ma, Z. Wu, X. You, Z. Xu, Y. Zhang, X. Huang, Acta Crystallogr. Sect. C Cryst. Struct. Commun. 52 (1996) 1875.
[53] X.Y. Huang, X.G. Zhou, H.Z. Ma, Y.P. Zhen, Y.Q. Yu, X.-Z. You, Z. Xu, Jiegou Huaxue 15 (1996) 223.
[54] J. Xia, X. Zhuang, Z. Jin, W. Chen, Polyhedron 15 (1996) 3399.
[55] M.M. Edelstein, P.G. Allen, J.J. Bucher, D.K. Shuh, C.D. Sofield, N. Kaltsoyannis, G.H. Maunder, M.R. Russo, A. Sella, J. Am. Chem. Soc. 118 (1996) 13115.
[56] L.F. Rybakova, O.P. Syutkina, T.A. Starostina, E.S. Petrov, Zh. Obshch. Khim. 65 (1995) 1600.
[57] K. Takaki, M. Maruo, T. Kamata, Y. Makioka, Y. Fujiwara, J. Org. Chem. 61 (1996) 8332.
[58] T. Kamata, T. Nishiyama, M. Maruo, K. Takaki, Y. Taniguchi, Y. Fujiwara, Kidorui 28 (1996) 280.
[59] S. Caron, D. Stoermer, A.K. Mapp, C.H. Heathcock, J. Org. Chem. 61 (1996) 9126.
[60] A. Krief, A.-M. Laval, B.E. Shastri, E. Badaoui, Acros. Org. Acta 2 (1996) 20.
[61] Y. Kawasaki, H. Shiraishi, M. Yakeno, Y. Nishiyama, S. Sakaguchi, Y. Ishii, Kidorui 28 (1996) 320.
[62] P. Merino, S. Anoro, E. Castillo, F. Merchan, T. Jejero, Tetrahedron Asymm. 7 (1996) 1887.
[63] E. Ihara, K. Katsura, Y. Adachi, K. Koyama, K. Tanaka, N. Kitamura, K. Sekiya, M. Tanaka, H. Yasuda, Kidorui 28 (1996) 92.
[64] T. Sakuragi, S. Myake, S. Inasawa, H. Yasuda; Jpn. Kokai Tokkyo Koho Jp 08,245,711 [96,245,711] (Cl. C08F4/52), 24 Sep 1996, Appl.95/51,321, 10 Mar 1995; 6 pp.
[65] W.J. Evans, D.M. DeCoster, J. Greaves, Organometallics 15 (1996) 3210.
[66] L. Jia, X. Yang, A.M. Seyam, I.D.L. Albert, P.-F. Fu, S. Yang, T.J. Marks, J. Am. Chem. Soc. 118 (1996) 7900.
[67] Y. Li, T.J. Marks, Organometallics 15 (1996) 3770.
[68] Y. Li, T.J. Marks, J. Am. Chem. Soc. 118 (1996) 9295.
[69] T.J. Marks, P.-F. Fu; Eur. Pat. Appl. EP 739,910 (Cl. C08F10/02), 30 Oct 1996, US Appl. 431,521, 28 Apr 1995; 10 pp.
[70] J.-F. Pelletier, A. Mortreux, X. Olonde, K. Bujadoux; Angew. Chem. 108 (1996) 1980; Angew. Chem. Int. Ed. 35 (1996) 1854.
[71] J.-F. Pelletier, K. Bujadoux, X. Olonde,E. Adisson, A. Mortreux, Eur. Pat. Appl. EP 736,536 (Cl. C07F3/02), 9 Oct. 1996, FR Appl. 95/4,203, 7 Apr. 1995.
[72] R. Nomura, Y. Shibasaki, T. Endo, Polym. Bull. 37 (1996) 597.
[73] A. Yanagase, H. Ishita, S. Tone, T. Tokinitsu; (Mitsubishi Rayon, Japan) Jpn. Kokai Tokkyo Koho JP 08,269,149 [96,269,149] (Cl. C08F297/06), 15 Oct 1996, Appl. 95/97,600, 31 Mar 1995; 6 pp. (Japan).

[74] H. Yasuda, E. Ihara, A. Yanagase, H. Ige, S. Tone, T. Tokimitsu (Mitsubishi Rayon, Japan) PCT Int. Appl. WO 96 19,513 (Cl. C08F297/06), 27 Jun 1996, JP Appl. 94/335,456, 22 Dec 1994; 22 pp. (Japan).
[75] F. Ota, T. Ishimaru (Hitachi Chemical Co., Japan), Jpn. Kokai Tokkyo Koho Jp 08,123,025 [96, 123, 025] (Cl. G03f7/033), 17 May 1996, Appl. 94/264,072, 27 Oct 1994; 11 pp. (Japan).
[76] M.R. Leonov, V.A. Il'yushenkov, N.V. Il'yushenkova, Radiokhimiya 38 (1996) 49.
[77] D. Baudry, A. Dormond, A. Hafid, C. Raillard, J. Organomet. Chem. 511 (1996) 37.
[78] M.R. Leonov, V.A. Il'yushenkov, N.V. Il'yushenkova, Zh. Obshch. Khim. 66 (1996) 721.
[79] S.M. Cendrowski-Guillaume, M. Ephritikhine. J. Chem. Soc. Dalton Trans. (1996) 1487.
[80] D.S.J. Arney, R.C. Schnabel, B.C. Scott, C.J. Burns, J. Am. Chem. Soc. 118 (1996) 6780.
[81] R.P. Hughes, J.R. Lomprey, A.L. Rheingold, B.S. Haggerty, G.P. Yap, J. Organomet. Chem. 517 (1996) 89.
[82] T. Straub, W. Frank, G.J. Reiss, M.S. Eisen. J. Chem. Soc. Dalton Trans. (1996) 2541.
[83] C. Boisson, J.C. Berthet, M. Lance, M. Nierlich, M. Ephritikhine, Chem. Commun. (1996) 2129.
[84] Y.-X. Chen, C.L. Stern, S. Yang, T.J. Marks, J. Am. Chem. Soc. 118 (1996) 12451.
[85] M.-R. Spirlet, J. Rebizant, C. Apostolidis, E. Dornberger, B. Kanellakopulos, B. Powietzka, Polyhedron 15 (1996) 1503.
[86] P.C. Leverd, M. Ephritikhine, M. Lance, J. Vigner, M. Nierlich, J. Organomet. Chem. 507 (1996) 229.
[87] D.J.A. De Ridder, C. Apostolidis, J. Rebizant, B. Kanellakopulos, R. Maier, Acta Crystallogr. Sect. C Cryst. Struct. Commun. 52 (1996) 1436.
[88] C. Boisson, J.C. Berthet, M. Ephritikhine, M. Lance, M. Nierlich, J. Organomet. Chem. 522 (1996) 249.
[89] A. Haskel, T. Straub, M.S. Eisen, Organometallics 15 (1996) 3773.